Using an Automated Skilled Reaching Task to Investigate Predictors of Motor Impairment and Recovery following Photothrombotic Stroke

Rana Abdelhalim

Thesis Submitted to the University of Ottawa in partial fulfillment of the requirements for the Master of Science in Neuroscience

Department of Cellular and Molecular Medicine

Faculty of Medicine

University of Ottawa

Abstract

Accurate assessment of sensorimotor function in rodent models of stroke is essential for understanding how brain reorganization or plasticity contribute to functional recovery. We recently developed the Home-cage Automated Skilled Reaching Apparatus (HASRA) that allows automated training and assessment of mice engaged in a skilled reaching task. To validate the HASRA as a sensitive tool for assessing post-stroke performance, group-housed mice were trained on the reaching task for 14-21 days, followed by an M1 photothrombotic stroke or sham procedure, after which performance was monitored for 4 weeks. Performance at baseline, acutely, and at endpoint was compared. Stroke mice had a significantly reduced performance acutely compared to baseline but improved by endpoint. The stroke group was divided into two sub-groups: 1) high endpoint success and 2) low endpoint success groups. We found that training success, acute success, and learning rate were significant predictors of endpoint success. Furthermore, using a novel semi-automated lesion localization workflow, we were able to find that the percentage of damage in the secondary motor area was also a predictor of endpoint performance. Overall, using automated tools like the HASRA for the quantification of post-stroke motor impairments and semi-automated tools for the quantification of lesion location are essential for investigating potential predictors of stroke recovery and designing effective therapies.

Table of Contents

List of Figures

List of Tables

List of Supplemental Figures

List of Abbreviations

9HPT	9-Hole Peg Test
AMBA	Allen Mouse Brain Atlas
AP	Anterior-Posterior
ARAT	Action Research Arm Test
BBT	Box And Block Test
CIMT	Constraint-Induced Movement Therapy
dACC	Dorsal Anterior Cingulate Area
ET-1	Endothelin-1
EWMN	Eshkol-Wachmann Movement Notation
FDI	First Dorsal Interosseous Muscle
FPS	Frames Per Second
H&E	Hematoxylin Eosin
HASRA	Home-Cage Automated Skilled Reaching Apparatus
IR	Infrared
IVT	Intravenous Thrombolysis
Little's MCAR	Little's Missing Completely At Random
M1	Primary Motor Cortex
M2	Secondary Motor Cortex
MCA	Middle Cerebral Artery
ML	Mediolateral
MT	Mechanical Thrombectomy
RFID	Radio Frequency Identification
RM	Repeated Measures
rtPA	Recombinant Tissue Plasminogen Activator
S1FL	Forelimb Primary Somatosensory Cortex
S1HL	Hindlimb Primary Somatosensory Cortex
SEM	Standard Error of the Mean
SPRT	Single Pellet Reaching Task
vACC	Ventral Anterior Cingulate Area

Acknowledgements

For the supervision and guidance provided throughout my master's thesis, I would like to thank Dr. Greg Silasi. I am grateful for the opportunity to expand my knowledge in the field of neuroscience, gain valuable research skills, and uncover my passion for motor neuroscience research. To Matthew Jeffers, thank you for all your help with the experimental design, all the experimental efforts, and for all the guidance provided.

I would also like to especially thank my advisory committee Dr. Diane Lagace and Dr. Maxime Rousseaux for always providing me with support, feedback, and stimulating conversations. To the staff at ACVS and at the Faculty of Medicine Graduate Studies Office, thank you for always being there to answer my questions, your efforts are greatly appreciated.

In addition, a huge thank you to my friends and colleagues at the Silasi lab: Beatriz Romero Quineche, Irina Morozov, Zanna Vanterpool, Zachary Eckert, Danya Alomar, Katie Neale, Segolene Chevallier Rufigny, Eilia Eslami Dizgah, and Shafik Algharbi. Thank you all for being such wonderful people, I will definitely miss our lunch time chats.

Lastly, to my family, thank you for always believing in me. Your encouragement and support have given me the strength to persevere despite any and all challenges.

1. INTRODUCTION

1.1 Ischemic stroke in humans

1.1.1 Pathophysiology of Thrombotic Ischemic Stroke

Ischemic stroke is the most common type of stroke, accounting for 85% of all cases (Musuka et al., 2015; Sacco et al., 2013). Generally, it is caused by an abrupt and sustained reduction in blood and oxygen supply to the brain resulting in damage and localized death in the affected brain tissue (Chugh et al., 2019). Ischemic stroke can be divided into two subtypes: thrombotic and embolic stroke (Musuka et al., 2015). Thrombotic stroke is the most common type of ischemic stroke and occurs when a blood clot (known as a thrombus) forms in a blood vessel affected by atherosclerosis (Kuriakose et al., 2020; Sacco et al., 2013). Atherosclerosis is a condition in which the vessel becomes narrower due to plaque build-up along the lining of the blood vessel. Plaque is made up of cell lesions, foam cells, calcium, cholesterol esters, fibrin, and a mass of fatty substances (Rafieian-Kopaei et al., 2014). As the plaque continues to build up in the vessel, the vessel will continue to become narrower, and it becomes more likely to be occluded by a blood clot (Kuriakose et al., 2020).

The transition from plaque build-up to thrombus formation is not fully understood; although it is known that plaque destabilization (fissuring and rupture) is the most frequent cause of thrombosis (Bentzon et al., 2014; Deb et al., 2010). Plaque fissuring (thinning) involves two concurrent mechanisms. One of which involves the loss of smooth muscle cells from the fibrous cap of the plaque; the other involves foam cells infiltrating the plaque and degrading the collagen-rich cap matrix (Bentzon et al., 2014; Deb et al., 2010; Slager et al., 2005). When the plaque ruptures, circulating platelets come into contact with the subendothelial collagen,

becoming activated, then aggregating and adhering to the endothelial surface of the vessel (Deb et al., 2010). Next, a coagulation cascade ensues. The activated platelets contain an enhanced capacity to catalyze interactions between activated coagulation factors. This capacity results in the formation of fibrin molecules, which aggregate together and trap platelets, erythrocytes, and leukocytes, leading to thrombus formation in the vessel and blockage of blood flow (Deb et al., 2010; Stoll et al., 2008).

Cerebrovascular tissue undergoing thrombotic ischemia consists of two regions. One is the inner core of severe ischemia, with blood flow levels below 10% to 25%. In this inner layer, both neuronal and glial cells undergo necrosis (Deb et al., 2010). The second layer is the outer layer surrounding the ischemic core and is known as the penumbra. The penumbra undergoes less severe ischemia and is often supplied by collaterals to support the tissue. Neurons in the penumbra are mostly dysfunctional but may recover if reperfused in time. Furthermore, penumbral cells can also be retrieved later by therapeutic intervention (Deb et al., 2010; Meschia et al., 2017).

1.1.2 Treatments and Interventions

To date, there is only one approved pharmacological systemic treatment for ischemic stroke: intravenous thrombolysis (IVT) with recombinant tissue plasminogen activator (rtPA or alteplase; NINDS et al., 1995; Hacke et al., 2008; Berge et al., 2021; Powers et al., 2019). It is recommended that IVT with rtPA is administered within 4.5 hours of symptom onset. If the time of symptom onset is beyond 4.5 hours, then imaging techniques such as computed tomography (CT) and magnetic resonance imaging (MRI) may be used to assess the brain tissue perfusion status and determine if IVT with rtPA is the appropriate treatment option (Lansberg et al., 2017; Thomalla et al., 2011). When rtPA is administered, it attaches to the fibrin on the surface of the

blood clot. During its attachment, rtPA cleaves the fibrin-bound plasminogen, resulting in the formation of plasmin, a serine protease. Plasmin is an endogenous fibrinolytic enzyme that breaks the cross-links between the fibrin molecules, providing structural support for the blood clot; this causes the clot to dissolve (Collen et al., 1987). Although there are other thrombolytic drugs with a similar mechanism of action as rtPA, such as reteplase and tenecteplase, rtPA continues to be the most effective IVT drug (Kuriakose et al., 2020).

IVT can be administered alone or in combination with mechanical thrombectomy (MT), which is an endovascular technique for the removal of a blood clot from large vessels. The MT procedure should be performed within 6 hours of symptom onset. Although MT has been shown to be safe and effective in reducing neurological disability in patients with large cerebral artery occlusions, only 10% to 20% of patients are eligible. Furthermore, access to thrombectomy centres within 6 hours of symptom onset may not be feasible for many individuals (Berkhemer et al., 2015; Saver et al., 2015). Due to the tight time window for these interventions administration, ischemic strokes can leave patients with motor impairments that lead to short- and long-term disabilities (Kuriakose et al., 2020).

1.1.3 Upper Limb Motor Impairments

Motor impairments resulting from ischemic stroke can significantly affect one's quality of life, with common daily activities like reaching, gripping, and picking up objects becoming challenging to do (Hatem et al., 2016; Bleyenheuft & Gordon, 2014). The most common impairment following stroke is hemiparesis of the contralateral upper limb, which affects more than 80% of stroke patients acutely, and more than 40% of patients chronically (Cramer et al., 1997). Common manifestations of upper limb motor impairment include muscle weakness, immobility, sarcopenia, and spasticity (Hatem et al., 2016; Raghavan, 2015).

Weakness is the most common impairment post-stroke and the primary contributor to impairment in chronic stroke (Kamper et al., 2006). Normally, to generate a movement impulse, a signal is transmitted from the motor cortex to the spinal cord, which sends signals to the muscles for movement execution (Teka et al., 2017). However, following stroke, the signal from the motor cortex is not transmitted, which leads to a delay in the initiation and termination of muscle contractions and may result in an inability to move quickly or at all (Chae et al., 2002; Canning et al., 1999). Suresh et al., (2008) investigated changes in neural input to muscles in stroke patients experiencing weakness in their affected upper limb. They measured muscle response in the first dorsal interosseous muscle (FDI) while stroke patients and healthy subjects moved their second digit. A larger magnitude of muscle force was observed from recordings of the FDI in patients' affected limb compared to that of their unaffected limb and of healthy subjects, suggesting that a greater muscle force was required for movement of the affected limb's second digit. These observed changes are likely due to a combination of abnormal firing patterns and changes in motor unit control (Suresh et al., 2008). Weakness of the upper limb may affect all muscle groups, or some muscle groups more than others (Raghavan, 2015). A study by Renner et al., (2009) examined this further by exploring the relationship between upper limb weakness and the strength of muscle groups in stroke patients. They were unable to identify any correlations between the pattern of weakness across muscle groups, the absolute strength of muscle groups, and upper limb functional motor ability. But they did find that the rate of change in force development in hand grip and wrist extension strength was correlated with functional recovery of the upper limb (Renner et al., 2009).

One consequence of upper limb weakness is immobility, which can lead to further impairments. These impairments include changes in bone mineral density, increasing the risk of

developing osteoporosis, and changes in soft-tissue, such as muscle tissue, leading to muscle fibrosis (Hamdy et al., 1993; Stecco et al., 2014). Additionally, immobility could lead to stiffness in connective tissue, causing stroke-related pain through the stimulation of nerve endings and proprioceptors in the tissue (Raghavan, 2015). Chronic pain is a common symptom following stroke and is experienced by up to one-half of stroke patients; with nearly 70% of affected patients experiencing this pain daily (Naess et al., 2012; Klit et al., 2011). Another impairment that may appear alongside the weakness of the affected limb is spasticity. Spasticity is characterized as a velocity-dependent increase in tonic stretch reflexes with exaggerated tendon jerks due to hyperexcitability of the stretch reflex (Feldman et al., 1980). Put simply, in post-stroke spasticity, muscles are very tight, even when not contracted, due to their increased tone and resistance. Normally, the excitability of the stretch reflex circuit is predominantly regulated by a balance of excitatory and inhibitory descending supraspinal signals (Gracies et al., 2005; Li et al., 2017). In post-stroke spasticity, these signals are disrupted, causing disinhibition of the stretch reflexes and a reduction in the threshold for reflex activity (Gracies et al., 2005; Li et al., 2017; Raghavan, 2015).

Weakness, immobility, stroke-related pain, and spasticity can lead to the use of compensatory motor strategies to complete daily tasks (McCrea et al., 2005). Motor compensation is defined as the appearance of new motor patterns resulting from the adaptation of remaining motor elements or the substitution of the previous motor elements (Levin et al., 2008). For the upper limbs, motor compensation includes the use of movement patterns incorporating trunk displacement and rotation, scapular elevation, shoulder abduction, and internal rotation (Levin et al., 2002; Roby-Brami et al., 2003). Post-stroke, patients may use trunk movements instead of elbow extension to enable the transport of their arm and hand for reaching movements;

forearm pronation and wrist flexion instead of neutral forearm position and wrist extension to orient the hand for grasping; and metacarpophalangeal joint flexion instead of proximal interphalangeal joint flexion for grasping movements (Cirstea & Levin, 2000; Ustinova et al., 2004; Raghavan et al., 2010). The degree of compensatory motor strategies used is related to the severity of hemiparesis (Levin et al., 2002; Thielman et al., 2004). When therapeutic interventions are aimed at the reacquisition of motor elements involved in functional task accomplishment, it can lead to an overall reduction in impairment. For instance, this is observed in interventions where the trunk is restrained during reach practice, resulting in the use of a more normal pattern of reaching by extending the elbow (Michaelsen et al., 2001; Woodbury et al., 2008). To design such appropriate rehabilitative interventions, accurate assessment of upper-limb motor impairment is crucial.

1.2 Clinical Assessment and Rehabilitation of Upper Limb Impairments

1.2.1 Upper Limb Impairment Assessment

The presence and severity of upper limb impairments vary considerably among stroke patients, partly due to the variability in lesion size and location (Adolphs et al., 2000; Karnath et al., 2004; Fellows & Farah, 2007). There are a variety of clinical assessments that can be used to evaluate these impairments following stroke, such as the Action Research Arm Test (ARAT), the 9-hole peg test (9HPT), the box and block test (BBT), and many more (Lang et al., 2013; Salter et al., 2013).

The ARAT was first described by Ronald Lyle in 1981 as a modification of an earlier test known as the Upper Extremity Function test (Lyle, 1981; Carrol, 1965). This test consists of 19

items, which are grouped into four subtests of arm motor function: grasp, grip, pinch, and gross arm movement. These tests require various pieces of equipment, such as differently sized blocks of wood, cricket ball, stone, jug and glass, a tube, washer and bolt, a ball bearing, and marble. In the ARAT, a researcher observes a patient's movement at each test and transforms that observation into a score on an ordinal 4-point scale ranging from 0 to 3. The higher the score, the better the motor status. These scores are then summed up to obtain the total ARAT score (Lyle, 1981). This test has been shown to have a high inter-rater and retest reliability, and efforts to further standardize the test by detailing scoring guidelines have also been made (Van der Lee et al., 2001; Yozbatiran et al., 2008).

In contrast to the ARAT, the 9HPT is logistically simpler to administer. In this assessment, participants are asked to use their hands to quickly pick up nine small pegs from a holding well, and place them into holes on a board, and then move them back into the well. Multiple trials of this test are often performed for the affected and unaffected upper limbs. The time, in seconds, spent on the completion of one trial with one limb is scored (Salter et al., 2013). The 9HPT is a standardized and well-established assessment that has been demonstrated to be a reliable measure of hand function for adults of a broad range of ages (Haaxma et al., 2010; Kellor et al., 1971; Mathiowetz et al., 1985).

Similarly to the 9HPT, the BBT requires precise reaching and grasping movements to measure gross manual dexterity. The BBT apparatus consists of a box divided into two spaces by a partition (Mathiowetz et al., 1985). One compartment of the box is filled with 150 blocks, while the other compartment, on the opposite side of the partition, is empty. In the BBT, participants are required to reach into the compartment filled with blocks to grasp and obtain one block to be transported over the partition and released into the empty compartment. To score this

assessment, the number of blocks carried from one compartment to the other in one minute is evaluated for each hand over two trials. Participants can select blocks in any order for their transport to the other compartment; this may lead to some variability in the number of blocks transported among different participants. For this reason, modified versions of the standard BBT, such as the targeted BBT, have been developed (Herbert & Lewicke, 2012; Herbert et al., 2014). In the targeted BBT, participants are required to accurately place a specific block at a target position in the other compartment, reducing variability among participants and allowing for the analysis of the same movements (Herbert & Lewicke, 2012; Herbert et al., 2014). Overall, the BBT is especially useful due to its reproducibility, reliability, ease, and speed of implementation (Kontson et al., 2017). Moreover, in one study examining the predictive validity of the BBT compared to various other upper limb motor assessments (9HPT, Frenchay Arm Test, Grip Strength, and the Stroke Rehabilitation Assessment of Movement), it was found to be the best predictor of upper limb function at 5 weeks post-stroke (Higgins et al., 2005).

All three of the above upper limb motor assessments are highly interrelated as they quantify deficits in dexterity and coordinated movements. Through the use of highly correlated motor assessments, experimenters and therapists can further validate their evaluations of a patient's upper limb motor function to allow for the design of appropriate rehabilitative interventions.

1.2.2 Rehabilitative Interventions for Upper Limb Recovery

Upper limb rehabilitation interventions are mostly delivered by physical and occupational therapists, but they can also be delivered by other health and non-health professionals (Coupar et al., 2010; Coupar et al., 2012). These interventions are usually selected following an assessment of a patient's upper limb impairment and with the patient's goals and quality of life in mind

(Langhorne et al., 2011). Other important considerations that health professionals keep in mind are the particular deficits that the patients are experiencing, which can range from general muscle weakness to difficulty with specific functional movements like grasping and releasing objects. There are various interventions that can be delivered to address deficits like these as well as others, such as constraint-induced movement therapy (CIMT), bilateral or unilateral arm training, and task-specific training (e.g., reach-to-grasp exercises).

In CIMT, the unimpaired limb is placed in an arm sling or a mitt that prevents its use during fine movements (Page et al., 2001; Page et al., 2002; Taub et al., 1993; Uswatte et al., 2006; Wolf et al., 2006). By restraining this limb, patients are forced to learn to use their impaired hand when performing daily tasks following a stroke. Shaping programs are also used to train the affected limb to perform progressively more challenging motor tasks.

In contrast, in bilateral arm training, both arms are simultaneously used to perform identical movements (Waller & Whitall, 2008; Mudie & Matyas, 2000; Stewart et al., 2006). Through interlimb coupling in this intervention, interhemispheric inhibition is thought to be rebalanced, allowing for the activation of the stroke-affected hemisphere and improvement of the affected limb's motor control (Stinear et al., 2008). Although studies comparing bilateral arm training and unilateral arm training (exercises performed only by the impaired limb) have shown that unilateral training is more effective than bilateral training at improving upper limb function and performance of activities of daily living (van Delden et al., 2012).

Similarly to CIMT and unilateral arm training, task-specific training involves the use of the impaired limb to complete a task (Shumway-Cook & Woollacott, 2001). Although there is no conclusive definition for task-specific training, tasks used for upper limb rehabilitation are usually reach-to-grasp exercises (Rensink et al., 2009). Thus far, there has been inconclusive

evidence related to the efficacy of these exercises on improving upper limb function post-stroke (Pelton et al., 2012; Urton et al., 2007). However, multiple studies have shown that restriction of trunk movements with reach and grasp training led to further arm reaching and diminished trunk bending during grasping in chronic stroke patients (Michaelsen & Levin, 2004; Michaelsen et al., 2006). Recently, there has been an investigation into the use of home-based reach-to-grasp exercises, which can reduce the barriers related to accessing rehabilitative interventions that many patients face (Turton et al., 2016; Cunningham et al., 2016). Moreover, reach-to-grasp exercises can be used to investigate the use of compensatory strategies during upper limb movement post-stroke. In a study by Xie et al., (2022), they used markerless motion tracking to assess the kinematic parameters of the patients' upper limb movement during a reach-to-grasp-pen exercise. They were able to characterize patients' reaching behaviour and identify compensatory strategies like a longer reaching duration, less smooth movement trajectories, more trunk rotation, and greater extension of metacarpophalangeal and proximal interphalangeal joints. This study demonstrates that the reach-to-grasp task can be very useful for evaluating the recovery and motor compensation of the impaired upper limb.

1.2.3 Mechanism Underlying Rehabilitation

One mechanism underlying rehabilitation that has been identified is brain plasticity. Brain plasticity refers to changes in brain networks that carry behavioural implications over time. The cortex has been found to be an ideal site for plasticity to take place due to its multitude of synaptic connections (Donoghue, 1995). One way through which plastic change can take place in the cortex is through motor skill learning, which has been associated with dendrite growth, an increase in dendritic spines, and synaptogenesis in animal models (Ivanco & Greenough, 2000; Rioult-Pedotti et al., 1998). Furthermore, through clinical studies, there has been evidence of

these cortical changes in human motor learning as well (Bütefisch et al., 2000; Ziemann et al., 2004).

Following stroke injury, behavioural training has been found to promote neural recovery in animals by inducing synaptogenesis in the lesioned hemisphere (22, 23). Similarly, clinical studies have demonstrated that targeted physical training post-stroke induces physiological and structural changes in the brain to promote neural recovery (25, 26). As discussed earlier, task-specific training (e.g., reach-to-grasp exercises) is a rehabilitative paradigm that involves the repeated practice of new functional skills that make up a functional task (French et al., 2007; Bütefisch et al., 1995). Through this paradigm, stroke patients engage in motor learning, leading to neuroplastic changes in the brain once new motor skills are learned (Carr & Shepherd, 1987; Ada et al., 1990; Carr & Shepherd, 1998; Nudo et al., 2000; Nudo et al., 2003a; Nudo et al., 2003b).

1.3 Rodent Models of Ischemic Stroke

Preclinical research in animal models allows for the informed development of novel therapeutics to be translated and further investigated in clinical studies (Drude et al., 2021). Various animal models can be used in preclinical stroke research, with mice and rats being the most commonly used species (Bacigaluppi et al., 2010; Boboc et al., 2023; Ruan & Yao, 2020). Rodents are often used due to their similar vascular anatomy to humans, high reproductive rates, low maintenance costs, and availability of transgenic models, particularly in mice (Ruan & Yao, 2020). Furthermore, by using rodents, experimenters can control lesion location, lesion size (in some rodent models), and longitudinally track impairment and recovery among animals. These

advantages allow for the creation of a homogenous sample population in which within-subject comparisons can be made across the experimental timeline, from the pre-stroke to the post-stroke time periods. For this reason, this thesis uses a mouse model of ischemic stroke.

1.3.1 Endovascular Filament Middle Cerebral Artery Occlusion

The intraluminal thread occlusion of the middle cerebral artery (MCA) is the most commonly used model of focal ischemic stroke (Howells et al., 2010). This model involves the insertion of a round-tip filament into the external carotid artery, then advancing it through the internal carotid artery to block the origin of the MCA (Uluç et al., 2011). The filament remains inserted for a fixed period of time, between 30 and 180 minutes, before its removal to allow for reperfusion (Buchan et al., 1992; Olsen, 1986). The severity of the resulting ischemic stroke is dependent on the duration of the occlusion (Buchan et al., 1992; Olsen, 1986). Occlusion of the MCA for more than 180 minutes leads to damage in other regions than just the cortex, such as the lateral caudate putamen (Nagasawa & Kogure, 1989). Moreover, transient and permanent MCA occlusions involve different pathophysiological processes, making them difficult to compare (Shah et al., 2019). Another disadvantage of this model is the variability in infarct size and distribution, which can be further affected by the rat or mouse strain and type of filament used (Oliff et al.,1995; Connolly et al., 1996; Bouley et al., 2007). Despite these disadvantages, this can be a useful model due to its ease of manipulation, control of ischemic duration, and use in both mouse and rat models (Hata et al., 1998).

1.3.2 Endothelin-1 Occlusion

Endothelin-1 (ET-1) is a 21-amino acid peptide with potent vasoconstrictor properties (Masaki, 1998). ET-1 can be used to induce ischemic injury in a variety of ways. One way is through the

direct administration of ET-1 to a surgically exposed MCA, which leads to a reduction in cerebral blood flow (CBF) to the caudate nucleus, genu of the corpus callosum, and cortical regions near the MCA (Robinson et al., 1990; Robinson et al., 1991). Another method through which similar infarct volumes can be achieved is by a stereotaxic injection of ET-1 into the superficial cortex adjacent to the MCA (Sharkey, 1993; Macrae et al., 1993). Lastly, ischemic injury can also be induced in other brain regions, such as the internal capsule and the frontoparietal cortex, via a cortical stereotaxic injection of ET-1 (Frost et al., 2006; Ono et al., 2016; Fuxe et al., 1997). The extent of damage produced by ET-1 administration is dependent on the dosage of ET-1 and the use of anesthetics during the stroke procedure. The greater the dosage of ET-1, the greater the damage produced (Macrae et al., 1993). Anesthetized rats require approximately four times the dose of ET-1 as awake rats to produce similar infarct volumes (Bogaert et al., 2000). This model is widely used in rats due to its ease of manipulation and ability to target specific regions for infarction (Horie et al., 2008).

1.3.3 Photothrombosis Model

The photothrombosis model was introduced by Watson et al., (1985) to produce a more reproducible cortical infarct without a craniotomy. This model involves the injection of a photosensitive dye (Rose Bengal, erythrosine B), which circulates through the brain vasculature, and then a specific brain region is irradiated through the intact cranium using stereotaxic coordinates and a laser beam of a particular wavelength. When the laser illuminates the photosensitive dye, this leads to dye-sensitized photooxygenation, which causes endothelial damage, followed by platelet adhesion and aggregation to form a thrombus, thereby blocking cerebral blood vessels (Watson et al., 1985). This ischemic stroke model is advantageous as it is reproducible, easy to manipulate, allows for the control of infarct size and location, and is widely

used in rats and mice (Lee et al., 2007). Due to these many advantages, our study uses the photothrombotic model in mice. More information on our photothrombotic stroke procedure is available in section **3.2**. Lastly, although there are many advantages of this model, it is important to discuss its drawbacks. One such drawback is the greater neuroinflammation induced by photothrombosis compared to other ischemic stroke models, such as the MCA occlusion (Feng et al., 2017). Increased neuroinflammation can promote further injury; however due to our small stroke sizes, this is not likely a great concern in our study.

1.4 Assessment and Rehabilitation of Post-Stroke Upper Limb Impairments in Rodents

1.4.1 Assessment and Rehabilitation Assays

There are various motor and sensorimotor assays that can be used to assess post-stroke upper limb impairments in rodents. Some of these assays require minimal training and are easy to execute, such as the foot-fault test, cylinder test, adhesive removal test, and wire hanging test described in Table 1 (Ruan & Yao, 2020). Despite their ease of use, these assays can only assess impairment and spontaneous recovery, and cannot be used as a rehabilitative paradigm. In contrast, the single pellet reaching task (SPRT), a type of skilled reaching task, can be used as an assessment assay for post-stroke upper limb impairments as well as a rehabilitative paradigm to improve forelimb motor function (Whishaw & Pellis, 1990; Farr & Whishaw, 2002). The SPRT requires a great deal of training since rodents need to engage in motor learning to perform complex sequences of movements for the successful execution of the task. In the SPRT, rodents are placed in a plexiglass reaching box with a narrow slot in the middle of the front wall. A tray with two indentations, each located 1 cm away from the left and right edges of the slot, is placed in front of the slot. During the shaping period (three to seven days), millet seeds are placed on the tray at a distance closest to the rodents' mouths so that the animals can engage with the task

by obtaining the millet seed using their tongue. The tray is then gradually moved farther away from the slot to encourage the animals to use their forelimbs to reach and retrieve a millet seed. Once the rodents are reaching, their preferred forelimb is determined by placing the millet seeds on the left and right indentations, and the most frequently used limb is considered the preferred forelimb. During the training period (eight days), millet seeds are placed in the indentation opposite the preferred forelimb so that animals can only obtain the seed using their preferred limb. Twenty millet seeds are given to each rodent during each training day, and the number of successful reaches (millet seeds successfully retrieved by reaching) and failed trials (millet seeds knocked down or dropped) is scored. Upper limb impairment and recovery following ischemic stroke can be evaluated by the percentage of successful reaches using the contralateral forelimb (Whishaw & Pellis, 1990; Farr & Whishaw, 2002; Ruan & Yao, 2020). This task has been shown to be sensitive in detecting acute upper limb impairments and long-term recovery through its use as a rehabilitative paradigm following ischemic stroke in rodents (Kleim et al., 2003; Maldonado et al., 2008; Liu et al., 2011; Farr & Whishaw, 2002).

The SPRT is analogous to the reach-to-grasp exercises (e.g., BBT and 9HPT) used for the assessment and rehabilitation of upper limb impairments in stroke patients. This is evident from the similar sequences of movements taken by rodents in the SPRT as they reach for the millet seed, grasp it, retrieve it, and then release it into their mouths (Whishaw & Pellis, 1990; Farr & Whishaw, 2002; Salter et al., 2013; Mathiowetz et al., 1985). Furthermore, the SPRT can be used to investigate compensatory motor strategies of the impaired forelimb in rodents (Alaverdashvili & Whishaw, 2013), similarly to reach-to-grasp tasks in humans. As previously discussed, following stroke, compensatory strategies can develop to compensate for any present functional impairments so that the animal can execute the task (Alaverdashvili & Whishaw, 2013; Finger,

1978). Motor compensation can impede rehabilitation of the impaired limb and interfere with the evaluation of the animals' recovery pattern post-stroke (Finger, 1978). In the past, compensatory motor strategies were described using the Eshkol-Wachmann Movement Notation (EWMN), a conceptual framework that describes the movement of different body parts in relation to each other (Farr & Whishaw, 2002). Some of the compensatory strategies identified using the EWMN in stroke mice include an ipsiversive trunk rotation made to bring a mouse's forelimb to an aiming position for reaching instead of the usual elbow adduction made for forelimb positioning. In addition, during millet seed retrieval, trunk rotary movements along with the use of the non-reaching forelimb for assistance were observed (Farr & Whishaw, 2002). Technological advancements have led to the placement of physical reflective markers on a rodent, which can then be used to track the movements of different body parts during reaching (Balbinot et al., 2021). More recently, further technological advancements have led to the development of markerless deep neural networks that can provide detailed information on the movement of different body parts and their kinematics during reaching behaviour (Ryait et al., 2019; O'Neill et al., 2022).

Overall, the SPRT is considered the gold standard for assessing forelimb motor function in rodents due to its ability to predict lasting upper limb impairment, its use as a rehabilitative paradigm, and its high translatability to the clinical population.

Table 1. Behavioural assays for assessing stroke impairments in rodents. *Illustrations created using BioRender.*

Assay	Purpose	Description	Illustration
Unskilled Assays			

Foot-Fault Test	Assesses motor function and limb coordination in rodents (Colle et al., 1986; Hernandez & Schallert, 1988; Zhang et al., 2002).	Animals are allowed to move across an elevated grid with score openings. If the limb slips off the frame of the grid, then a foot-fault is recorded (OG source). Post-stroke, rodents display increased foot-faults toward the contralateral side (Zhang et al., 2002).	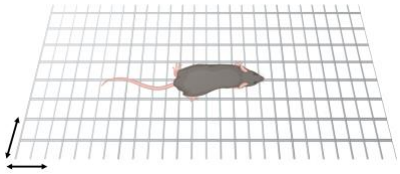
Cylinder Test	Assesses sensorimotor asymmetry in limbs (Schallert et al., 2000).	Animals are placed in a clear cylinder container and their use of forelimbs to contact the wall of the cylinder is recorded. Post-stroke, rodents may use the ipsilateral forelimb more frequently than the contralateral forelimb (Li et al., 2004).	
Adhesive Removal Test	Assesses sensorimotor dysfunction and motor asymmetry (Schallert et al., 2000; Modo et al., 2000).	Animals are placed into a transparent box and tape is placed on the hairless part of each rodent's hand. The time spent removing the tape from each hand is recorded. Generally, rodents would spend more time removing the tape from the contralateral hand post-stroke (Schallert et al., 2000; Modo et al., 2000).	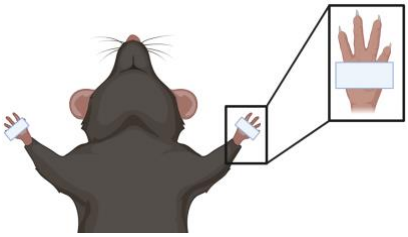

Wire Hanging Test	Assesses grip strength, endurance, and body corporation (Ikegami, 2000; Joseph et al., 1986; Dean et al., 1981).	Animals are placed hanging from a wire using their forelimbs. The latency before falling from the wire is recorded, which reflects muscle strength (Ikegami, 2000; Joseph et al., 1986; Dean et al., 1981). Rodents would have more trouble hanging on to the wire and a smaller latency before falling post-stroke (Fan et al., 2006; Fan et al., 2005).	
Skilled Assay			
Single Pellet Reaching Task	Assesses skilled upper limb motor function (Whishaw & Pellis, 1990; Farr & Whishaw, 2002).	Rodents are placed in a plexiglass reaching box containing a narrow slot in the front wall. Millet seeds are placed in front of the slot at a fixed position that is opposite the animal's preferred limb. Rodents are required to reach through the slot, grasp the millet seed, and retrieve it for consumption. The percentage of successful reaches is scored. Stroke animals would have a decreased percentage of successful reaches during the acute period. Animals can also use this task as a rehabilitative paradigm, enabling an improvement in their	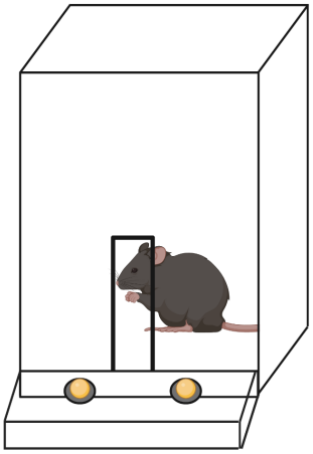

		performance at the task and allowing for recovery of their impaired limb (Whishaw & Pellis, 1990; Farr & Whishaw, 2002; Ruan & Yao, 2020).	

1.4.2 Challenges and limitations of the Single Pellet Reaching Task

Despite the utility of the SPRT in assessing upper limb impairment and recovery post-stroke, there are several challenges that can arise due to the nature of the task. One major challenge of the traditional SPRT is that it is laborious. This is because the experimenter can only work with one animal at a time, which results in a limited number of trials performed by each animal (20 trials per day) and a limited number of animals that can be trained for an experiment (Fouad et al., 2013). One consequence of the limited number of trials that each animal can perform is the high variability in performance that is observed from day to day (Fouad et al., 2013). Perhaps if more numerous trials were conducted, such variability would be reduced. Furthermore, SPRT training is often done during the animals' light-cycle, which can impact the performance of nocturnal rodents, which are more active during the dark-cycle (Fouad et al., 2013; Fenrich et al., 2015). Moreover, disruption of rodents' circadian rhythms through training during the day cycle can significantly influence the animals' stress levels (Dauchy et al., 2010). Other stressors that can influence rodents' performance and lead to further variability include animal handling, social isolation when rodents are individually placed in the reaching chamber, and changes in the experimenter working with the animals (Fouad et al., 2013; Balcombe et al., 2004).

In addition, another source of variability within and between laboratories is the different experimenters conducting the task (Fenrich et al., 2015; Torres-Espin et al., 2018). This is due, in

part, to individual differences between experimenters' methodologies for shaping and training animals on the SPRT and to the variability in the time of day or week in which training was performed. For instance, if an experimenter does not train animals during the weekend, a trend of lower success rates early in the week and higher success rates later in the week may be observed. This trend may be due to animals having a lower motivation to engage with the SPRT early in the week since they had access to food *ad libitum* during the weekend (Fenrich et al., 2015).

To address many of these challenges that introduce variability into the data, several research groups have developed an automated version of the SPRT. In a study by Torres-Espin et al., (2018), researchers found that the use of a motorized delivery arm to present millet seeds at a fixed position to rodents (without experimenter interference) resulted in a reduction in the variability in success rate between and within experiments compared to that observed when millet seeds were manually presented by experimenters. Other automated reaching tasks allow for reduced experimenter interaction by enabling animals to self-initiate trials through the activation of a sensor in the reaching chamber (Wong et al., 2015; Ellens et al., 2016). This paradigm can also allow multiple animals to be trained simultaneously, leading to an increase in sample size. All these different paradigms have alleviated several challenges of the manual SPRT. But various limitations, such as the stress induced by animal handling, social isolation, and circadian rhythm disruption, continue to persist. To address these remaining limitations, the Silasi lab has developed the Home-cage Automated Skilled Reaching Apparatus, HASRA (Salameh et al., 2020).

1.4.3 Home-cage Automated Skilled Reaching Apparatus

The HASRA is a newly designed task, adapted from the SPRT, that can be used to assess upper limb motor function in mice following stroke (Salameh et al., 2020). In the HASRA, mice are

group-housed in their home-cage; this is unlike the manual SPRT and the automated skilled reaching paradigms described in the previous section **1.4.2**. When an animal is interested in interacting with the reaching task, they can enter the reaching tunnel of the apparatus from their home-cage environment and initiate the task themselves by activating a sensor in the tunnel (Fig. 3; more information is provided in section **3.3**). Similarly to the SPRT, mice reach through a slot at the front of the HASRA's reaching tunnel to grasp and retrieve a millet seed presented at a fixed position on a motorized delivery arm. Once the mouse's preferred limb is determined, the motorized delivery arm will present millet seeds more laterally in either the left or right position, depending on which limb is preferred. This is done so that animals can retrieve the seed only using their preferred limb. Since the HASRA task is completely automated and requires little experimenter interference, a reduction in inter-experimenter variability and animal stress levels should be observed. Moreover, due to the mice's ability to self-initiate the task in the HASRA, mice can interact with the task at any time of the day without disrupting their circadian rhythm, including during the dark-cycle when they are typically most active. Overall, through using the HASRA, many of the challenges and limitations experienced with the manual SPRT are overcome. It has been demonstrated that the HASRA can be used to efficiently train mice on the skilled reaching task and is sensitive to measuring motor impairments acutely following photothrombotic stroke (Salameh et al., 2020). In this study, we will use the HASRA to further assess long-term motor impairments and recovery post-stroke in mice. More information on the materials and methodology of the HASRA is available in section **3.3**.

1.5 Factors Impacting Motor Assessment and Rehabilitation in Rodents

1.5.1 Behavioural Training in Skilled Reaching Tasks

As touched upon in previous sections, many variables can influence rodents' performance at a skilled reaching task, such as differences in how experimenters train animals (Fouad et al., 2013). These differences can include the day of the week, the time of day, and even the time of year that animals are trained (Fenrich et al., 2015; Dauchy et al., 2010; O'Bryant et al., 2011). Experimenter-related variability aside, differences in the rate of motor learning and task acquisition among rodents can introduce variability in the overall performance during the training period and following stroke (O'Bryant et al., 2011; Fouad et al., 2013). The typical motor learning curve for skilled reaching tasks consists of two main phases: an initial acquisition phase where animals' performance at the task progressively improves, and a consolidation phase near the end of the training period where the animals' performance has plateaued (Chen et al., 2014). The learning curves of individual mice can vary as different mice may take a different number of days to reach the consolidation phase; furthermore, some animals' performance during the training period can be more variable day-to-day compared to others (Chen et al., 2014). Due to these differences in the rate of motor learning, by the end of the training period and at the timepoint for stroke induction, different animals may be at different phases of motor learning and thereby be differently impacted by a stroke targeted at the forelimb primary motor area. In this example, other brain regions, such as the striatum, may be involved in the storage and execution of the learned motor skills in animals that have reached the consolidation phase prior to stroke induction (Hwang et al., 2019; Kawai et al., 2015; Wolff et al., 2022). These animals may not be as impacted by damage to the primary motor area as animals that have not yet reached the consolidation phase of learning. As a result, variability in these animals' performance post-stroke and in their level of impairment and recovery may be observed.

1.5.2 Stroke Size and Location

In preclinical experiments using rodent models of ischemic stroke, animals are often sacrificed at the experimental endpoint so that the animals' brains can be extracted and sectioned coronally for subsequent lesion volume calculation. Stroke damage can be visualized using a histological stain such as hematoxylin eosin (H&E) or Cresyl violet which allows for the detection of infarcted brain tissue (Sommer, 2016). To determine the size of the stroke, these areas of damage in coronal brain sections can be manually delineated using *NIH ImageJ* (Schneider et al., 2012), and the sum of the sectional infarct areas are multiplied by the interval thickness to calculate lesion volume (Sommer, 2016). Stroke size has been shown to be correlated with severity of impairments both preclinically and clinically (Rogers et al., 1997; Brott et al., 1989). Unlike lesion volume measurements which are routinely calculated in preclinical stroke studies in rodents, precise lesion location determination is often neglected. This is an issue as the relationship between stroke location and motor impairment cannot be explored, which may limit the translatability of preclinical stroke models. In clinical studies, however, lesion location has been shown to be correlated with motor and cognitive impairments following ischemic strokes (Shelton & Reding, 2001; Liepert et al., 2005; Ernst et al., 2018; Zhao et al., 2018).

There are various limitations that can limit one's ability to precisely delineate lesion location, such as the great amount of time and expertise lesion localization would require. The standard method for the quantification of features in 2D histological samples is through stereological analysis which requires the use of an expert in the field for the delineation of different anatomical features (Schmitz and Hof, 2005). This method is difficult to apply due to the shortage of anatomical expertise and the time-consuming nature of manual analysis. Recently, a semi-automated workflow has been developed for the quantification and spatial analysis of histological features from 2D images (Puchades et al., 2019; Yates et al., 2019). This

workflow uses four open-source software (*QuickNII, VisuAlign, Ilastik,* and *Nutil*) which allow for the registration of coronal and sagittal histological sections to the Allen Mouse Brain Atlas (AMBA), and the subsequent quantification of histological features of interest (Puchades et al., 2019; Yates et al., 2019; Bjerke et al., 2021). This workflow and its associated software have been successfully utilized and adapted to explore various research questions, such as the expression of calcium-binding proteins (parvalbumin and calbindin) involved in spatial navigation and memory (Bjerke et al., 2021), the role of layer 6 corticothalamic neurons in primary somatosensory cortex (Whilden et al., 2021), and the localization of microemboli in the rodent brain (McDonald et al., 2021). Thus, adaptation of this workflow to preclinical rodent lesion studies can enable us to investigate the relationship between lesion location and upper limb motor performance. More information on the QUINT workflow is available in section **3.8**.

1.6 Study Rationale

In summary, it is evident that there are a few persisting obstacles in the assessment of stroke impairment and recovery in preclinical rodent studies. For example, although tasks like the SPRT are considered the "gold standard" for the assessment of post-stroke upper limb impairments, the manual nature of the task introduces various challenges. These challenges include inter-experimenter variability due to differences in training methodology between different experimenters. Additionally, since the SPRT is laborious, only a limited number of animals can be trained at a time, thereby limiting experimental sample sizes. Another major obstacle in the preclinical stroke field is the precise delineation of lesion location, which is difficult to accomplish with standard stereological analysis as it is time-consuming and requires a high level of anatomical expertise. This obstacle limits the translatability of preclinical studies

since stroke location has been demonstrated to be a significant predictor of impairment in the clinical population.

To overcome these obstacles, my thesis will use the HASRA for the training and longitudinal assessment of upper limb impairments and recovery following photothrombotic ischemic stroke in mice. Additionally, we will investigate the adaptation of the QUINT workflow for lesion localization. These approaches will allow us to obtain a fuller picture of the different factors at play that may be impacting forelimb motor function post-stroke.

2. HYPOTHESIS & OBJECTIVES

Hypothesis

Metrics of reaching behaviour in the HASRA and of lesion location may be used as predictors of post-stroke forelimb motor impairment and recovery in mice.

Objectives

1. Characterize the time course of post-stroke motor impairment and recovery in mice using the HASRA.
2. Identify behavioural and lesion-related parameters that correlate with endpoint forelimb performance.

3. MATERIALS & METHODS

3.1 Animals and Experimental Design

All animal care and research procedures were carried out in accordance with the University of Ottawa's animal care committee's regulations. This study used 57 Thy1-ChR2-YFP mice (The Jackson Laboratory, stock #007612, 35 females, 22 males) between the ages of 36 and 136 days at the start of the experiment. Mice were group-housed in groups of 4 to 5 mice per cage, amounting to a total of 12 cages used.

To prepare animals for placement in the home-cage of the HASRA, a unique radio frequency identification (RFID) tag (Sparkfun, SEN-09416) was subcutaneously implanted between the scapula while animals were under 4% isoflurane anesthesia in room air (Salameh et al., 2020). These RFID tags allow for the identification of each individual mouse interacting with the skilled reaching task in the HASRA. Two days after RFID tag implantation, millet seeds were sprinkled within the mice's cages for three days to habituate them to the novel food (Fig. 1). RFID tag implantation and millet seed habituation were separated by two days so that the mice do not associate the implantation procedure with receiving millet seeds.

Following millet seed habituation, mice were then transferred to a new home-cage in the HASRA and were allowed to start their training period which ranged from 13 to 20 days (Fig. 1). In the HASRA, mice were food restricted to 1g of lab chow per mouse per day to ensure they maintained at least 80% of their baseline weight. Mice were able to supplement their restricted diet *ad libitum* by successfully obtaining seeds through the reaching task in the HASRA. Water was also accessible *ad libitum*. At the start of the training period, a seed was presented on the pedestal positioned 0.4 cm from the front slot. Once mice were able to obtain these pellets by

licking, the pedestal was gradually moved further back to encourage reaching behaviour. Early in the training phase, each mouse's preferred hand was determined by identifying the hand that was used in more than 50% of reaching trials. Once the preferred hand was determined, the presenting pedestal was moved laterally so that each mouse could only use their preferred limb to retrieve a seed. More information on how the pedestal position was changed and customized for each mouse is provided in section **3.2**. At the end of the training period, on day 0, mice that acquired the task were removed from the home-cage to receive a photothrombotic stroke or sham surgery (Fig. 1). Shortly after mice recovered from surgery, they were returned to their corresponding home-cages and allowed to continue engaging with the HASRA task for 29 days.

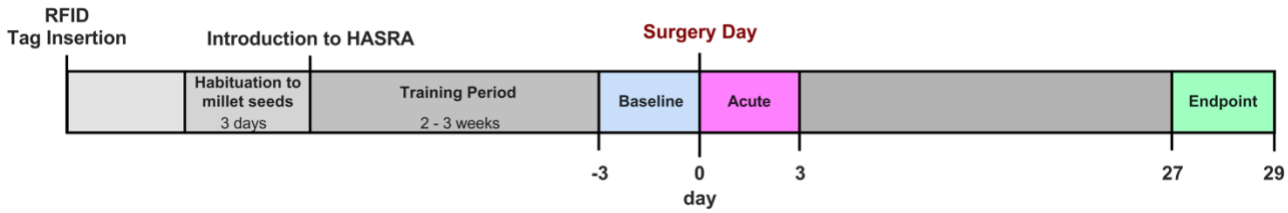

Figure 1. Experimental timeline. Full timeline of preparation and training in the HASRA. Time periods of interest (baseline, acute, and endpoint period) are indicated on the timeline and are represented relative to surgery day (day zero).

From the 57 mice used in this experiment, the final sample size was n = 32 (sham: n = 16 [n = 11 females and n = 5 males] and stroke: n = 16 [n = 10 females and n = 6 males]; Table 2). This is because animals that were either not able to engage in reaching behaviour to obtain a millet seed (n = 16) or were not able to achieve a 15% success rate at the reaching task by the last three days of the training period (n = 5) were excluded from the study. These excluded animals did not undergo surgery (n = 21). In addition, following post-mortem analysis of brain sections belonging to stroke animals, four stroke animals were excluded from our analysis due to tissue damage during sectioning (n = 2) and an absence of stroke damage (n = 2).

Table 2. Number of experimental animals.

Experimental Timepoint	Initial Sample Sizes	Number of Excluded Animals	Reason for Exclusion
Start of Training Period	57	16	Unable to engage in reaching behaviour
End of Training Period	41	5	Unable to achieve a 15% success rate
Post-mortem	36	4	No stroke present (n=2), Not quantifiable lesions (n=2)
Final Sample Size: Sham: n=16, Stroke: n=16			

3.2 Photothrombotic stroke and sham surgeries

To prepare mice for the photothrombotic stroke procedure, mice were anaesthetized using 4-5% isoflurane, secured in a stereotaxic frame, and an incision was made along the midline of the scalp to expose the skull (Salameh et al., 2020). Next, 100 mg/kg Rose Bengal, a photosensitive dye, diluted in PBS was injected intraperitoneally and allowed to circulate systemically for two minutes for the dye to travel through the brain vasculature (Fig. 2). A green laser (532 nm, 1.5 mm in diameter, 20 mW power) was positioned 5 cm above the surface of the skull and directed at the forelimb motor cortical area (1 mm anterior and ± 1.5 mm lateral to bregma) on the hemisphere contralateral to each animal's preferred hand for 13 minutes (Fig. 2). When the Rose Bengal dye was activated by the green laser, single oxygen species are produced, damaging the endothelial cells of the vessels, and inducing a blood clotting cascade to form thrombosis (Talley et al., 2015). For sham animals, the order of events was reversed to expose them to the same procedure without inducing any lesions. First, they were exposed to the green laser and then received a Rose Bengal injection after the laser was turned off. Once the procedure was complete, the scalp was sutured and bupivacaine, a topical analgesic, was applied on the incision

site. Mice were allowed to regain mobility prior to being returned to their home-cage on the same day. Stroke and sham surgeries did not result in any mortality.

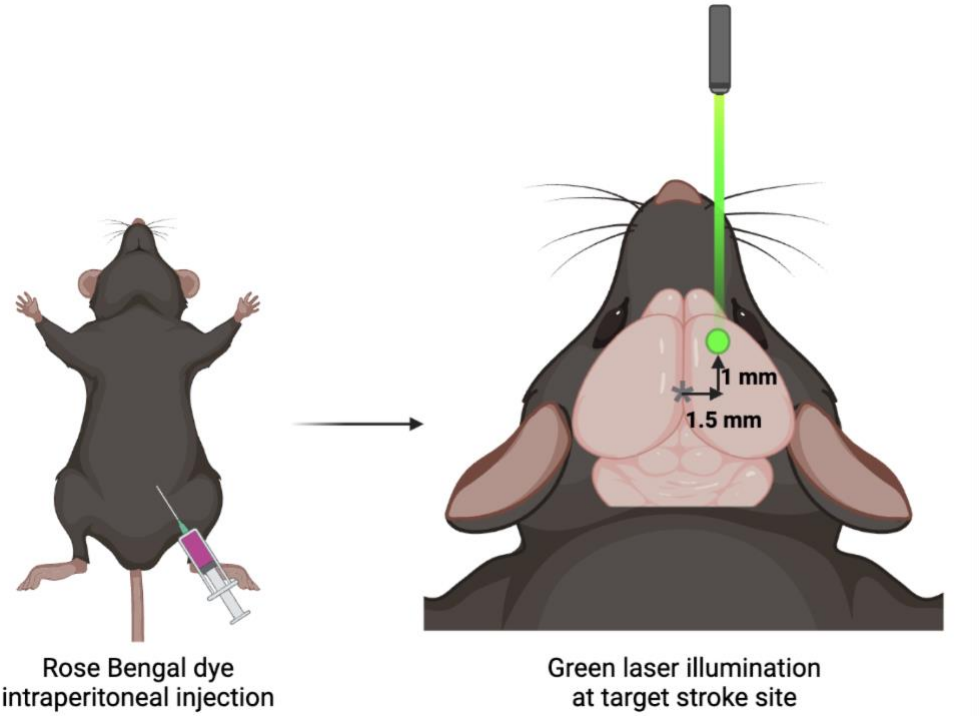

Figure 2. Photothrombotic stroke procedure. Following Rose Bengal injection, a green laser (green circle, 532 nm) stereotaxically positioned 1 mm anterior and 1.5 mm lateral to bregma (*) activated the photosensitive dye to induce stroke.

3.3 HASRA

Mice were placed in the HASRA to train them on the skilled reaching task, and to assess forelimb motor function prior to and following stroke (Salameh et al., 2020). The HASRA was composed of a reaching tunnel that was connected to the home-cage containing the group-housed animals (Fig. 3A). This tunnel had an RFID reader placed on top and an infrared (IR) beam breaker in a mounting bracket placed on its sides (Fig. 3A, B). When a mouse entered the reaching tunnel, the IR beam was broken, and the mouse's unique RFID tag was read by the

RFID reader. When these two events occurred, a reaching session was started by moving the seed hopper (containing the millet seeds) into the correct position through the activation of the left/right and front/back stepper motors (Pololu, 1205) (Fig. 3A).

Next, a servo motor (Hitec, HS-82MG), mounted on the backside of the seed hopper, was activated to enable the motorized pedestal to present a seed (Fig. 3A, B). This servo motor controls both the speed and height of the presenting pedestal (Salameh et al., 2020). An Arduino Nano (Arduino, 7630049200173) was used to control these motors. Most components of the HASRA were 3D printed using a fused deposition modeling printer (FlashForge 3D printer, Creator Pro) (Salameh et al., 2020). Two pedestal presentation modes were used in this study: 1) continuous 5-s cycling (n = 10) and 2) stationary presentation (n = 22). The 5-s cyclical presentation mode involved presenting a seed to the mouse for 5 seconds, after which the pedestal would descend into the hopper and present again. In contrast, in the stationary presentation mode, the pedestal would present a seed and remain ascended until the seed was no longer detected on the pedestal. Real-time pellet seed detection was achieved through a custom Python script that used the intensity value of a region of interest within the presenting pedestal to determine if a seed was located on the pedestal. The presence of a lightly colored seed increased image intensity values beyond a pre-set threshold, thus indicating the presence of a seed. When a seed was not being presented on the pedestal (empty presentation), the light intensity within the region of interest decreased below the pre-set threshold and the pedestal descended into the seed hopper to retrieve a seed.

All the animals' interactions with the presented seeds were recorded using either a video camera (ELP, USBFHD08S-LC1100) facing the reaching slot (n = 20; Fig. 3B) or a Raspberry Pi Camera V2 (insert RRID and megapixels here) placed overhead the reaching slot (n = 12; Fig.

3A). Both cameras recorded videos at 60 frames per second (fps) and video acquisition was automatically started upon the recognition of a mouse's RFID tag by the RFID tag reader. To enable recording during the dark cycle, two IR light sources (HonYan, 191094177157) were placed at each edge of the hopper (Fig. 3B).

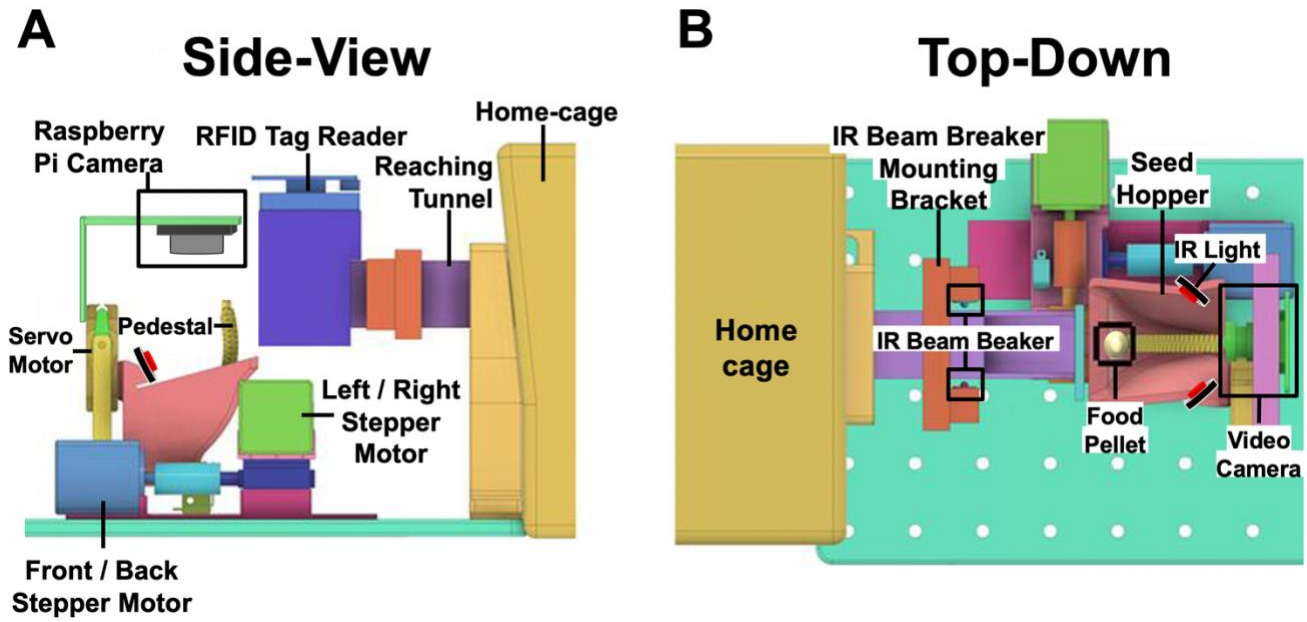

Figure 3. Labelled HASRA diagram. (A) Side-view of the HASRA with the following components labelled: Overhead Raspberry Pi Camera V2, servo motor, left / right and front / back stepper motors, pedestal, RFID tag reader, and reaching tunnel. (B) Top-down view of the HASRA with the following components labelled: Video camera facing the reaching slot, IR light, seed hopper, IR beam breaker, and IR beam breaker mounting bracket. Modified from Salameh et al., 2020.

Each animal in the home-cage had their own individual, custom text file which was accessible by the main Python script responsible for running the task (Fig. 4). This text file contained each mouse's unique RFID tag, number within the home-cage (each mouse was numbered using an ear notch system), position of the pedestal in the x (left / right), y (height), and z (front / back) dimensions, total number of entries, and the full path of the text file (Fig. 4A). The pedestal's position in the x, y, and z dimensions was represented on an ordinal scale with values ranging from zero to ten (Fig. 4B). For the x dimension, a value of zero

corresponded with the right-most position and a value of ten corresponded with the left-most pedestal position (Fig. 4B*i*). For the y dimension, zero corresponded with the highest height and ten corresponded with the lowest height of the pedestal (Fig. 4B*ii*). Lastly, for the z dimension, zero corresponded with the front-most and ten corresponded with the back-most pedestal position (Fig. 4B*iii*). Changes in values for the x and z dimensions resulted in a change in the number of "steps" and the direction of "steps" taken by the corresponding left / right and front / back stepper motors. While a change in value for the y dimension resulted in a change in "steps" taken by the servo motor. These changes in the z dimension allowed the pedestal to be moved farther back from each mouse to encourage reaching behaviour, and changes in the x dimension allowed for the lateral presentation of a seed on the pedestal to accommodate each mouse's preferred hand. Overall, by making custom changes to the pedestal's left / right and front / back positions in the text file, we were able to individualize each mouse's training and enable food pellet delivery in accordance with each mouse's hand preference.

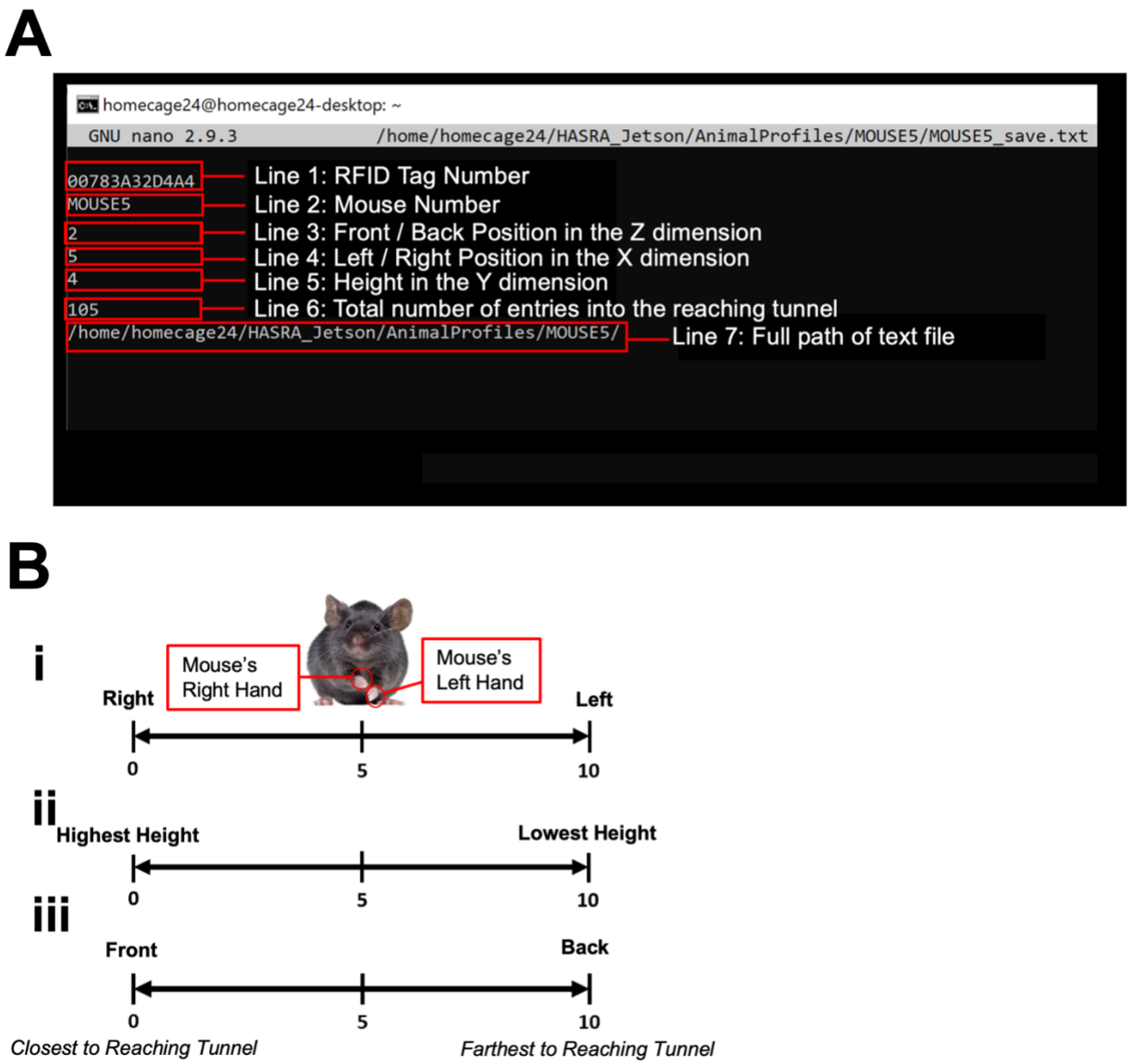

Figure 4. Mouse text file. (A) Labelled image of a mouse's text file. (B) Ordinal scales for the (i) x, (ii) y, and (iii) z dimensions.

3.4 Scoring HASRA Videos

Videos were manually scored in chronological order starting with the earliest video at 12:00 am. Scoring was performed every other day apart from certain time periods of interest (baseline, acute period, and endpoint period) during which videos were scored daily. The baseline period

consisted of the last three days of the training period (days –3 to –1 relative to surgery day), the acute period represented days 1 to 3 following surgery day, and the endpoint period represented days 27 to 29 relative to surgery day which were the last three days of our experimental timeline (Fig. 1). For each day of scoring, 20 trials of events were scored. There were four categories of events observed: “lick”, “miss”, “knock-down”, and “success” (Fig. 5). A “lick” was identified as pellet retrieval using the tongue and not the forelimbs (Fig. 5A). A “miss” was a reach where the forelimb did not disrupt the position of the pellet (Fig. 5B). A “knock-down” was defined as a reach that displaced the pellet from its position on the pedestal but did not successfully retrieve it (Fig. 5C). A “success” was defined as a reach where the pellet was grasped, retrieved, and consumed by the mouse (Fig. 5D). A trial was defined as an event where the pellet was displaced by a “lick”, “knock-down”, or “success”. A “lick” was only scored if one or more “miss” events were observed prior to the “lick”.

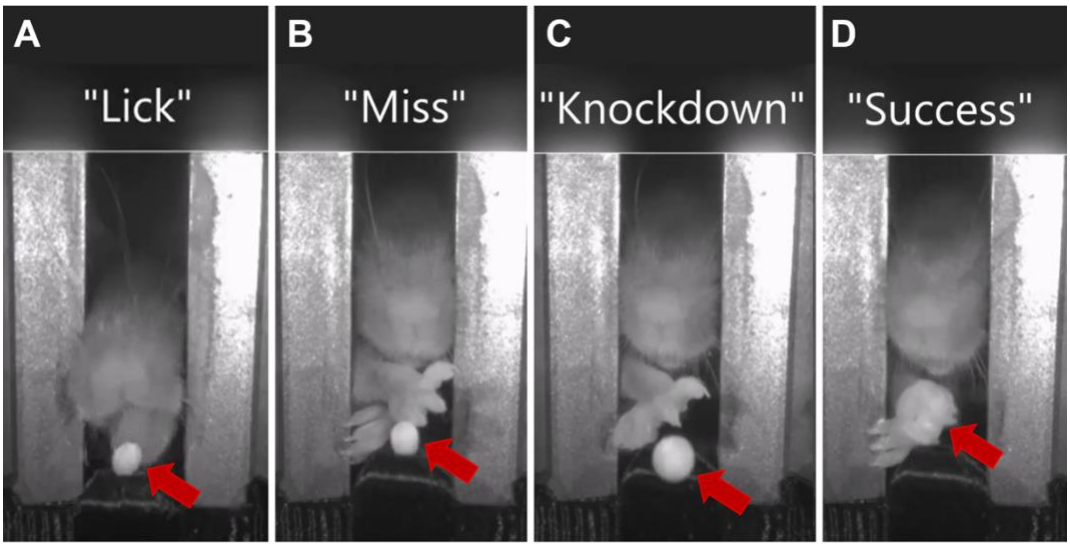

Figure 5. HASRA events. Events were categorized as (A) “Lick”, (B) “Miss”, (C) “Knockdown”, and “Success”. The red arrow points to the food pellet.

3.5 Assessing performance and engagement at the HASRA task

To assess the animals' performance at the task, different measures of success rate were calculated, such as 1) success rate by reaching events = $\frac{\text{Success}}{(\text{Miss} + \text{Knockdown} + \text{Success})} \times 100\%$, 2) trial success rate = % of successful trials, and 3) first reach success rate = % of trials where a successful reach was completed on the first attempt. The success rate by reaching events metric was used as our primary metric of performance and is referred to in this thesis simply as 'success rate'. To investigate each animals' engagement with the task, we extracted the number entries into the reaching tunnel and the time spent in the reaching tunnel (minutes) from our task's python script which recorded the time and date at which each animal entered and exited the reaching tunnel. To explore changes in the animals' performance and engagement with the reaching task following surgery, a recovery metric was obtained for our performance (success rate) and task engagement (number of entries into the reaching tunnel and time spent in the reaching tunnel) parameters by calculating the difference of these parameters between the endpoint and acute time periods. Performance and engagement parameters at time periods of interest were used to explore changes in behaviour acutely and long-term following stroke compared to pre-stroke.

3.6 Quantification of lesion volume

Following the completion of behavioural testing, mice were euthanized with euthanyl (1 mL/g) and transcardially perfused (3.8 mL/min) with phosphate buffered saline (pH 7.4) followed by 4% paraformaldehyde. Brains were extracted, photographed dorsally, sectioned coronally on a vibratome at 100 mm thickness, and stained with Cresyl violet. Slides were scanned using a

flatbed slide scanner (Canon 900F MKII) at a resolution of 1200 dpi. The location of stroke damage was identified using the Anterior-Posterior (AP) coordinate system relative to bregma (AP 0.0). *NIH ImageJ* (Schneider et al., 2012) was used to determine the area of damaged stroke tissue with total infarct volume calculated using the following equation:

Σ (area of damage on each section) × tissue volume between each section (100 μm^3). The most anterior coordinate of damage, the most posterior coordinate of damage, and the greatest damage coordinate (AP coordinate with greatest infarct area) relative to bregma were obtained from the data.

3.7 Qualitative identification of dorsal lesion location

Using dorsal images of the mouse brains, we were able to outline the area of stroke damage and align this mask to a dorsal mouse brain atlas with delineated functional regions (Watson et al., 2012). To perform this alignment, we obtained the range of AP coordinates relative to bregma that contained lesion damage from our Cresyl violet stained coronal sections since bregma was not identifiable in our dorsal images. We were then able to find the range of mediolateral (ML) coordinates containing damage by calculating the distances between the midline and the edges of the outlined dorsal area of damage using *NIH ImageJ* (Schneider et al., 2012). Using the identified ranges of AP and ML coordinates damaged, we were able to align our masks to a dorsal template of the AMBA.

3.8 Semi-automated lesion localization workflow

Open-source software from the semi-automated QUINT workflow was used to quantify the amount of lesion damage in various anatomical regions. Our Cresyl violet stained coronal serial sections with the lesion overlaid were registered to the AMBA using *QuickNII* v2.2 (RRID:SCR_016854; Puchades et al., 2019; Fig. 6 A-B). *QuickNII* is a three-dimensional brain atlasing tool that allows for the generation of atlas maps that are customised to match each section (Puchades et al., 2019). To accomplish this, our coronal section images were superimposed to the AMBA, and the correct alignment was determined using visual landmarks such as the corpus callosum, anterior commissure, lateral ventricles, Ammon's horn, and the dentate gyrus. This alignment process is termed "anchoring". During "anchoring", the reference atlas could be rotated, stretched, compressed, and its cutting angle could be adjusted to match our section images (Puchades et al., 2019; Yates et al., 2019).

The registered custom maps from *QuickNII* are then opened in *VisuAlign* v0.8 (RRID: SCR_017978; Blixhavn et al., 2023; Bjerke et al., 2021). Using *VisuAlign,* we further refined our registration by performing non-linear transformations to compensate for any brain deformations. Refinements were first made by fitting the atlas template to the contour of the section and then proceeding inwards to refine the alignment to the aforementioned visual landmarks (Fig. 6 C). Once the non-linear refinements were completed, the registration results were stored in JSON format and images of the refined atlas maps were exported in PNG format.

Prior to quantification of damage in each region, we also needed to obtain segmentation images of the lesion damage in each section. Using *NIH ImageJ* (Schneider et al., 2012), segmentation images were created using a simple macro that produced a binary image of the lesion in black and all other features in white by changing the image's brightness and contrast

(Fig. 6 D). This transformation was applied to all sections through *NIH ImageJ*'s batch processing feature. Additionally, *NIH ImageJ* was used to create lateralization masks for each section. To create the mask, a white polygon shape was used to cover the hemisphere containing the lesion and a black polygon shape was used to cover the other hemisphere (Fig. 6 D). These masks are critical so that only the hemisphere with lesion damage is taken into consideration during the quantification of damage in the anatomical regions affected. Lastly, the *Nutil* software (RRID: SCR_017183; Puchades et al., 2019) used the refined atlas maps, segmentation images, and lateralization masks to provide us with the percentage of lesion damage in select anatomical regions (primary motor cortex [M1], secondary motor cortex [M2], forelimb primary somatosensory cortex [S1FL], hindlimb primary somatosensory cortex [S1HL], dorsal anterior cingulate area [dACC], ventral anterior cingulate area [vACC], and the corpus callosum; Fig. 6 E).

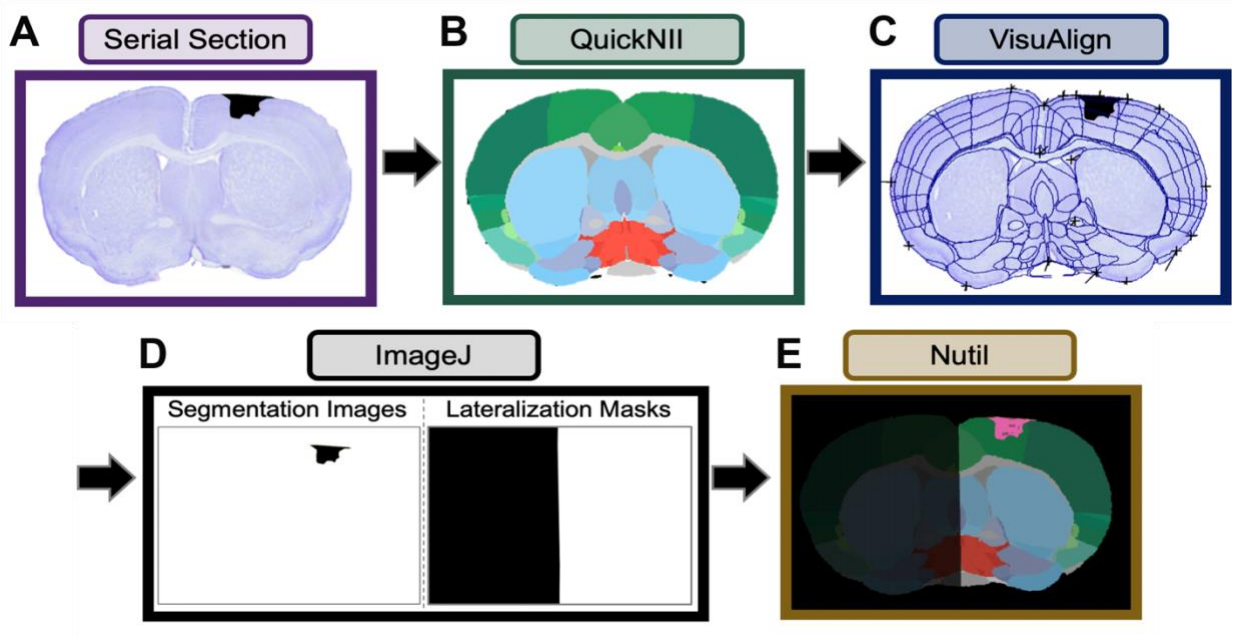

Figure 6. Workflow for lesion localization quantification. (A) Coronal serial section with the outlined lesion overlaid. (B) Sections were aligned to the AMB using the *QuickNII* software. (C) Non-linear transformations were achieved using the *VisuAlign* software. (D) *NIH ImageJ* was

used to create segmentation images and lateralization masks. (E) Lesion damage in each region was quantified using the *Nutil* software.

3.9 Statistical analysis

All behavioural, histological, and lesion localization data were expressed as mean ± standard error of the mean (SEM). Statistical analyses were performed using SPSS Statistics software (v27; IBM Corp., Armonk, USA) and all figures were created using GraphPad Prism (v9.4.1; San Diego, CA, USA).

A multiple imputation approach was used to impute missing data values for behavioural parameters (success rate, number of entries into the reaching tunnel, time spent in the reaching tunnel, and number of reaches during pellet presentation) on all scored days due to technical issues with the device. There was a total of 4.875% of values missing. In this approach, five imputations with ten iterations using a linear regression model were performed. An average was taken across the five imputations to impute the missing values. Prior to performing the multiple imputation approach, the Little's Missing Completely at Random (MCAR) statistical test was performed to determine if our missing data was missing in a random or non-random pattern. The Little's MCAR test showed that the missing values were missing randomly and that there was no systematic bias in the data ($X^2(1317) = 89.00$, $p = 1.00$) which allowed us to then perform the multiple imputation approach.

One-way repeated measures (RM) ANOVA analysis was used to investigate within-subject factors (success rate, number of entries into the reaching tunnel, time spent in the reaching tunnel, recovery of these performance and engagement parameters, and number of reaches during pellet presentation). Two-way RM ANOVA analysis was used to compare

between-subject factors (percentage of an anatomical region damaged by the lesion in total and at each cortical layer, stroke group versus sham group, and high residual success group versus low residual success group). Bonferroni-corrected t-tests were used for post-hoc analysis with an $\alpha = 0.05$ for statistical significance. Furthermore, independent samples t-tests for sham versus stroke and high versus low endpoint success groups were performed to identify significant differences between these groups' task performance and engagement at all scored timepoints.

Pearson bivariate correlations were used to investigate correlations 1) among behavioural parameters at time periods of interest and 2) between percentage of damage of an anatomical region and behavioural parameters at time periods of interest for all stroke animals. Forward step-wise binary logistic regression procedures were performed to identify behavioural and lesion location predictors of success rate at the endpoint period among stroke animals in the high and low endpoint success groups.

4. RESULTS

4.1 Sham and stroke animals behave similarly during the training period

Mice were placed in the HASRA and underwent a shaping period followed by a training period. The purpose of the shaping was to promote interaction with the pellet presentation device in the HASRA. During this shaping period, seeds were presented at the closest distance to the front slot to allow mice to obtain a seed by licking or grabbing with the mouth. Once mice were engaged with the task, seeds were presented at a progressively farther distance until they could no longer be retrieved by licking, forcing mice to reach with their forelimbs. Once animals started reaching for the presented seeds, this marked the start of the reaching phase of the training period. The animals' performance and engagement with the task during the training period are displayed in **Figure 7**.

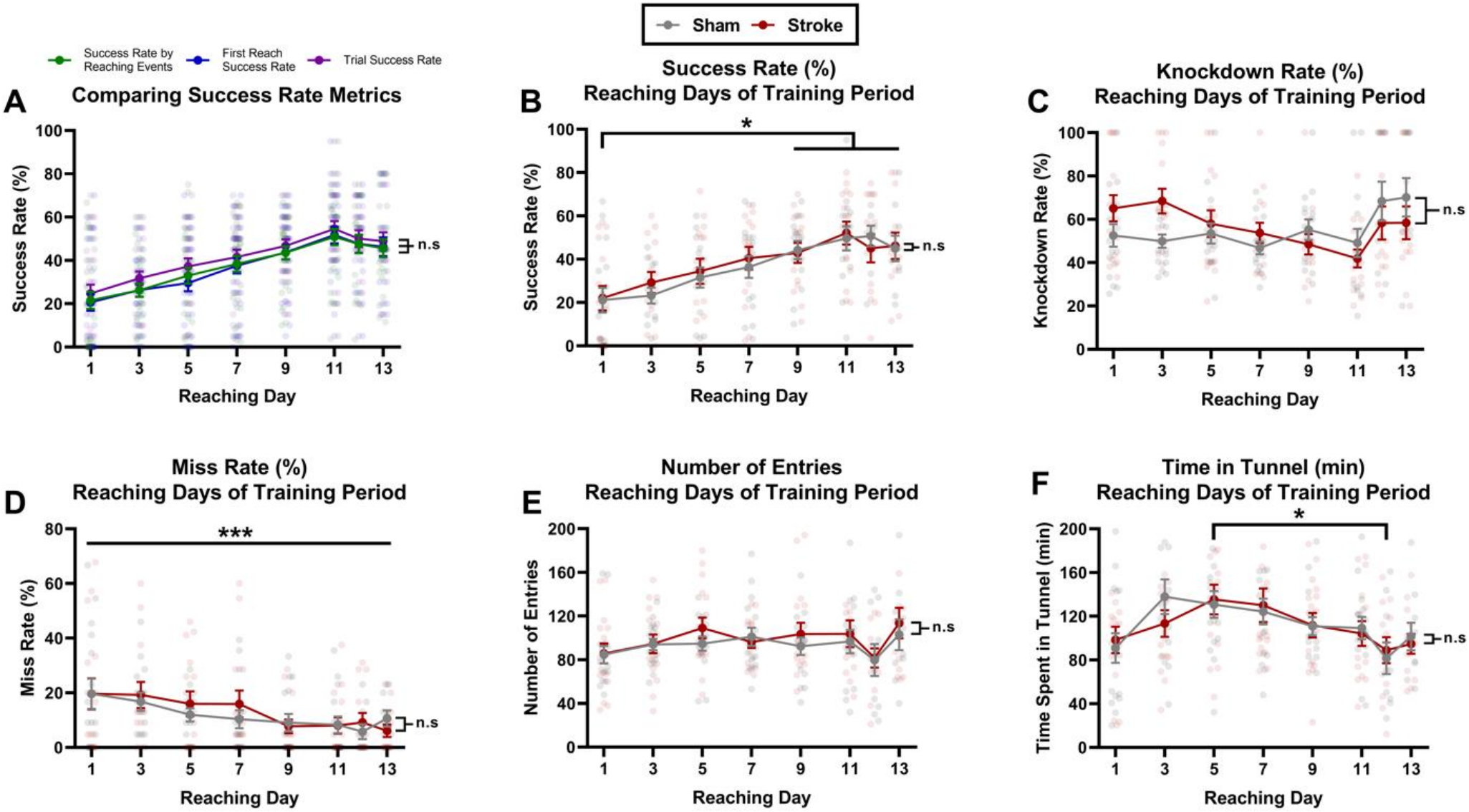

Figure 7. Sham (n = 16) and stroke (n = 16) mice had a similar performance and engagement with the HASRA task during the reaching days of the training period. (A) Comparing different success rate calculations among all mice (n = 32): Success rate by reaching events (green), first reach success rate (blue), and trial success rate (purple). (B – F) Compares sham (gray) and stroke (red) mouse groups. (B) Success rate, (C) miss rate, (D) knockdown rate, (E) number of entries, and (F) time spent in reaching tunnel (minutes) were compared between sham and stroke. All data was presented as mean ± SEM. Individual data points were displayed as translucent coloured dots. * depicts significance of $p < 0.05$. *** depicts significance of $p < 0.001$.

To determine the most appropriate metric of the animals' performance at the reaching task, various success rate calculations were compared among all mice (n = 32): success rate by reaching events, first reach success rate, and trial success rate (**Fig. 7 A**). A mixed-effects model (REML) demonstrated that there were no statistically significant differences among the three success rate calculations during the training period ($F_{(2, 93)} = 0.7368$, $p = 0.4814$; **Fig. 7 A**). We decided to use the success rate by reaching events calculation, simply referred to as 'success rate' throughout the remainder of this thesis, as our primary metric for task performance since it takes into consideration all the different reaching events that each mouse performs (knockdown, miss, and success).

Throughout the training period, we did not observe any significant differences between sham and stroke animals' mean success rate (sham: 37.95 ± 2.93%, stroke: 38.41 ± 4.29%; $F_{(1, 30)} = 0.007266$, $p = 0.9326$; **Fig. 7 B**), knockdown rate (sham: 55.96 ± 2.57%, stroke: 56.30 ± 3.34%; $F_{(1, 30)} = 0.005781$, $p = 0.9399$; **Fig. 7 C**), or miss rate (sham: 11.04 ± 2.11%, stroke: 12.82 ± 2.88%; $F_{(1, 30)} = 0.2247$, $p = 0.6389$; **Fig. 7 D**) as demonstrated by mixed-effects models (REML) analyses. These findings suggest that both groups of animals had similar performance at the reaching task during the training period.

We were also interested in investigating differences within the sham and stroke groups and found a main effect of time (day of training period) on success rate ($F_{(4.695, 122.7)} = 16.85$, $p < 0.0001$, mixed-effects model (REML); **Fig. 7 B**). Tukey's post-hoc tests showed that both groups had a statistically significant increase in success rate near the end of the training period, reaching days 9 to 13, compared to the start, day 1 ($p < 0.05$; **Fig. 7 B**). Mice in the sham and stroke groups had a mean increase in success rate of 23.66% and 24.01%, respectively, from day 1 to days 9 and 13. Interestingly, an opposite trend was observed in the miss rates of sham and stroke

mice, as there was a significant, progressive decrease in the percentage of missed reaches as the training period went on ($F_{(3.488, 90.70)} = 5.960$, $p = 0.0005$, mixed-effects model (REML); **Fig. 7 D**). The steady increase in success rates coupled with the decline in miss rates as the training period progresses indicates that over time, animals were able to learn, acquire, and become more skilled at successfully retrieving the presented millet seeds through optimization of their reaching strategies.

In addition to performance, we also investigated the animals' engagement with the reaching task in the HASRA through two metrics: the number of entries into the reaching tunnel and the amount of time spent in the reaching tunnel (min). Similar to their performance metrics, both groups appeared to have similar task engagement as there were no statistically significant differences between the sham and stroke groups' number of entries ($F_{(1, 30)} = 0.4230$, $p = 0.5204$; **Fig. 7 E**) and time in the reaching tunnel ($F_{(1, 30)} = 0.1715$, $p = 0.6817$; **Fig. 7 F**) during the training period. When investigating within-group differences, we did not observe any significant differences in the number of entries into the reaching tunnel ($F_{(3.272, 88.34)} = 2.410$, $p = 0.0670$; **Fig. 7 E)**. Although we did find a significant interaction between the reaching day and the time spent in the reaching tunnel per day ($F_{(3.514, 94.89)} = 4.968$, $p = 0.0018$; **Fig. 7 F**). Post-hoc analysis with a Tukey adjustment showed that both groups had a statistically significant decrease in the time spent in the tunnel on day 12 compared to day 5 of the training period ($p < 0.05$; **Fig. 7 F**). This finding suggests that, near the end of the training period, as animals become more skilled at the reaching task, they may not require as much time engaging with the task to achieve success as they did at the beginning.

Overall, mice in the sham and stroke groups had similar task performance and engagement throughout the training period. All mice demonstrated acquisition of the task and

optimization of their reaching skills, as demonstrated by their progressively increasing success rate and decreasing miss rate during the training period.

4.2 Postoperative Outcomes

4.2.1 Stroke animals are persistently impaired postoperatively compared to baseline

Following sham and stroke surgeries, metrics of performance and engagement were investigated on all scored days of the baseline and postoperative period (presented relative to surgery day – day zero) and at our time periods of interest (baseline, acute, and endpoint) to assess animals' impairment and recovery following surgery. When comparing sham and stroke mice's success rates at baseline and post-surgery days, a two-way repeated measures ANOVA showed that there is a significant interaction between the surgery group and day relative to surgery ($F_{(19, 570)}$ = 1.919, p = 0.0110) and time periods of interest ($F_{(2, 60)}$ = 5.135, p =0.0087). Shortly after surgery, stroke mice had significantly lower mean success rates than sham animals on days 1 (sham: 46.24 ± 4.88%, stroke: 20.63 ± 5.30%; p = 0.0254, Sidak's post-hoc test) and 5 (sham: 47.81 ± 6.22%, stroke: 19.318 ± 5.17%; p = 0.0282, Sidak's test) relative to surgery day (**Fig. 8 A**). Similarly, this significant reduction in success rate was observed at the acute period in the stroke group (sham: 46.145 ± 4.021%, stroke: 22.80 ± 5.16%; p = 0.0035, Sidak's test; **Fig. 8 B**).

In addition to differences in performance between the sham and stroke groups, we also investigated differences within these groups over time. Using a two-way RM ANOVA, we identified a main effect of day relative to surgery ($F_{(9.286, 278.6)}$ = 3.314, p = 0.0006) and time periods of interest ($F_{(1.989, 59.67)}$ = 9.232, p = 0.0003) on success rate. Most interestingly, we found that the stroke group's mean success rate decreased by 24.98% and 19.21% at the acute and endpoint periods, respectively, compared to their baseline success rate of 47.78 ± 4.64%

(acute: 22.80 ± 5.16%, $p = 0.0035$; endpoint: 28.57 ± 6.27%, $p = 0.0092$, Tukey's post-hoc tests; **Fig. 8 B**). To explore the change in sham and stroke animals' performance post-surgery, we calculated the postoperative change in success rate by finding the difference in animals' success rates between the acute and endpoint periods. We found that stroke animals had a significantly greater postoperative change in success rate compared to sham animals (sham: -9.85 ± 5.95%, stroke: 5.77 ± 4.44%; $t_{(27.77)} = 2.103$, $p = 0.0446$, unpaired t-test; **Fig. 8 C**). This finding may suggest that some stroke mice experienced some recovery, as evidenced by their improved performance at the endpoint compared to the acute period.

Beyond success rate, we wanted to investigate other performance metrics, such as knockdown rate and miss rate, to obtain a complete picture of reaching behaviour in the HASRA. When comparing knockdown rates between sham and stroke groups across the scored baseline and postoperative days, a two-way RM ANOVA did not reveal any significant differences between groups ($F_{(19, 570)} = 1.157$, $p = 0.2898$, two-way RM ANOVA) or within groups ($F_{(8.943, 268.3)} = 1.669$, $p = 0.0969$, two-way RM ANOVA; **Fig. 8 D**). However, when investigating knockdown rates solely among our time periods of interest, we found a statistically significant effect of the time period on knockdown rates ($F_{(1.762, 52.86)} = 3.941$, $p = 0.0300$, two-way RM ANOVA). In contrast to the reduced mean success rates observed acutely following stroke surgery, we observed a 16.64% increase in stroke animals' mean knockdown rate at the acute period compared to baseline (baseline: 44.43 ± 3.10%, acute: 61.07 ± 3.60%; $p = 0.0010$, Tukey's test; **Fig. 8 E**). By endpoint, stroke mice's mean knockdown rate decreased to 52.96 ± 4.26% and was not significantly different from their baseline knockdown rates. In addition, although not significantly different, we found that stroke mice had a negative postoperative change in their mean knockdown rate, -8.11 ± 5.21%, between acute and endpoint periods, while

sham mice had nearly no change, 0.92 ± 5.52% ($t_{(29.90)} = 1.190$, $p = 0.2436$, unpaired t-test; **Fig. 8 F**). Stroke animals' negative change in knockdown rate postoperatively could further suggest that the performance some stroke animals improved by endpoint, as evidenced by their lower knockdown rates compared to acutely following stroke. Similar to knockdown rates, there were no significant differences in miss rates between the sham and stroke groups across the scored days relative to surgery ($F_{(19, 570)} = 0.7475$, $p = 0.7697$, two-way RM ANOVA; **Fig. 8 G**) and the time periods of interest ($F_{(2, 60)} = 1.132$, $p = 0.3293$, two-way RM ANOVA; **Fig. 8 H**). However, we observed a significant effect of time on miss rates (day relative to surgery: $F_{(7.363, 220.9)} = 2.172$, $p = 0.0350$, time periods of interest: $F_{(1.698, 50.93)} = 4.535$, $p = 0.0201$, two-way RM ANOVA; **Fig. 8 G-H**). In general, these significant effects suggested a trend towards increased miss rates at the acute and endpoint periods for the stroke group and increased miss rates only at the endpoint period for sham animals. Lastly, there were no significant differences post-operative change in miss rate between the sham and stroke groups ($t_{(29.88)} = 0.8840$, $p = 0.3838$, unpaired t-test; **Fig. 8 I**).

Altogether, our findings suggest that stroke mice were impaired acutely following stroke surgery, as evidenced by the significant decline in success rate, significant rise in knockdown rate, and slight numerical increase in miss rate during the acute period. Although stroke animals had a slight increase in success rate by endpoint, their endpoint performance was still significantly lower than at baseline, suggesting chronic impairment. However, other findings like the reduction in the knockdown rate at endpoint, positive postoperative change in success rate, and negative postoperative change in knockdown rate may suggest that some stroke animals had improved outcomes by endpoint and were able to make some recovery.

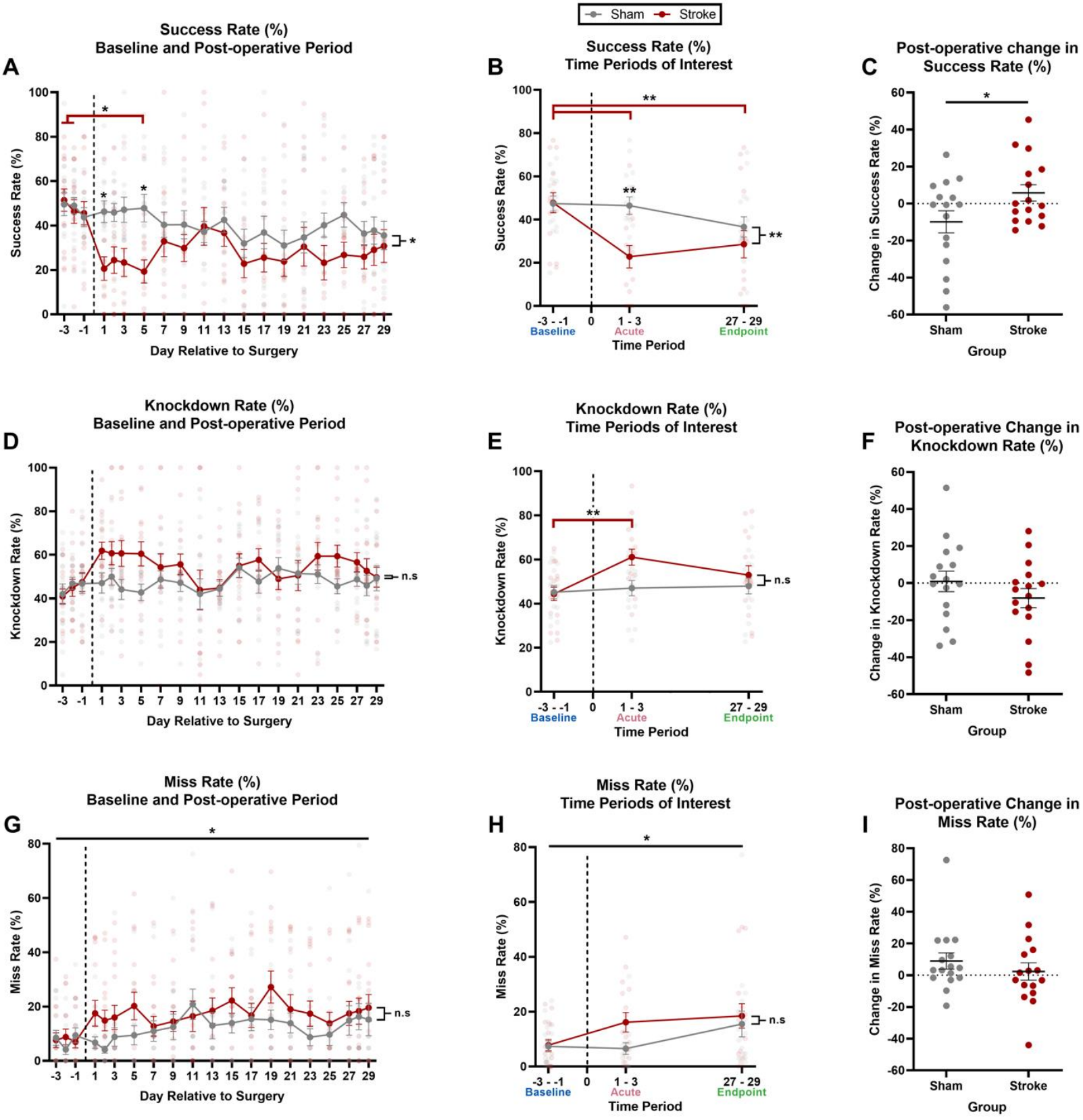

Figure 8. Stroke mice (n = 16) had acute and chronic impairment following surgery compared to shams (n = 16). Success rate at (A) each scored day of the baseline and post-operative period relative to surgery day (day zero) and at (B) time periods of interest (baseline,

acute, and endpoint). (C) Recovery of success rate (difference in metric between the endpoint and acute periods). Knockdown rate at (D) each scored day and at (E) time periods of interest. (F) Recovery of knockdown rate. Miss rate at (G) each scored and at (H) time periods of interest. (I) Recovery of miss rate. Data presented as mean ± SEM. Individual data points displayed as translucent gray- and red-coloured dots. Significance of $p < 0.05$ is represented by (*) and $p < 0.01$ is represented by (**).

4.2.2 No significant differences in task engagement observed between sham and stroke animals postoperatively

Along with performance metrics, we also examined changes in animals' engagement parameters following surgery. There were no significant differences in the mean number of entries into the reaching tunnel between the sham and stroke groups across the scored days ($F_{(1, 30)} = 0.06030$, $p = 0.8077$) and time periods of interest ($F_{(1, 30)} = 0.09061$, $p = 0.7655$). However, we found that time (days relative to surgery and time periods of interest) had a significant interaction with the number of entries into the reaching tunnel (days: $F_{(6.499, 195.0)} = 5.475$, $p < 0.0001$; time periods: $F_{(1.859, 55.76)} = 9.784$, $p = 0.0003$, two-way RM ANOVA; **Fig. 9 A-B**). Like the performance metrics, we observed a significant decline in the number of entries by stroke mice into the reaching tunnel at the acute period, 61.96 ± 5.80 entries, compared to that at baseline, 98.50 ± 8.77 entries ($p = 0.0003$, Tukey's test; **Fig. 9 B**). Although not statistically significant, stroke mice made more entries into the tunnel by endpoint, 81.99 ± 7.31 entries ($p = 0.1366$, Tukey's test). Moreover, both sham and stroke animals had a similar increase in their number of entries between the endpoint and acute periods (sham: 19.027 ± 8.80 entries, stroke: 20.03 ± 9.81 entries; $t_{(29.65)} = 0.07579$, $p = 0.9401$, unpaired t-test; **Fig. 9 C**).

Similarly to the number of entries, a two-way RM ANOVA did not reveal any significant differences in the time spent in the reaching tunnel between the sham and stroke groups across the scored days ($F_{(1, 30)} = 0.6827$, $p = 0.4152$; **Fig. 9 D**) and time periods of interest ($F_{(1, 30)} =$

2.023, $p = 0.1652$; **Fig. 9 E**). Interestingly, we observed a significant interaction of the time spent in the tunnel with the scored days relative to surgery ($F_{(7.178, 215.4)} = 3.515$, $p = 0.0012$; **Fig. 9 D**), but not with the time periods of interest ($F_{(1.974, 59.22)} = 3.020$, $p = 0.0570$; **Fig. 9 E**). These two findings suggest that time points between the acute and endpoint periods contributed to the significant interaction observed. Furthermore, this interaction may not be representative of the overall trend of the time spent in the reaching tunnel (min) due to the variability in this parameter between the individual days scored. Overall, there appeared to be little change in the time spent in the tunnel (min) across our experimental timeline. Indeed, we found that both sham and stroke groups had small postoperative changes in their time spent in the tunnel (min) following surgery (sham: 2.815 ± 9.41 minutes, stroke: 8.82 ± 9.57 minutes; $t_{(29.99)} = 0.4472$, $p = 0.6580$, unpaired t-test; **Fig. 9 F**).

Overall, sham and stroke animals had a similar engagement with the reaching task following surgery, despite the significant differences in performance parameters observed between the two groups postoperatively. When comparing performance and engagement parameters at the acute period compared to baseline, we found that stroke mice had significantly lower success rates and number of entries into the reaching tunnel and higher knockdown rates acutely following stroke surgery. At the endpoint, the success rates of stroke mice increased slightly but remained significantly lower than baseline. In addition, although not significantly different, the stroke group's knockdown rates were lower, and their number of entries into the reaching tunnel was higher at the endpoint compared to the acute period. Altogether, these findings suggest that stroke mice were greatly impaired at the acute period and that some of these animals continued to be chronically impaired while others may have had some recovery by the endpoint.

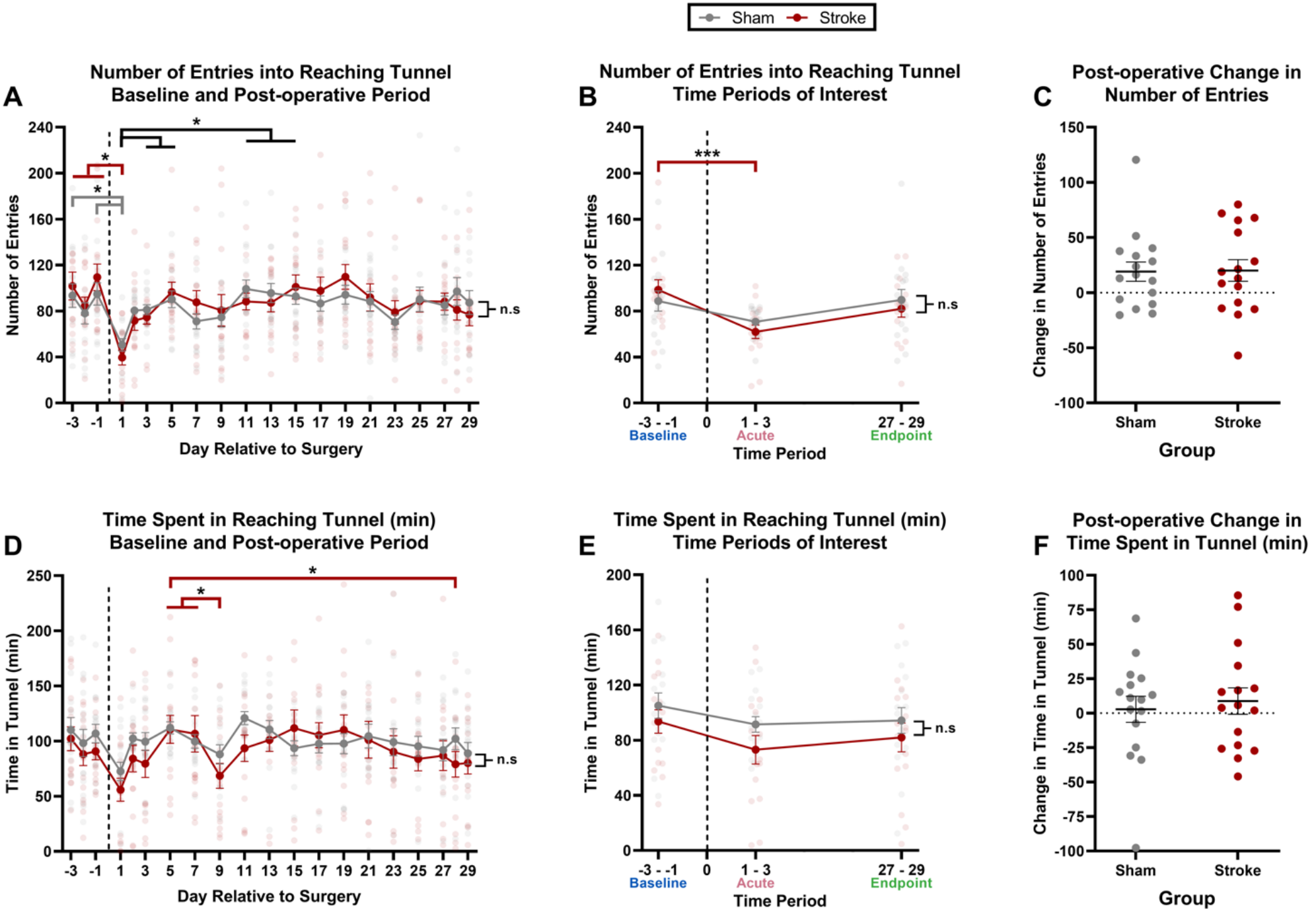
Sham
Stroke
A
Number of Entries into Reaching Tunnel
Baseline and Post-operative Period
Number of Entries
Day Relative to Surgery
n.s
B
Number of Entries into Reaching Tunnel
Time Periods of Interest
Number of Entries
-3 - -1
Baseline
0
1 - 3
Acute
27 - 29
Endpoint
Time Period
n.s
C
Post-operative Change in
Number of Entries
Change in Number of Entries
Sham
Stroke
Group
D
Time Spent in Reaching Tunnel (min)
Baseline and Post-operative Period
Time in Tunnel (min)
Day Relative to Surgery
n.s
E
Time Spent in Reaching Tunnel (min)
Time Periods of Interest
Time in Tunnel (min)
-3 - -1
Baseline
0
1 - 3
Acute
27 - 29
Endpoint
Time Period
n.s
F
Post-operative Change in
Time Spent in Tunnel (min)
Change in Time in Tunnel (min)
Sham
Stroke
Group

Figure 9. Sham (n = 16) and stroke (n = 16) mice had similar task engagement post-operatively. Number of entries at (A) each scored day relative to surgery day (day zero) and at (B) time periods of interest. (C) Recovery of number of entries. Time spent in the reaching tunnel at (D) each scored day and at (E) time periods of interest. (F) Recovery of time in tunnel (min). Data presented as mean ± SEM. Individual data points displayed as translucent gray- and red-coloured dots. Significance of $p < 0.05$ is represented by (*), $p < 0.01$ is represented by (**), $p < 0.001$ is represented by (***).

4.3 Stroke animals were divided into two sub-groups: "high endpoint success" and "low endpoint success" groups

Thus far, we have observed that stroke animals had a significant decrease in success rate, increase in knockdown rate, and decrease in number of entries into the reaching tunnel at the acute period compared to baseline. Altogether, these findings strongly suggest impairment in skilled reaching following stroke. By endpoint, we did not observe any significant changes in knockdown rate or number of entries, but we did find that stroke animals' success rates continued to be significantly lower than those at baseline. However, we also observed that some stroke animals had greater success rates, more entries into the reaching tunnel, and lower knockdown rates at the endpoint; this suggests that some stroke mice may have made some recovery by the endpoint. We wanted to investigate these findings further to provide insight into why some stroke animals had better performance by the endpoint while others did not. To conduct this investigation, we used a median split approach to divide the stroke group into two sub-groups based on their success rates at the endpoint: high endpoint success and low endpoint success sub-groups. The high endpoint success sub-group consisted of stroke animals with success rates greater than the median, 29.87%, while the low endpoint success sub-group contained animals with success rates lower than the median (**Fig. 10 A**). In the following sections, we explore differences between these two sub-groups during the postoperative and training periods.

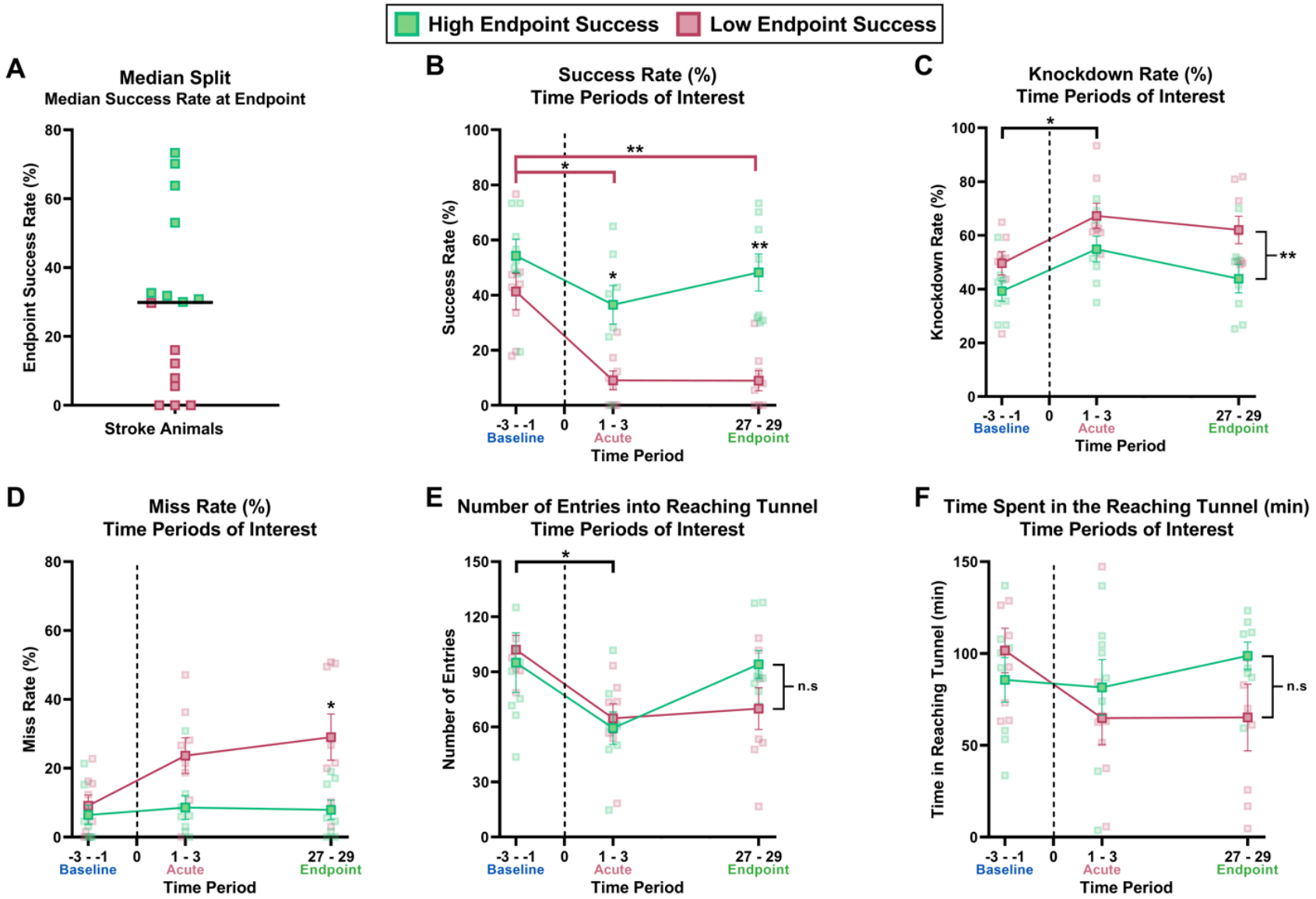

Figure 10. Comparing post-stroke profiles for high endpoint success (n = 8) and low endpoint success (n = 8) sub-groups. (A) Median split approach used to divide stroke group into high endpoint success (green) and low endpoint success (pink) sub-groups. (B - F) Compares high and low endpoint success groups at time periods of interest (baseline, acute, endpoint). (B) Success rate. (C) Knockdown rate. (D) Miss rate. (E) Number of entries into reaching tunnel. (F) Time spent in reaching tunnel (minutes). Data presented as mean ± SEM. Individual data points displayed as translucent green- and pink-coloured dots. Significance of $p < 0.05$ is represented by (*) and $p < 0.01$ is represented by (**).

4.3.1 Significant differences observed in post-stroke performance between high and low endpoint success sub-groups

Once the stroke group was divided into the high endpoint success and low endpoint success sub-groups, we compared their performance and engagement at time periods of interest (**Fig. 10**) and the scored baseline and post-stroke days (**Fig. S1**). We found that these two sub-groups had an overall statistically significant difference in success rates ($F_{(1, 14)} = 22.52$, $p = 0.0003$, two-way RM ANOVA; **Fig. 10 B**). More specifically, their success rates were significantly different at the acute period (high endpoint success: 36.53 ± 7.00%, low endpoint success: 9.08 ± 3.37%; $p = 0.0159$, Sidak's test) and at the endpoint (high endpoint success: 48.21 ± 6.71%, low endpoint success: 8.93 ± 3.65%; $p = 0.0010$, Sidak's test). Although not significantly different, when comparing the change within each sub-group's success rate between the endpoint and acute periods, we found that the high endpoint success sub-group had a positive change in their success rate of 11.68 ± 6.72%, while the low endpoint success sub-group had nearly no change with a decrease in their success rate of -0.14 ± 5.43% ($t_{(13.40)} = 1.369$, $p = 0.1936$, unpaired t-test; **Fig. S2 A**). Furthermore, at baseline, the high endpoint success group had a slightly higher success rate (54.28 ± 6.07%) than the low endpoint success group (41.29 ± 6.58%), but it was not a statistically significant difference. More notably, we found significant differences within the low endpoint success sub-group's success rates across time periods of interest ($F_{(1.598, 22.37)} = 13.06$, $p = 0.0004$, two-way RM ANOVA; **Fig. 10 B**). Compared to baseline (41.29 ± 6.58%), stroke animals in this sub-group had a 32.21% lower success rate acutely ($p = 0.0260$, Tukey's test) and a 32.36% lower success rate at the endpoint ($p = 0.0064$, Tukey's test).

When comparing changes in high and low endpoint success sub-groups' knockdown rates

compared to baseline ($F_{(1.748, 24.48)} = 6.341$, $p = 0.0078$, two-way RM ANOVA). Between the acute period and baseline, the low endpoint success sub-group had a 17.70% increase in knockdown rate (baseline: 49.59 ± 4.37%, acute: 67.28 ± 4.66%; $p = 0.0354$, Tukey's test), while the high endpoint success sub-group had a 15.58% increase in knockdown rate (baseline: 39.28 ± 3.81%, acute: 54.86 ± 4.78%; $p = 0.0441$, Tukey's test; **Fig. 10 C**). Despite having similar increases in knockdown rate post-stroke, a two-way RM ANOVA revealed that these two sub-groups had significantly different mean knockdown rates across our three time periods of interest ($F_{(1, 14)} = 12.36$, $p = 0.0034$; **Fig. 10 C**). Furthermore, there was an overall significant difference in mean miss rates between the sub-groups ($F_{(1, 14)} = 26.10$, $p = 0.0002$, two-way RM ANOVA; **Fig. 10 D**). At the endpoint, the low endpoint success sub-group had a 21.13% significantly greater miss rate than the high endpoint success group (low endpoint success: 29.03 ± 6.71%, high endpoint success: 7.90 ± 2.82%; $p = 0.0496$, Sidak's test; **Fig. 10 D**). No significant differences in post-stroke changes in knockdown rates ($t_{(12.35)} = 0.5372$, $p = 0.60$, unpaired t-test; **Fig. S2 B)** or miss rates ($t_{(7.924)} = 0.5474$, $p = 0.5992$, unpaired t-test; **Fig. S2 C**) were observed between high and low endpoint success groups.

In contrast to the performance parameters (success, knockdown, and miss rate), two-way RM ANOVAs did not reveal a significant difference in the mean number of entries ($F_{(1, 14)} = 0.1523$, $p = 0.7023$; **Fig. 10 E**) and mean time spent in the reaching tunnel ($F_{(1, 14)} = 0.6013$, $p = 0.4510$; **Fig. 10 F**) observed between the high and low endpoint success sub-groups. In addition, for time spent in the reaching tunnel, there were no significant differences observed within either sub-group across the different time periods ($F_{(1.882, 26.35)} = 1.833$, $p = 0.1814$, two-way RM ANOVA; **Fig. 10 F**). However, both sub-groups experienced significant and similar changes in their number of entries into the reaching tunnel ($F_{(1.636, 22.91)} = 7.588$, $p = 0.0046$, two-way RM

ANOVA; **Fig. 10 E**). Between baseline and the acute period following stroke, mice in the low endpoint success sub-group made 37.45 fewer entries (baseline: 102.04 ± 7.93 entries, acute: 64.59 ± 8.00 entries; $p = 0.0139$, Tukey's test) and those in the high endpoint success sub-group made 35.63 fewer entries (baseline: 94.96 ± 16.21 entries, acute: 59.33 ± 8.83 entries; $p = 0.0322$, Tukey's test) into the reaching tunnel (**Fig. 10 E**). Like the post-stroke changes in the performance parameters, there were no significant differences observed between high and low endpoint success sub-groups' changes in their number of entries or time in the tunnel (min) between the endpoint and acute periods (**Fig. S2 D – E**).

By comparing the high endpoint success and low endpoint success sub-groups' performance and engagement across different time periods, we gained a better understanding of how these two groups differ. We uncovered that despite a similar task engagement, the low endpoint success sub-group experienced a greater impact of stroke; this is evident by this group's lower success rates, higher knockdown rates, and higher miss rates observed acutely following stroke and at the endpoint. Therefore, these findings suggest that mice in the low endpoint success sub-group were more severely impaired post-stroke compared to mice in the high endpoint success sub-group.

4.3.2 Differences observed in the learning curves of high and low endpoint success groups.

We were interested in exploring if the differences in performance observed between the high and low endpoint success sub-groups are only present post-stroke or if these differences extend to earlier time points during the training period, before the stroke procedure. We compared mean success rates of high and low endpoint success sub-groups across the reaching days of the training period and found a significant difference between overall mean success rates ($F_{(1, 14)}$ =

5.849, $p = 0.0298$, mixed-effects model (REML) analysis; **Fig. 11 A**) and mean knockdown rates ($F_{(1, 14)} = 6.528$, $p = 0.0229$, mixed-effects model (REML) analysis; **Fig. 11 B**). In general, the high endpoint success sub-group had higher mean success rates and lower mean knockdown rates throughout the training period, including on both sub-groups' first day of reaching. There was not a significant difference between the two sub-groups' miss rates ($F_{(1, 14)} = 1.471$, $p = 0.2453$, mixed-effects model (REML) analysis; **Fig. 11 C**).

In addition, we found a significant main effect of time (reaching day) on success rate ($F_{(4.294, 53.37)} = 8.891$, $p < 0.0001$, mixed-effects model (REML) analysis; **Fig. 11 A**) and miss rate ($F_{(3.213, 39.48)} = 3.527$, $p = 0.0212$, mixed-effects model (REML) analysis; **Fig. 11 C**) during the training period. Tukey's post-hoc tests revealed that the low endpoint success sub-group had significantly greater success rates on reaching days 13 (37.03 ± 9.65%; $p = 0.0460$), 12 (38.81 ± 8.42%; $p = 0.0099$), and 11 (42.34 ± 7.57%; $p = 0.0086$) compared to their first day of reaching (11.80 ± 5.49%; **Fig. 11 A**). For the miss rate, we did not observe significant differences between specific reaching days within the high and low endpoint success sub-groups. But we observed that following the first day of reaching, the high endpoint success sub-group had slightly lower miss rates than the low endpoint success sub-group (**Fig. 11 C**). When investigating stroke animals' engagement at the reaching task, we did not observe any significant within-group or between-group differences for their number of entries into the reaching tunnel (within-group difference: $F_{(3.322, 43.18)} = 1.827$, $p = 0.1513$, between-group difference: $F_{(1, 14)} = 0.3804$, $p = 0.5473$, mixed-effects model (REML) analysis; **Fig. 11 D**) and time spent in the reaching tunnel (within-group difference: $F_{(2.943, 38.25)} = 2.781$, $p = 0.0550$, between-group difference: $F_{(1, 14)} = 0.1903$, $p = 0.6693$, mixed-effects model (REML) analysis; **Fig. 11 E**)

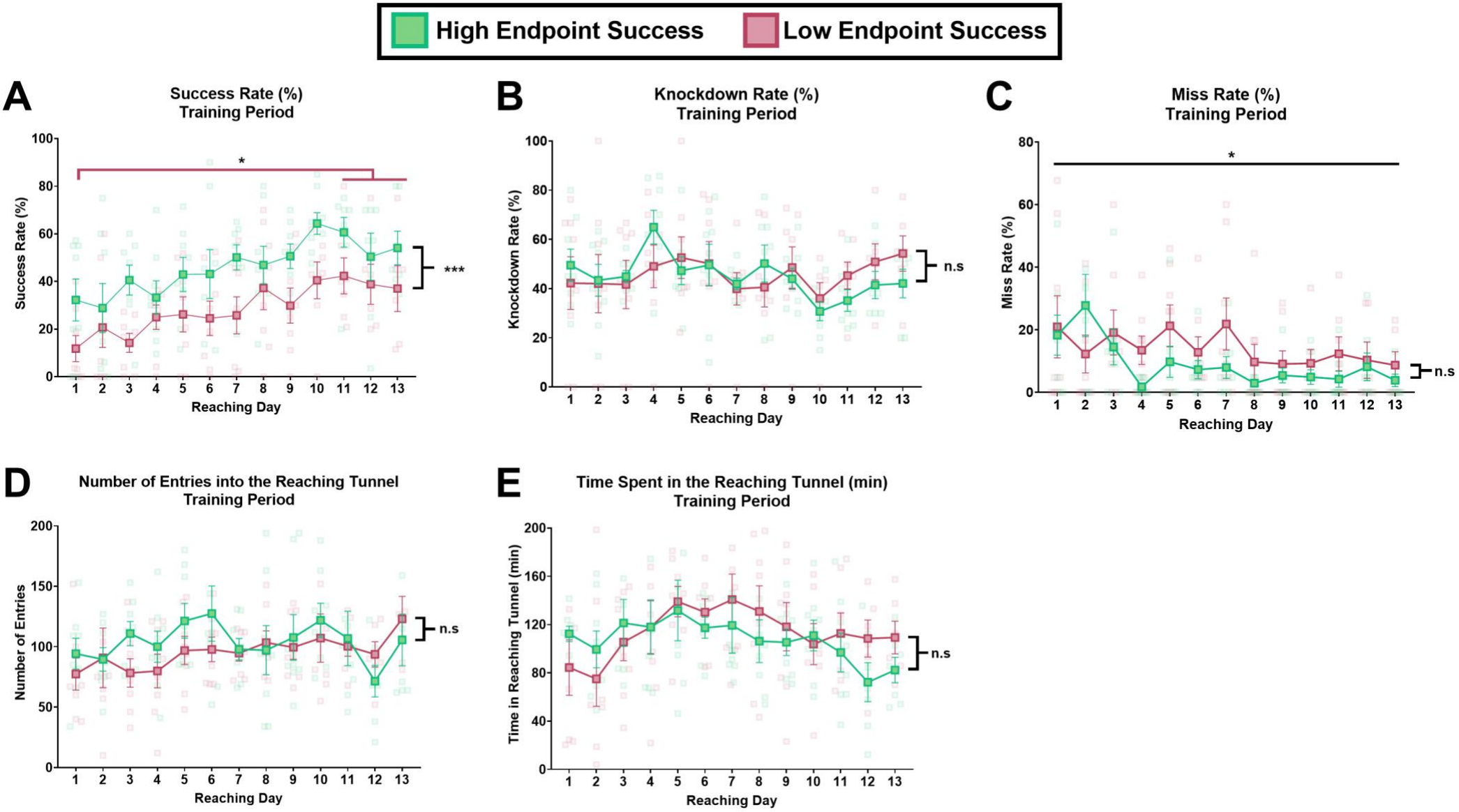

Figure 11. Comparing training profiles of high endpoint success (n = 8) and low endpoint success (n = 8) sub-groups. (A) Success rate. (B) Knockdown rate. (C) Miss rate. (D) Number of entries into the reaching tunnel. (E) Time spent in the reaching tunnel (min). All data is presented as mean ± SEM. Individual data points displayed as translucent green- and pink-coloured dots. Significance of $p < 0.05$ is represented by (*).

Since the main differences observed during the training period between the high and low endpoint success sub-groups were in their knockdown rates and success rates, we wanted to further explore any differences in the two sub-groups' learning curves. We found that the high endpoint success sub-group had an 18.90% significantly greater mean success rate during the training period than the low endpoint success sub-group (high endpoint success: 47.83 ± 5.09%, low endpoint success: 28.93 ± 5.24%; $t_{(13.99)} = 2.586$, $p = 0.0216$, unpaired t-test; **Fig. 12 A**). Due to this significant difference in performance, we were interested in exploring the animals' learning rate and their rate of improvement at the reaching task. Using animals' learning profiles (success rates over reaching days), we performed a linear regression analysis to identify each animal's learning rate, which is represented by the coefficient of the slope. This analysis was performed for each animal in both sub-groups. Although we did not find any significant differences between each sub-group's mean learning rate, we did observe that the low-endpoint sub-group had a slightly higher mean learning rate, suggesting a greater rate of improvement at the task during the training period (high endpoint success: 1.98 ± 0.71, low endpoint success: 2.74 ± 0.40; $t_{(11.15)} = 0.9330$, $p = 0.3706$, unpaired t-test; **Fig. 12 B**). This could be explained by our previous findings that the high endpoint success group had a better performance at the task throughout the training period. Since animals in the low endpoint success group were not as skilled at the reaching task from the start of the training period, they had to have more improvement in their reaching skills to improve their task outcomes. Lastly, both sub-groups had a significant correlation between their reaching days and their success rates during the training period (high endpoint success: slope = 1.78, $R^2 = 0.79$, $p = 0.0032$, low endpoint success: slope = 2.38, $R^2 = 0.91$, $p = 0.0002$; **Fig. 12 C**). The low endpoint success group's steeper slope further supports our findings in **Fig. 12 B** of a higher learning rate compared to that of the high endpoint

success group. Furthermore, our correlations in **Fig. 12 C** demonstrated that, in general, all animals' performance improved as time progressed during the training period.

Overall, our findings suggest that animals in the high endpoint success group were more skilled at the reaching task compared to those in the low endpoint success group, despite having similar task engagement. In summation, these two sub-groups had significant differences in their performance prior to and following stroke surgery.

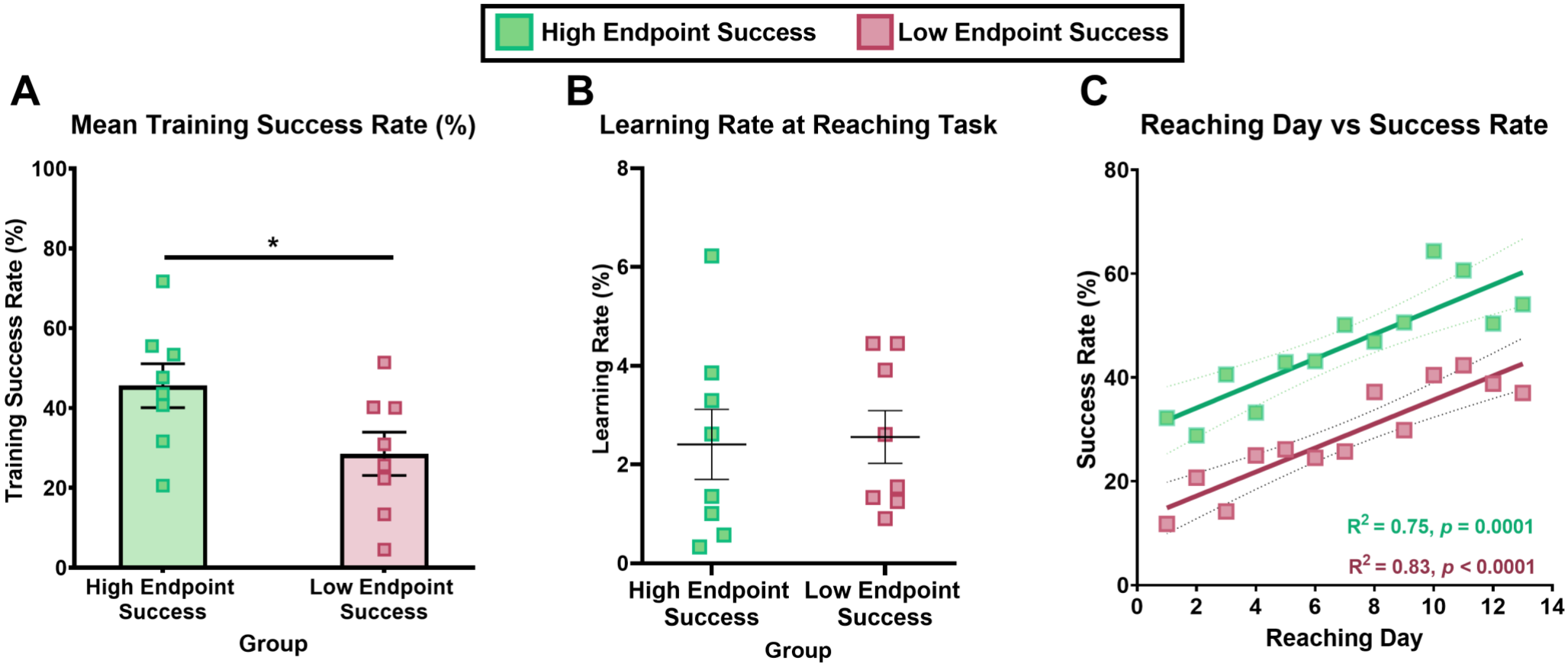

Figure 12. Learning curve analysis for high endpoint success (n = 8) and low endpoint success (n = 8) sub-groups. (A) Mean training success rate ± SEM. (B) Mean learning rate at reaching task ± SEM. (C) Correlations between success rate and reaching day of the training period. Significance of $p < 0.05$ is represented by (*).

4.4 Lesion volume and the anteroposterior and mediolateral range of damage

Lesion areas were traced and measured in *NIH ImageJ* to calculate the lesion volume induced by the photothrombotic stroke procedure resulting in a mean lesion volume of 1.034 ± 0.052 mm^3 (**Fig. 13 A, Bi**). We did not find any significant differences between high and low endpoint success groups' mean lesion volumes (high endpoint success: 1.082 ± 0.084 mm^3 , low endpoint success rate: 1.001 ± 0.063 mm^3; $t_{(13.01)} = 0.7681$, $p = 0.4561$, unpaired t-test, **Fig. 13 Bii**). Across all stroke animals, the location of the lesion on the AP coordinate system relative to bregma had a wide range with a maximum extent of +2.3 mm anterior to -0.5 mm posterior (**Fig. 13 C**). Furthermore, both high and low endpoint success groups had a wide range of damage across the AP coordinate system (high endpoint success: max = +2.3 mm and min = -0.5 mm, low endpoint success: max = +2.3 mm and min = -0.2 mm; **Fig. 13 C**). Due to these wide ranges in AP coordinates of damage, we were interested in exploring other approaches to localize the damage caused by the lesion.

Using our dorsal mouse brain images of the induced lesions, we were able to use the AP and ML coordinate systems to qualitatively visualize the location of the lesions on the dorsal mouse brain atlas (**Fig. 13 D**). From this approach, we found that, among all stroke animals, the following regions were impacted by the photothrombotic stroke: M2, M1, S1FL, and S1HL (**Fig. 13 Di-iii**). Since this is a qualitative approach, we could not accurately compare differences in lesion location between the high and low endpoint success groups (**Fig. 13 Dii-iii**).

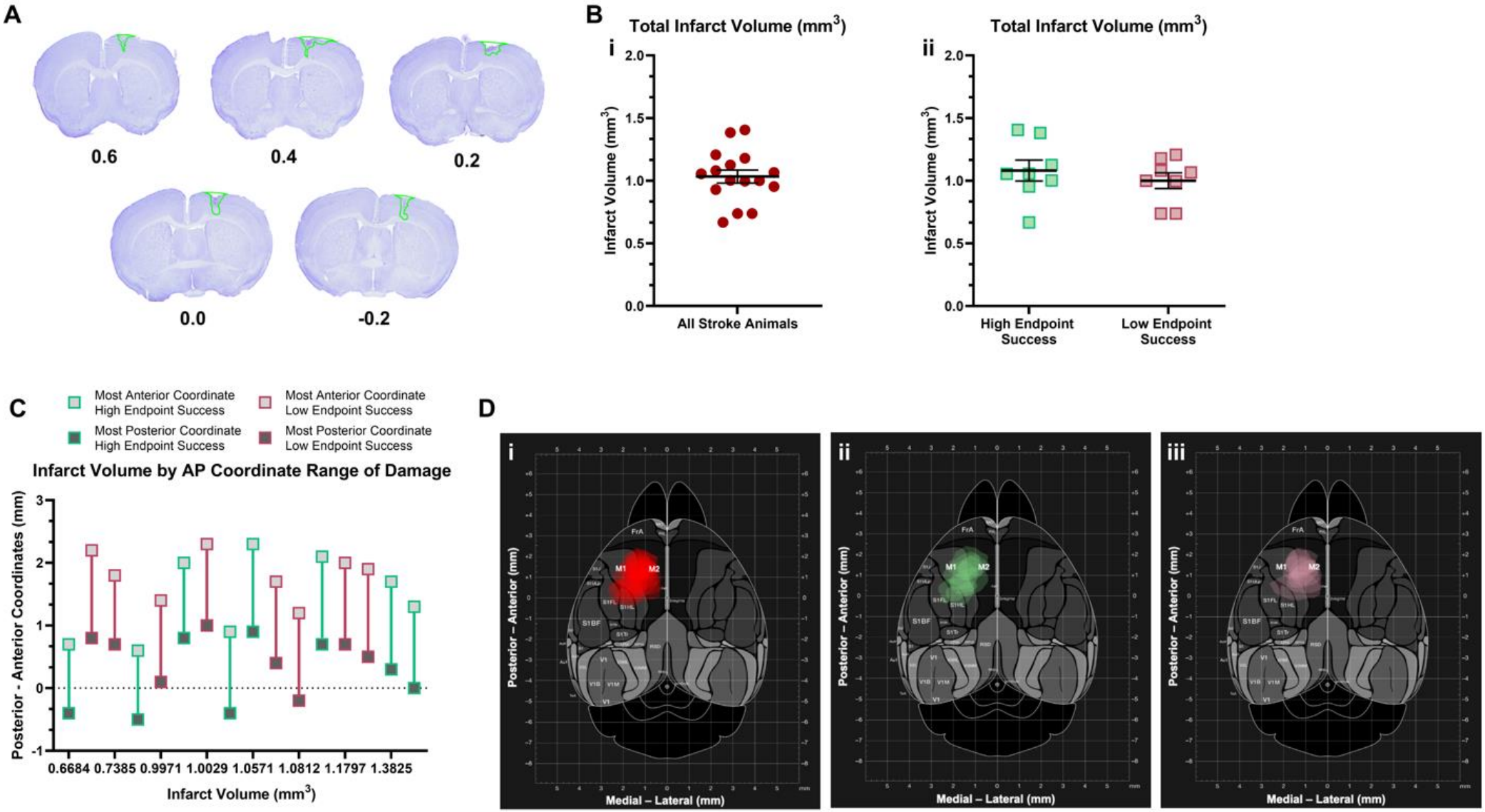

Figure 13. Lesion volume and location relative to bregma. (A) Cresyl violet stained sections showing outlined lesion areas in green. (B) Mean infarct volume ± SEM (i) among all stroke animals (n = 16) and (ii) stroke animals in the high endpoint success (n = 8) and low endpoint success (n = 8) groups. (C) Infarct volume by AP coordinate range of damage. (D) Dorsal localization of the induced lesions relative to bregma and the midline for (i) all stroke animals (n = 16), (ii) stroke animals in the high endpoint success group (n = 8), and (iii) stroke animals in the low endpoint success group (n = 8).

4.5 Quantifying lesion-induced damage in anatomical brain regions

For a more precise identification of the brain regions impacted by the stroke, we aligned our Cresyl violet stained coronal serial sections with the overlaid lesion areas to the AMBA using *NIH ImageJ*, *QuickNII*, *VisuAlign*, and *Nutil* as described in the methods section **3.8**. These tools allowed us to quantify the percentage of damage caused by the induced lesion in the following anatomical regions: M1, M2, S1FL, S1HL, dACC, vACC, and corpus callosum. But only regions that had a mean damage of 1% or more among all stroke animals were considered in our analysis: M1, M2, S1FL, and dACC. When comparing the regions damaged among all stroke animals, a two-way ANOVA revealed significant differences in the percentage of damage in the affected brain regions (M1 = 7.88 ± 1.26% damaged, M2 = 17.09 ± 2.248% damaged, S1FL = 1.80 ± 1.601% damaged, and dACC = 2.56 ± 0.81% damaged; $F_{(3, 45)} = 19.59$, $p < 0.0001$; **Fig. 14 A**). We found that M2 had the greatest amount of damage, which a post-hoc Tukey's test revealed was significantly greater than damage in M1 ($p = 0.0010$), S1FL ($p < 0.0001$), and dACC ($p < 0.0001$).

In addition, we were also interested in exploring any differences in the amount of damage in these brain regions between the high and low endpoint success groups. Within each endpoint success group, we found significant differences in the percentage of damage in the affected anatomical regions ($F_{(3, 42)} = 22.86$, $p < 0.0001$, two-way RM ANOVA; **Fig. 14 B**). Within the low endpoint success group, we found that M2 had significantly more damage, 21.52 ± 2.91%, than all the other analyzed regions (M1 = 6.56 ± 1.55%, S1FL = 0.027 ± 0.022%, dACC = 3.58 ± 1.22%; $p < 0.0001$, Sidak's test). In contrast, within the high endpoint success group, M2 had significantly more damage, 12.66 ± 2.75%, than S1FL (3.58 ± 3.17%, $p = 0.0215$) and dACC (1.53 ± 1.03%, $p = 0.0030$) but not M1 (9.20 ± 1.98%, $p = 0.8183$). Moreover, when comparing

the percentage of damage in the affected brain regions between the high and low endpoint success groups, we found that the low endpoint success group had significantly more damage in M2 compared to the high endpoint success group ($t_{(14)} = 2.211$, $p = 0.04420$, multiple unpaired t-tests; **Fig. 14 B**).

Through our semi-automated lesion localization workflow, we were able localize and quantify the induced lesion damage; this led us to our finding that stroke animals with lower success rates at endpoint had significantly more damage in M2 compared to stroke animals who achieved higher success rates by the endpoint of our experimental timeline.

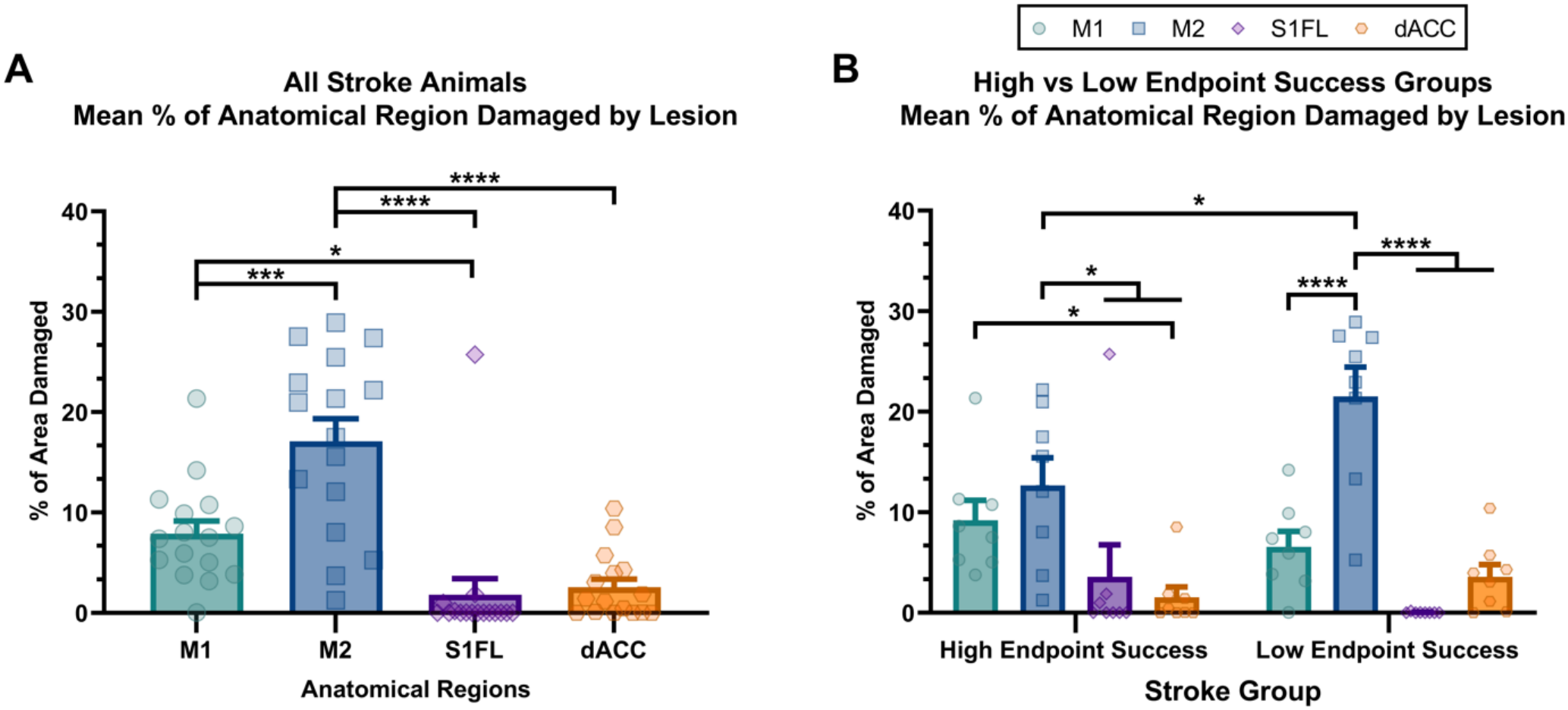

Figure 14. Lesion localization to the Allen Mouse Brain Atlas (n = 16). Mean percentage of anatomical region damaged by lesion + SEM for (A) all stroke animals (n =16) and (B) stroke animals in the high endpoint success (n = 8) and low endpoint success (n = 8) groups.

4.6 Correlates and predictors of endpoint performance among stroke animals

Following behavioural assessment post-stroke and the identification of the anatomical regions impacted by stroke, we were interested in investigating the relationships between task performance, task engagement, and lesion localization metrics among stroke animals. Using Pearson bivariate correlations, we first investigated the relationship between task performance and engagement at endpoint. We found that stroke animals' endpoint success rates were significantly correlated with time spent in the reaching tunnel ($R^2 = 0.3118$, $p = 0.0246$; **Fig. 15 A**) and number of entries into the reaching tunnel ($R^2 = 0.2488$, $p = 0.0493$; **Fig. 15 B**) at endpoint. These positive correlations show that animals with higher endpoint success rates entered the reaching tunnel more frequently and spent more time inside the reaching tunnel at endpoint (**Fig. 15 A-B**).

In addition to task engagement, we also found significant correlations between endpoint success rate and other task performance metrics. For instance, we found that endpoint success rate had a significant negative correlation with baseline, acute, and endpoint knockdown rates (baseline: $R^2 = 0.2649$, $p = 0.0414$, acute: $R^2 = 0.3112$, $p = 0.0248$, endpoint: $R^2 = 0.4971$, $p = 0.0023$; **Fig. 15 C**). Similarly, we observed a significant negative correlation between endpoint success rate and endpoint miss rate ($R^2 = 0.5396$, $p = 0.0012$; **Fig. 15 D**). These results demonstrate that stroke animals that made fewer reaching errors (knockdowns and misses) prior to and following stroke induction, achieved more success at endpoint. To further support these findings, we found that animals' mean baseline success rate, acute success rate, and training success rate were significantly and positively correlated with their success rate at the endpoint (baseline: $R^2 = 0.2670$, $p = 0.0404$, acute: $R^2 = 0.5098$, $p = 0.0019$, training success rate: $R^2 = 0.4905$, $p = 0.0025$; **Fig. 15 E**). Moreover, we found that stroke animals with lower learning rates

had a higher endpoint success rate ($R^2 = 0.3459$, $p = 0.0166$; **Fig. 15 F**). Since the learning rate represented the rate of improvement in performance throughout the training period, this correlation could suggest that animals requiring less improvement to successfully perform the reaching task during the training period had higher success rates at endpoint. Once more, these findings suggest that animals that were more successful at the reaching task throughout their training period were also more successful acutely following stroke and particularly at the endpoint.

When exploring the correlations between metrics of performance and lesion damage, we found that the acute miss rate was significantly and positively correlated with the % of M2 damaged ($R^2 = 0.5006$, $p = 0.0022$) and the % of dACC damaged ($R^2 = 0.5543$, $p = 0.0009$; **Fig. 15 G**). These correlations illustrate that stroke animals with higher miss rates at the acute period had more damage in M2 and dACC (**Fig. 15 G**). Conversely, we found a significant negative correlation between the acute success rate and the % of dACC damaged ($R^2 = 0.3151$, $p = 0.0237$; **Fig. 15 H**). Although not statistically significant, we observed a moderate negative correlation between the acute success rate and the % of M2 damaged ($R^2 = 0.2449$, $p = 0.0513$; **Fig. 15 H**). Overall, these correlations suggest that animals with more damage in M2 and dACC had poorer performance at the reaching task acutely following stroke.

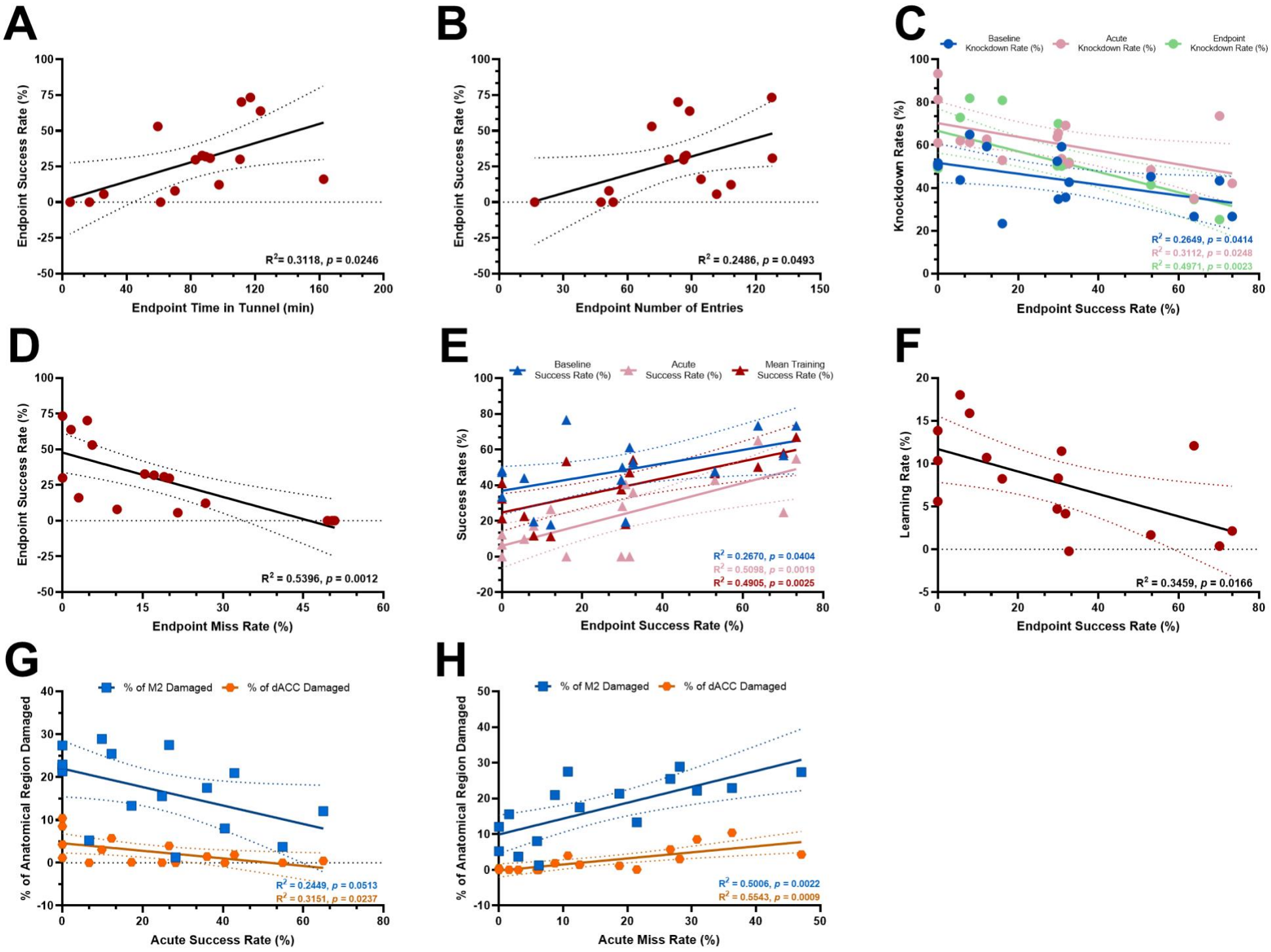
A
Endpoint Success Rate (%)
Endpoint Time in Tunnel (min)
R²= 0.3118, p = 0.0246
B
Endpoint Success Rate (%)
Endpoint Number of Entries
R² = 0.2486, p = 0.0493
C
Baseline Knockdown Rate (%)
Acute Knockdown Rate (%)
Endpoint Knockdown Rate (%)
Knockdown Rates (%)
Endpoint Success Rate (%)
R² = 0.2649, p = 0.0414
R² = 0.3112, p = 0.0248
R² = 0.4971, p = 0.0023
D
Endpoint Success Rate (%)
Endpoint Miss Rate (%)
R² = 0.5396, p = 0.0012
E
Baseline Success Rate (%)
Acute Success Rate (%)
Mean Training Success Rate (%)
Success Rates (%)
Endpoint Success Rate (%)
R² = 0.2670, p = 0.0404
R² = 0.5098, p = 0.0019
R² = 0.4905, p = 0.0025
F
Learning Rate (%)
Endpoint Success Rate (%)
R² = 0.3459, p = 0.0166
G
% of M2 Damaged
% of dACC Damaged
% of Anatomical Region Damaged
Acute Success Rate (%)
R² = 0.2449, p = 0.0513
R² = 0.3151, p = 0.0237
H
% of M2 Damaged
% of dACC Damaged
% of Anatomical Region Damaged
Acute Miss Rate (%)
R² = 0.5006, p = 0.0022
R² = 0.5543, p = 0.0009

Figure 15. **Investigating correlations among performance, engagement, and lesion damage localization parameters.** Mean endpoint success rate was significantly correlated with engagement parameters, such as (A) endpoint time spent in the reaching tunnel (min) and (B) endpoint number of entries into the reaching tunnel. Mean endpoint success rate was significantly correlated with performance parameters, such as (C) baseline, acute, and endpoint knockdown rates, (D) endpoint miss rate, (E) baseline, acute, and mean training success rate. (F) Learning rate and mean endpoint success rate were significantly correlated with each other. The percentages of M2 and dACC damaged by the induced lesions were significantly correlated with (G) acute success rate and (H) acute miss rate.

Lastly, we wanted to explore if any of the correlates discussed could be predictors of reaching performance at the endpoint, as well as predictors of whether stroke animals would be in the high endpoint success or low endpoint success groups. To explore this, a forward stepwise binary logistic regression was performed to investigate if variables of performance, engagement, and lesion damage could be predictors of endpoint success rate (**Table 3**). One statistically significant model we found ($\chi^2(1) = 9.618$, $p = 0.002$) showed that acute success rate was a significant predictor of endpoint success rate ($p = 0.032$; **Table 4**). This significant model explained 60.2% (Nagelkerke R^2) of the variance observed in endpoint success rate and correctly classified 87.5% of cases. This model showed that animals with higher success rates acutely following stroke were 1.26 times more likely to achieve higher success rates at the endpoint. Another significant model identified ($\chi^2(1) = 5.867$, $p = 0.015$) illustrated that training success rate was a significant predictor of endpoint success rate ($p = 0.049$). This model explained 40.9% (Nagelkerke R^2) of the variance in endpoint success rate and classified 81.3% of cases correctly. The last significant model we found ($\chi^2(2) = 13.459$, $p = 0.001$) revealed that the learning rate and % of M2 damaged were predictors of endpoint success rate, although they were not found to be significant individually (learning rate: $p = 0.165$, % of M2 damaged: $p = 0.156$). This model was able to explain 75.8% of the variance in endpoint success rate and had a classification accuracy of 87.5%. Through this model, we found that stroke animals that had greater learning

rates and more damage in M2 had a decreased likelihood of achieving higher success rates at endpoint.

Table 3. Variables used in conditional forward stepwise binary logistic regression to identify predictors of mean endpoint success rate.

Dependent Measure	Variables
Mean Endpoint Success Rate (%)	Baseline Number of Entries
	Acute Number of Entries
	Endpoint Number of Entries
	Baseline Time Spent in the Reaching Tunnel (min)
	Acute Time Spent in the Reaching Tunnel (min)
	Endpoint Time Spent in the Reaching Tunnel (min)
	Baseline Success Rate (%)
	Acute Success Rate (%)
	Endpoint Success Rate (%)
	Mean Training Success Rate (%)
	Learning Rate (%)
	Infarct Volume (mm^3)
	% of M1 damaged by Lesion
	% of M2 damaged by Lesion
	% of S1FL damaged by Lesion
	% of dACC damaged by Lesion

Table 4. Predictors of mean endpoint success rate among stroke animals (n = 16). Identifying predictors of stroke animals being in the high endpoint success or low endpoint success groups using a conditional forward stepwise binary logistic regression.

Dependent Measure	Predictor(s)	Nagelkerke R^2	Percentage Accuracy in Classification (%)	Significance of Model	Significance of Change to Model if Predictor is Removed	Significance of Individual Predictors	Odds Ratio
Mean Endpoint Success Rate (%)	Acute Success Rate (%)	60.2%	87.5%	0.002	0.002	0.032	1.126
	1. Mean Training Success Rate (%) & 2. % of M2 Damaged	69.0%	81.3%	0.003	1. 0.004 & 2. 0.001	1. 0.0146 & 2. 0.108	1. 1.203 & 2. 0.746

5. DISCUSSION

5.1 Summary of findings

In this study, we demonstrated that the HASRA can be used to characterize the time course of post-stroke upper limb motor impairments and recovery. We were also able to compare different behavioural parameters across the experimental timeline to each other and to lesion damage metrics. First we found that both sham and stroke animals had similar task performance and engagement during the training period, but differed post-operatively. Two of our performance metrics, success rate and knockdown rate, showed that stroke animals were most impaired acutely following stroke induction. Despite a slight increase by the endpoint, stroke animals' success rate was still significantly lower than baseline. Although, a reduction in knockdown rate was observed at the endpoint compared to the acute period, resulting in the endpoint knockdown rate to not be significantly different from baseline. This slight increase in success rate and the reduction in knockdown rate at the endpoint suggested to us that there may be some stroke animals with greater recovery and fewer impairments by the endpoint, and other stroke animals with a poorer recovery and more impairments.

To explore these findings further, we used a median split approach to divide the stroke group into two sub-groups based on the median success rate at the endpoint: high endpoint success and low endpoint success sub-groups. We then compared the performance and engagement parameters of these two sub-groups at time periods of interest and the training period. Although we did not find any significant differences between the two sub-groups' task engagement, we found that the high endpoint success group had a significantly better performance at the acute and endpoint periods post-stroke and during the training period. Moreover, when we calculated the learning rate, rate of improvement in performance during the

training period, we found that the low endpoint success sub-group had a higher learning rate suggesting that they needed to make more improvement in their performance to become successful at the reaching task. Whereas, for the high endpoint success group, they had a better performance at the reaching task from the start of the training period, and thus did not need to make as much improvement in their performance.

Next, we were interested in investigating the effect of stroke size and location on behavioural deficits and recovery. In our study, stroke size did not have an effect on performance or engagement post-stroke. Interestingly, we found that the low endpoint success sub-group had significantly more damage in M2 compared to the high endpoint success group, suggesting that stroke location could affect post-stroke performance and recovery. Lastly, we found that the acute success rate, training success rate, learning rate, and percentage of M2 damaged were significant predictors of endpoint performance. These predictors demonstrate that training performance, acute impairments and stroke location are important factors when predicting chronic impairment and recovery following stroke.

5.2 Comparing impairment and recovery in our photothrombotic stroke mouse model to other rodent models and to the clinical stroke population

Using the HASRA, we found that stroke animals were most impaired at the acute period following stroke as evidenced by the significant reduction in success rate and the significant increase in knockdown rate. These findings are corroborated by various skilled reaching studies of ischemic stroke mouse and rat models (Alaverdashvili et al., 2008; Alaverdashvili & Whishaw, 2010; Mirza Agha et al., 2021; Clarkson et al., 2013; Gharbawie & Whishaw, 2006; Nemchek et al., 2021). Generally, these studies have shown a large decline in success rate lasting

up to seven days post-stroke, thereby suggesting upper limb impairment acutely following stroke (Clarkson et al., 2013; Mirza Agha et al., 2021; Alaverdashvili et al., 2008). Following this acute period of impairment, a steady increase in success rate was observed resulting in success rates close to baseline values by roughly three to four weeks following stroke surgery (Clarkson et al., 2013; Mirza Agha et al., 2021; Nemchek et al., 2021; Gharbawie and Whishaw, 2006; Alaverdashvili et al., 2008). In our study, we did not find that all stroke animals recovered to baseline levels. In fact, our stroke animals' endpoint success rates were significantly lower than that at baseline. Although, when investigating our high endpoint success stroke animals' performance, we found that their post-stroke performance at the reaching task improved over time leading to endpoint success rates that were similar to baseline.

These improvements in reaching performance are possible since the skilled reaching task can be used as a rehabilitative paradigm. Through rehabilitative training post-stroke, synaptogenesis can be induced in the lesioned hemisphere leading to the promotion of neural recovery in animals (Jones et al., 1999). Furthermore, this motor training following stroke leads to relearning in the damaged brain and cortical reorganization which leads to the improved behavioural function observed (Kleim and Jones, 2008). Similarly in humans partaking in rehabilitative reach-to-grasp exercises, neuroplastic changes in the brain are observed as new motor skills are learned (Carr & Shepherd, 1998; Nudo et al., 2000; Nudo et al., 2003a; Nudo et al., 2003b).

As discussed earlier, stroke animals are most impaired acutely following stroke with some recovery made over time through rehabilitative training. Similar findings have also been observed in stroke patients. In a recent study by Saes et al., researchers investigated upper limb impairments and smoothness of motor movements longitudinally following unilateral ischemic

stroke in a reach-to-grasp task (2021). This study used the Fugl-Meyer motor assessment of the upper extremity (FM-UE) measure to assess motor function in the impaired upper limb from the first to the 26th week following stroke. Similarly to preclinical findings, stroke patients had the lowest upper extremity motor performance in the first week following stroke. FM-UE showed that motor performance increased over time and levelled off by the fifth week. The smoothness of stroke patients reaching movements followed a similar trend as the observed motor performance, with a gradual increase in smoothness of movements that began to stabilize by the 5th week of post-stroke training. Between the fifth and the 26th weeks of reach-to-grasp training, both motor performance and movement smoothness were comparable to that of the healthy control group. Together, these findings suggest that stroke patients had the most impairment acutely following stroke, but through rehabilitative training with the reach-to-grasp task were able to achieve some recovery by the fifth week (Saes et al., 2021).

It is also important to note that improvement in motor performance over time does not necessarily equate to recovery, the restoration of the original movement. Following an ischemic stroke, animals and humans alike may show improvement in motor performance through the use of compensatory strategies. Among the clinical stroke patients, common compensatory strategies include trunk displacement and rotation, scapular elevation, shoulder abduction, and internal rotation (Levin et al., 2002; Roby-Brami et al., 2003). Similarly, preclinical rodent models of ischemic stroke have shown the use of compensatory strategies such as ipsiversive trunk rotary movements, reduced elbow adduction, and non-reaching forelimb use for assistance during the skilled reaching task (Alaverdashvili & Whishaw, 2013; Farr & Whishaw, 2002; Finger, 1978). Our study did not examine the use motor compensation during reaching so it is difficult for us to identify the amount of recovery made by the stroke animals. In the future, we can use a

markerless pose estimation software like DLC to track the movement of the rodent's different body parts and their kinematics during reaching behaviour (Nath et al., 2019).

5.3 Automating the single pellet reaching task is advantageous

As discussed before, the manual nature of the SPRT leads to several challenges arising, such as experimenter related variability, disruption of animals' circadian rhythm, handling stress in the animals, and a limited number of trials due to time constraint (Balcombe et al., 2004; Dauchy et al., 2010; Fouad et al., 2013). Our lab has designed the HASRA to investigate upper limb motor impairments and recovery following ischemic stroke while overcoming the challenges of the manual SPRT through automation (Salameh et al., 2020). Animals in the HASRA were able to engage with the task completely autonomously and without disruption to their day-night cycles. Moreover, experimenters had nearly no direct contact with the animals, except once weekly when the animals' home-cages are cleaned. Through our study, we demonstrated that the HASRA can be used longitudinally to characterize the time course of forelimb motor function in a mouse model of stroke. We were also able to investigate the effect of different behavioural variables on impairment and recovery which lead us to our findings that acute success rate and training success rate were significant predictors of post-stroke performance.

Beyond the HASRA, there have been several efforts to automate the SPRT to study forelimb motor function in healthy rodents and in rodents with neurological conditions. Ellens et al., designed an automated version of the SPRT to train rats on skilled reaching for twelve days (2016). Animals were placed in a skilled reaching chamber by an experimenter and rats were allowed to reach for the automatically delivered seeds for a total of 100 reaches or 60 minutes, whichever occurs first. Animals' reaching behaviour was recorded using a high frame rate

camera (300 fps). Similar to the mice in the HASRA, rats were successfully trained on this task as shown by the gradual increase in success rate and first reach success rate as the training period progressed. Also like our study, they did not observe any significant differences between animals' success rates and first reach success rates. Although this automated task was able to successfully train rats, there are still some challenges similar to that of the manual SPRT. Firstly, animals still need to be handled to be placed in the reaching chamber and then to be returned to their home-cage. Secondly, since researchers need to be present to allow rats to engage with the task, the experiments would likely be taking place during the day when animals are not as active leading to disruption of their day-night cycle. Lastly, animals only have a limited amount of time and number of reaches that can be made in a training session.

Another automated version of the SPRT by Fenrich et al., combats the residual challenges mentioned above (2015). They designed an automated *ad libitum* full-time training robot in which rats were housed in their home-cage in groups of two to five. To participate in the reaching task, each rat could then cross a tunnel to enter a task enclosure where a sensor would detect when the animal is at the front of the enclosure to then allow for the automatic presentation of a food pellet. Animals were able to interact with the task completely autonomously and at any time of the day (Fenrich et al., 2015). This design is very similar to the HASRA, although the HASRA is used for training mice and does not require animals to enter another enclosure to interact with the task resulting in the HASRA's more compact design. Another advantage of our HASRA design is that each mouse had an identification tag so that we can track each individual animal's engagement with the task through their number of entries and time spent in the reaching tunnel. Furthermore, through our unique identification tags, we can personalize the task to accommodate each mouse's handedness during millet seed presentation.

These advantages make the HASRA an ideal device for the assessment of forelimb motor function in mice.

5.4 The effect of training level on performance post-stroke

Through our analysis, we found that performance and learning rates during the training period were significant predictors of endpoint performance. These findings suggest that training performance could have an effect of post-stroke recovery. There have been a few studies which investigated the role of baseline training on the execution of motor skills following damage or inactivation to M1 (Hwang et al., 2019; Kawai et al., 2015). For instance, in a study by Hwang et al., researchers investigated motor performance and M1 involvement following long-term training on a forelimb two-dimensional joystick task (2019). In their study, they had three groups of animals whose training ended at three different timepoints: 1) Early (around 10 days of training), 2) middle (around 25 days of training), and 3) late (more than 60 days of training). Once the training period for each of these groups of animals was completed, experimenters used optogenetic techniques to temporarily inactivate M1 through the activation of parvalbumin expressing inhibitory interneurons. Following M1 inactivation, performance of the three groups was assessed and they found that forelimb movements in the early and middle training groups were impaired but not movements for the late training group.

In another study by Kawai et al., researchers were able to show that the motor cortex is required for learning but not the execution of a motor skill (2015). This study demonstrated this by showing how rats that were well trained on a temporally precise lever-pressing task had a preservation in their performance following a lesion made to the motor cortex compared to untrained animals (Kawai et al., 2015). Collectively, these findings suggest that M1 was less

engaged for well learned tasks and suggest a role for subcortical structures, such as the striatum, in the storage and execution of well learned motor movements (Hwang et al., 2019; Kawai et al., 2015). Thus, it would be interesting in the future for our group to investigate differences in performance following a stroke targeting M1 in one group of animals who are experts at the reaching task, and in another group of animals who are at the novice level.

5.5 The importance of lesion location to stroke impairment and recovery

The effect of lesion location on upper limb motor functioning is more commonly investigated in the clinical stroke population than in preclinical rodent studies. Various clinical studies have shown that the location of the lesion is correlated with functional outcomes following stroke (Shelton & Reding, 2001; Liepert et al., 2005; Ernst et al., 2018; Zhao et al., 2018). Since lesion location appears to be an important factor in recovery for stroke patients, it is important that this aspect also be explored in preclinical rodent models. For this reason, we used software from the QUINT workflow to design our lesion localization workflow and quantify damage in the different anatomical regions affected (Puchades et al., 2019; Yates et al., 2019; Bjerke et al., 2021). From our workflow, we found that mice in the low endpoint success group had significantly more damage in M2 than those in the high endpoint success group. Furthermore, we found that M2 was a predictor of endpoint success rate, with animals containing more M2 damage, having lower success rates by endpoint.

These findings can be explained by previous studies which demonstrated the importance of M2 in reaching and grasping movements (Wang et al., 2017; Galiñanes et al., 2018). In a study investigating the role and organization of corticospinal neurons in the execution of a skilled forelimb food-pellet retrieval task, the researchers found that the highest concentration of

corticospinal “pre-grasping” neurons were located in M2 (Wang et al., 2017). Similarly, another study investigated reaching movements for water droplets prior to and following optogenetic inactivation of the motor cortex (Galiñanes et al., 2018). These researchers found that optogenetic inactivation of M2 during an ongoing reach resulted in motor impairments and found that inactivation of M1 did not affect ongoing reaching movements (Galiñanes et al., 2018). Altogether, these findings further suggest that the execution of well learned reaching and grasping movements become independent of M1 but may still require input from M2 to maintain motor vigor (Wang et al., 2017; Galiñanes et al., 2018).

5.6 Limitations and future directions

Although this study revealed interesting and significant findings, there are still some limitations that exist. One limitation of our study is the limited number of trials used for our success rate measurements. Despite animals having unlimited access to the reaching task, we were only able to manually score 20 trials every other day for each animal, except the time periods of interest where every day was scored. This limited number of trials assessed could limit our success rate measurements. To obtain a more complete view of the animals’ performance, all trials would need to be scored which would require automation of our scoring methods. In a study by Kakanos et al., researchers designed a benchtop device that allows for the automation of the SPRT (2022). In their experiments, animals would be removed from their home-cage and allowed to engage with the reaching task in the benchtop device for 20 minutes per day, 5 days a week while a video camera was used to record each trial. All recorded trials would be put through two supervised machine learning algorithms to allow for automatic scoring of trials. They used DLC to train, label, and analyze their videos. Then, using the DLC outputs, they used

a recurrent neural network (RNN) to predict trial outcomes (Kakanos et al., 2020). Similarly to this study, in the future we hope to combine our DLC outputs with a RNN to obtain an automated calculation of success rate for all trials performed on all experimental days. This automated approach could reveal more about the time course of impairment and recovery and could allow us to discover additional predictors of recovery and performance at the residual impairment period.

Another limitation of our study is that we did not investigate if compensatory strategies were used by mice following the stroke procedure since that could affect the animals' recovery. There are various changes in reaching behaviour that could suggest motor compensation, such as trunk rotation, variable and unsmooth reaching trajectories, abnormal kinematic synergies, elbow flexion, shoulder adduction, and shoulder rotation (Balbinot et al., 2022; Balbinot et al., 2018). A recent study by O'Neill et al., successfully used DLC to track mouse forepaw movements during reaching and pellet retrieval at the SPRT to investigate compensation and recovery after spinal cord injury (2022). To do this, they used a camera with a 120 fps and labelled the following in DLC: nose, thumb, dorsal ulnar edge, middle knuckle, index knuckle, ring knuckle, and pinky knuckle, index tip, middle tip, ring tip, and pinky tip. Through labelling the individual digits of the mice's hands, they were able to detect deficits in pronation following surgery. In the future, we could use a similar labelling strategy in DLC combined with a higher frame rate to explore motor compensation post-stroke.

6. CONCLUSION

Overall, the HASRA allows animals to autonomously interact with the reaching task within a home-cage environment and allows experimenters to assess these animals' motor impairments and recovery following stroke. In our study, we were also able to investigate reaching behaviour

and quantify damage in different brain regions. This study demonstrates how the HASRA can also be used to better understand how different aspects of motor training, task engagement, and stroke location impact the animals' performance post-stroke.

7. SUPPLEMENTAL FIGURES

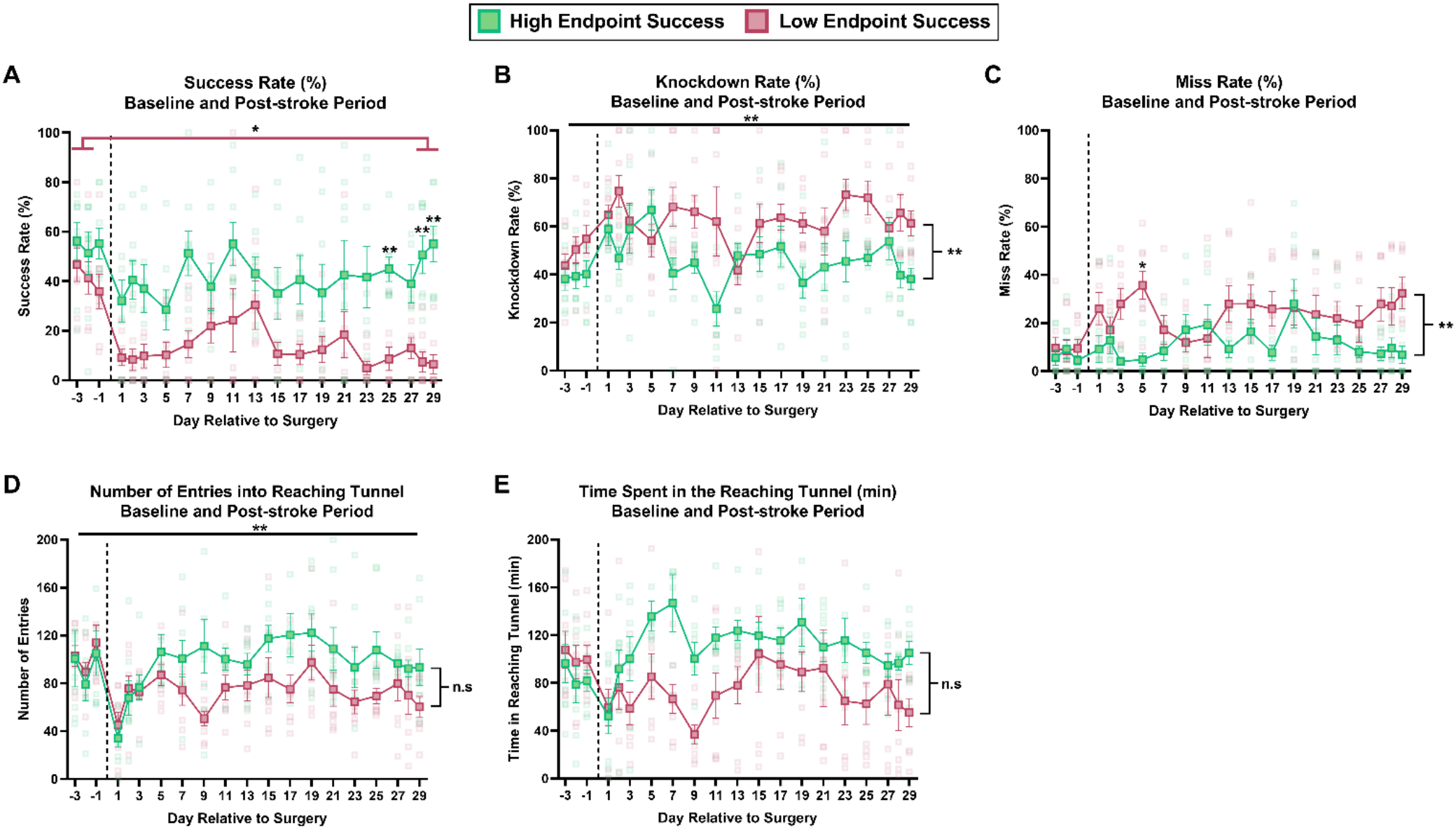

Figure S1. Baseline and post-stroke scored days comparing the high and low endpoint success groups. (A) Success rate. (B) Knockdown rate. (C) Miss rate. (D) Number of entries into the reaching tunnel. (E) Time spent in the reaching tunnel (min). All data is presented as mean ± SEM. Individual data points displayed as translucent green- and pink-coloured dots. Significance of $p < 0.05$ is represented by (*).

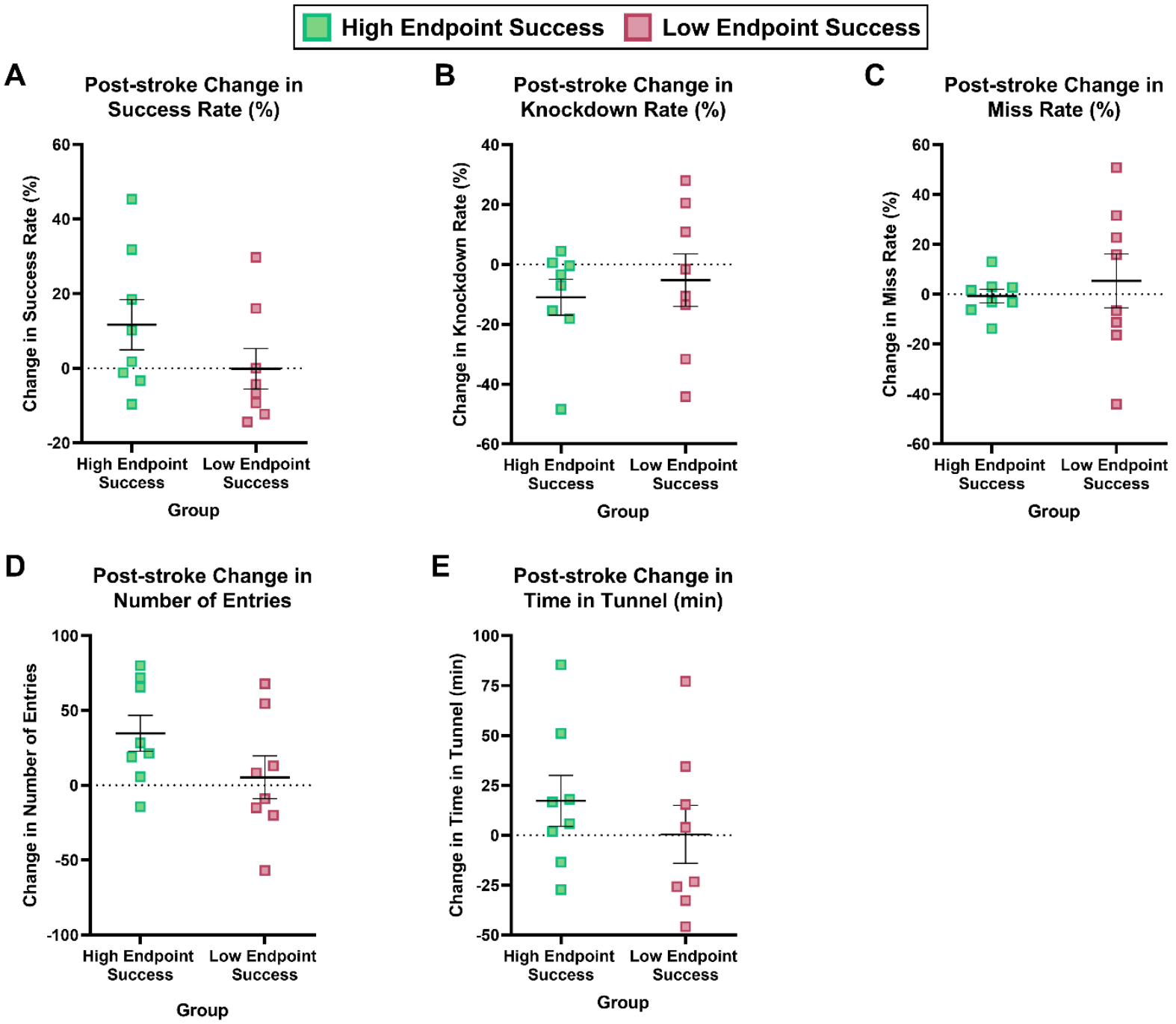

Figure S2. Change in performance and engagement parameters between the endpoint and acute periods for mice in high endpoint success (n = 8) and low endpoint success (n = 8) sub-groups. Post-stroke changes in (A) success rate, (B) knockdown rate, (C) miss rate, (D) number of entries into reaching tunnel, and (E) time spent in reaching tunnel (min).

Bibliography

Adolphs, R., Damasio, H., Tranel, D., Cooper, G., & Damasio, A. R. (2000). A role for somatosensory cortices in the visual recognition of emotion as revealed by three-dimensional lesion mapping. *The Journal of Neuroscience*, *20*(7), 2683–2690. http://doi.org/10.1523/jneurosci.20-07-02683.2000

Alaverdashvili, M., Moon, S.-K., Beckman, C. D., Virag, A., & Whishaw, I. Q. (2008). Acute but not chronic differences in skilled reaching for food following motor cortex devascularization vs. photothrombotic stroke in the rat. *Neuroscience*, 157(2), 297–308. doi:10.1016/j.neuroscience.2008.09.015

Alaverdashvili, M., & Whishaw, I. Q. (2010). Compensation aids skilled reaching in aging and in recovery from forelimb motor cortex stroke in the rat. *Neuroscience*, 167(1), 21–30. doi:10.1016/j.neuroscience.2010.02.001

Alaverdashvili, M., & Whishaw, I. Q. (2013). A behavioral method for identifying recovery and compensation: Hand use in a preclinical stroke model using the single pellet reaching task. *Neuroscience Biobehavioral Reviews*, *37*(5), 950–967. http://doi.org/10.1016/j.neubiorev.2013.03.026

Bacigaluppi, M., Comi, G., & Hermann, D. M. (2010). Animal models of ischemic stroke. part Two: Modeling cerebral ischemia. *The Open Neurology Journal*, *4*(2), 34–38. http://doi.org/10.2174/1874205x01004020034

Balbinot, G., Denize, S., & Lagace, D. C. (2022). The emergence of stereotyped kinematic synergies when mice reach to grasp following stroke. *Neurorehabilitation and Neural Repair*, *36*(1), 69–79. http://doi.org/10.1177/15459683211058174

Balbinot, G., Schuch, C. P., Jeffers, M. S., McDonald, M. W., Livingston-Thomas, J. M., & Corbett, D. (2018). Post-stroke kinematic analysis in rats reveals similar reaching abnormalities as humans. *Scientific Reports*, 8(1). doi:10.1038/s41598-018-27101-0

Balcombe, J. P., Barnard, N. D., & Sandusky, C. (2004). Laboratory routines cause animal stress. *Contemporary Topics in Laboratory Animal Science*, *43*(6), 42–51.

Bentzon, J. F., Otsuka, F., Virmani, R., & Falk, E. (2014). Mechanisms of plaque formation and rupture. *Circulation Research*, *114*(12), 1852–1866. http://doi.org/10.1161/circresaha.114.302721

Berge, E., Whiteley, W., Audebert, H., De Marchis, G. M., Fonseca, A. C., Padiglioni, C., … Turc, G. (2021). European Stroke Organisation (ESO) guidelines on intravenous thrombolysis for acute ischaemic stroke. *European Stroke Journal*, *6*(1). http://doi.org/10.1177/2396987321989865

Berkhemer, O. A., Fransen, P. S. S., Beumer, D., van den Berg, L. A., Lingsma, H. F., Yoo, A. J., … Dippel, D. W. J. (2015). A randomized trial of intraarterial treatment for acute ischemic stroke. *New England Journal of Medicine*, *372*(1), 11–20. http://doi.org/10.1056/nejmoa1411587

Bjerke, I. E., Yates, S. C., Laja, A., Witter, M. P., Puchades, M. A., Bjaalie, J. G., & Leergaard, T. B. (2021). Densities and numbers of calbindin and parvalbumin positive neurons across the rat and Mouse Brain. *IScience*, *24*(1), 101906. http://doi.org/10.1016/j.isci.2020.101906

Bleyenheuft, Y., & Gordon, A. M. (2014). Precision Grip in congenital and acquired hemiparesis: Similarities in impairments and implications for neurorehabilitation. *Frontiers in Human Neuroscience*, *8*. http://doi.org/10.3389/fnhum.2014.00459

Blixhavn, C. H., Haug, F.-M. Š., Kleven, H., Puchades, M. A., Bjaalie, J. G., & Leergaard, T. B. (2023). A Timm-Nissl multiplane microscopic atlas of Rat Brain zincergic terminal fields and metal-containing glia. *Scientific Data*, *10*(1). http://doi.org/10.1038/s41597-023-02012-6

Boboc, I. K., Rotaru-Zavaleanu, A. D., Calina, D., Albu, C. V., Catalin, B., & Turcu-Stiolica, A. (2023). A preclinical systematic review and meta-analysis of behavior testing in mice models of ischemic stroke. *Life*, *13*(2), 567. http://doi.org/10.3390/life13020567

Bogaert, L., Scheller, D., Moonen, J., Sarre, S., Smolders, I., Ebinger, G., & Michotte, Y. (2000). Neurochemical changes and laser Doppler flowmetry in the endothelin-1 rat model for focal cerebral ischemia. *Brain Research*, *887*(2), 266–275. http://doi.org/10.1016/s0006-8993(00)02959-0

Bouley, J., Fisher, M., & Henninger, N. (2007). Comparison between coated vs. uncoated suture middle cerebral artery occlusion in the rat as assessed by perfusion/diffusion weighted imaging. *Neuroscience Letters*, *412*(3), 185–190. http://doi.org/10.1016/j.neulet.2006.11.003

Brott, T., Marler, J. R., Olinger, C. P., Adams, H. P., Tomsick, T., Barsan, W. G., … Walker, M. (1989). Measurements of acute cerebral infarction: Lesion size by computed tomography. *Stroke*, *20*(7), 871–875. http://doi.org/10.1161/01.str.20.7.871

Buchan, A. M., Xue, D., & Slivka, A. (1992). A new model of temporary focal neocortical ischemia in the rat. *Stroke*, *23*(2), 273–279. http://doi.org/10.1161/01.str.23.2.273

Bütefisch, C., Hummelsheim, H., Denzler, P., & Mauritz, K.-H. (1995). Repetitive training of isolated movements improves the outcome of motor rehabilitation of the centrally Paretic Hand. *Journal of the Neurological Sciences*, *130*(1), 59–68. http://doi.org/10.1016/0022-510x(95)00003-k

Canning, C. G., Ada, L., & O'Dwyer, N. (1999). Slowness to develop force contributes to weakness after stroke. *Archives of Physical Medicine and Rehabilitation*, *80*(1), 66–70. http://doi.org/10.1016/s0003-9993(99)90309-x

Carr, J. H., & Shepherd, R. (1998). *Neurological Rehabilitation: Optimizing Motor Performance* (1st ed.). Oxford: Churchill Livingstone.

Carr, J. H., & Shepherd, R. B. (1987). *A Motor Relearning Programme for Stroke* (2nd ed.). London: Heinemann Medical.

Carr, J. H., & Shepherd, R. B. (1990). A motor learning model for rehabilitation of the movement disabled. In L. Ada & C. Canning (Eds.), *Key Issues in Neurological Physiotherapy*. (pp. 1–24). Chapter, Oxford: Heinemann Medical.

Carroll, D. (1965). A quantitative test of upper extremity function. *Journal of Chronic Diseases*, *18*(5), 479–491. http://doi.org/10.1016/0021-9681(65)90030-5

Chae, J., Yang, G., Park, B. K., & Labatia, I. (2002). Delay in initiation and termination of muscle contraction, motor impairment, and physical disability in Upper Limb Hemiparesis. *Muscle & Nerve*, *25*(4), 568–575. http://doi.org/10.1002/mus.10061

Chen, C. C., Gilmore, A., & Zuo, Y. (2014). Study Motor Skill Learning by single-pellet reaching tasks in mice. *Journal of Visualized Experiments*, (85). http://doi.org/10.3791/51238

Chugh, C. (2019). Acute ischemic stroke: Management approach. *Indian Journal of Critical Care Medicine*, *23*(S2), 140–146. http://doi.org/10.5005/jp-journals-10071-23192

Cirstea, M. C., & Levin, M. F. (2000). Compensatory strategies for reaching in stroke. *Brain*, *123*(5), 940–953. http://doi.org/10.1093/brain/123.5.940

Clarkson, A. N., López-Valdés, H. E., Overman, J. J., Charles, A. C., Brennan, K., & Carmichael, S. T. (2013). Multimodal examination of structural and functional remapping in the mouse photothrombotic stroke model. *Journal of Cerebral Blood Flow & Metabolism*, 33(5), 716–723. doi:10.1038/jcbfm.2013.7

Colle, L. M., Holmes, L. J., & Pappius, H. M. (1986). Correlation between behavioral status and cerebral glucose utilization in rats following freezing lesion. *Brain Research*, *397*(1), 27–36. http://doi.org/10.1016/0006-8993(86)91366-1

Collen, D. (1987). Molecular mechanism of action of newer thrombolytic agents. *Journal of the American College of Cardiology*, *10*(5), 11B–15B. http://doi.org/10.1016/s0735-1097(87)80422-9

Connolly, E. S., Winfree, C. J., Stern, D. M., Stern, D. M., Solomon, R. A., & Pinsky, D. J. (1996). Procedural and strain-related variables significantly affect outcome in a murine model of focal cerebral ischemia. *Neurosurgery*, *38*(3), 523–532. http://doi.org/10.1097/00006123-199603000-00021

Coupar, F., Pollock, A., Legg, L. A., Sackley, C., & van Vliet, P. (2012). Home-based therapy programmes for upper limb functional recovery following stroke. *Cochrane Database of Systematic Reviews*. http://doi.org/10.1002/14651858.cd006755.pub2

Coupar, F., Pollock, A., van Wijck, F., Morris, J., & Langhorne, P. (2010). Simultaneous bilateral training for improving arm function after stroke. *Cochrane Database of Systematic Reviews*. http://doi.org/10.1002/14651858.cd006432.pub2

Cramer, S. C., Nelles, G., Benson, R. R., Kaplan, J. D., Parker, R. A., Kwong, K. K., … Rosen, B. R. (1997). A functional MRI study of subjects recovered from Hemiparetic stroke. *Stroke*, *28*(12), 2518–2527. http://doi.org/10.1161/01.str.28.12.2518

Cunningham, P., Turton, A. J., Van Wijck, F., & Van Vliet, P. (2016). Task-specific reach-to-grasp training after stroke: Development and description of a home-based intervention. *Clinical Rehabilitation*, *30*(8), 731–740. http://doi.org/10.1177/0269215515603438

Dauchy, R. T., Dauchy, E. M., Tirrell, R. P., Hill, C. R., Davidson, L. K., Greene, M. W., … Blask, D. E. (2010). Dark-phase light contamination disrupts circadian rhythms in plasma measures of endocrine physiology and metabolism in rats. *Comparative Medicine*, *60*(5), 348–356.

Dean, R. L., Scozzafava, J., Goas, J. A., Regan, B., Beer, B., & Bartus, R. T. (1981). Age-related differences in behavior across the life span of the C57BL/6J mouse. *Experimental Aging Research*, *7*(4), 427–451. http://doi.org/10.1080/03610738108259823

Deb, P., Sharma, S., & Hassan, K. M. (2010). Pathophysiologic mechanisms of acute ischemic stroke: An overview with emphasis on therapeutic significance beyond thrombolysis. *Pathophysiology*, *17*(3), 197–218. http://doi.org/10.1016/j.pathophys.2009.12.001

Dickinson, A. (1985). Actions and habits: The development of Behavioural Autonomy. *Philosophical Transactions of the Royal Society of London. B, Biological Sciences*, *308*(1135), 67–78. http://doi.org/10.1098/rstb.1985.0010

Donoghue, J. P. (1995). Plasticity of adult sensorimotor representations. *Current Opinion in Neurobiology*, *5*(6), 749–754. http://doi.org/10.1016/0959-4388(95)80102-2

Drude, N. I., Martinez Gamboa, L., Danziger, M., Dirnagl, U., & Toelch, U. (2021). Improving preclinical studies through replications. *ELife*, *10*. http://doi.org/10.7554/elife.62101

Ellens, D. J., Gaidica, M., Toader, A., Peng, S., Shue, S., John, T., … Leventhal, D. K. (2016). An automated rat single pellet reaching system with high-speed video capture. *Journal of Neuroscience Methods*, *271*, 119–127. http://doi.org/10.1016/j.jneumeth.2016.07.009

Ernst, M., Boers, A. M. M., Forkert, N. D., Berkhemer, O. A., Roos, Y. B., Dippel, D. W. J., … Gellissen, S. (2018). Impact of ischemic lesion location on the MRS score in patients with ischemic stroke: A voxel-based approach. *American Journal of Neuroradiology*, *39*(11), 1989–1994. http://doi.org/10.3174/ajnr.a5821

Fan, L. W., Lin, S., Pang, Y., Lei, M., Zhang, F., Rhodes, P., & Cai, Z. (2005). Hypoxia-ischemia induced neurological dysfunction and brain injury in the neonatal rat. *Behavioural Brain Research*, *165*(1), 80–90. http://doi.org/10.1016/j.bbr.2005.06.033

Fan, L. W., Lin, S., Pang, Y., Rhodes, P. G., & Cai, Z. (2006). Minocycline attenuates hypoxia-ischemia-induced neurological dysfunction and brain injury in the juvenile rat. *European Journal of Neuroscience*, *24*(2), 341–350. http://doi.org/10.1111/j.1460-9568.2006.04918.x

Farr, T. D., & Whishaw, I. Q. (2002). Quantitative and qualitative impairments in skilled reaching in the mouse (mus musculus) after a focal motor cortex stroke. *Stroke*, *33*(7), 1869–1875. http://doi.org/10.1161/01.str.0000020714.48349.4e

Feldman, R. G., & Lance, J. W. (1980). Pathophysiology of spasticity and clinical experience with baclofen. In R. G. Feldman, W. P. Koella, & R. R. Young (Eds.), *Spasticity, disordered motor control* (pp. 485–494). Book, Chicago, Illinois: Book Medical Publishers.

Fellows, L. K., & Farah, M. J. (2007). The role of ventromedial prefrontal cortex in decision making: Judgment under uncertainty or judgment per se? *Cerebral Cortex*, *17*(11), 2669–2674. http://doi.org/10.1093/cercor/bhl176

Feng Y, Liao S, Wei C, Jia D, Wood K, Liu Q, Wang X, Shi F-D, Jin W-N (2017). Infiltration and persistence of lymphocytes during late-stage cerebral ischemia in middle cerebral artery occlusion and photothrombotic stroke models. *Journal of Neuroinflammation 14: 1-12*. https://doi.org/10.1186/s12974-017-1017-0

Fenrich, K. K., May, Z., Hurd, C., Boychuk, C. E., Kowalczewski, J., Bennett, D. J., … Fouad, K. (2015). Improved single pellet grasping using automated ad libitum full-time training robot. *Behavioural Brain Research*, *281*, 137–148. http://doi.org/10.1016/j.bbr.2014.11.048

Finger, S. (1978). *Recovery from brain damage: Research and theory*. New York: Plenum Press.

Fouad, K., Hurd, C., & Magnuson, D. S. (2013). Functional testing in animal models of spinal cord injury: Not as straight forward as one would think. *Frontiers in Integrative Neuroscience*, *7*. http://doi.org/10.3389/fnint.2013.00085

French, B., Thomas, L. H., Leathley, M. J., Sutton, C. J., McAdam, J., Forster, A., … McMahon, N. (2007). Repetitive task training for improving functional ability after stroke. *Cochrane Database of Systematic Reviews*. http://doi.org/10.1002/14651858.cd006073.pub2

Frost, S. B., Barbay, S., Mumert, M. L., Stowe, A. M., & Nudo, R. J. (2006). An animal model of capsular infarct: Endothelin-1 injections in the rat. *Behavioural Brain Research*, *169*(2), 206–211. http://doi.org/10.1016/j.bbr.2006.01.014

Fuxe, K., Bjelke, B., Andbjer, B., Grahn, H., Rimondini, R., & Agnati, L. F. (1997). Endothelin-1 induced lesions of the frontoparietal cortex of the rat. A possible model of focal cortical ischemia. *NeuroReport*, *8*(11), 2623–2629. http://doi.org/10.1097/00001756-199707280-00040

Galiñanes, G. L., Bonardi, C., & Huber, D. (2018). Directional reaching for water as a cortex-dependent behavioral framework for Mice. *Cell Reports*, 22(10), 2767–2783. doi:10.1016/j.celrep.2018.02.042

Gharbawie, O. A., & Whishaw, I. Q. (2006). Parallel stages of learning and recovery of skilled reaching after motor cortex stroke: “oppositions” organize normal and compensatory movements. *Behavioural Brain Research*, 175(2), 249–262. doi:10.1016/j.bbr.2006.08.039

Goodale, M. A., & Milner, A. D. (1992). Separate visual pathways for perception and action. *Trends in Neurosciences*, *15*(1), 20–25. http://doi.org/10.1016/0166-2236(92)90344-8

Gracies, J.-M. (2005). Pathophysiology of spastic paresis. II: Emergence of muscle overactivity. *Muscle & Nerve*, *31*(5), 552–571. http://doi.org/10.1002/mus.20285

Haaxma, C. A., Bloem, B. R., Overeem, S., Borm, G. F., & Horstink, M. W. I. M. (2010). Timed Motor tests can detect subtle motor dysfunction in early parkinson's disease. *Movement Disorders*, *25*(9), 1150–1156. http://doi.org/10.1002/mds.23100

Hacke, W., Kaste, M., Bluhmki, E., Brozman, M., Dávalos, A., Guidetti, D., … Toni, D. (2008). Thrombolysis with alteplase 3 to 4.5 hours after acute ischemic stroke. *New England Journal of Medicine*, *359*(13), 1317–1329. http://doi.org/10.1056/nejmoa0804656

Hamdy, R. C., Krishnaswamy, G., Cancellaro, V., Whalen, K., & Harvill, L. (1993). Changes in bone mineral content and density after stroke. *American Journal of Physical Medicine & Rehabilitation*, *72*(4), 188–191. http://doi.org/10.1097/00002060-199308000-00003

Hata, R., Mies, G., Wiessner, C., Fritze, K., Hesselbarth, D., Brinker, G., & Hossmann, K.-A. (1998). A reproducible model of middle cerebral artery occlusion in mice: Hemodynamic, biochemical, and magnetic resonance imaging. *Journal of Cerebral Blood Flow & Metabolism*, *18*(4), 367–375. http://doi.org/10.1097/00004647-199804000-00004

Hatem, S. M., Saussez, G., della Faille, M., Prist, V., Zhang, X., Dispa, D., & Bleyenheuft, Y. (2016). Rehabilitation of motor function after stroke: A multiple systematic review focused on techniques to stimulate upper extremity recovery. *Frontiers in Human Neuroscience*, *10*. http://doi.org/10.3389/fnhum.2016.00442

Hebert, J. S., & Lewicke, J. (2012). Case report of modified box and blocks test with motion capture to measure prosthetic function. *The Journal of Rehabilitation Research and Development*, *49*(8), 1163. http://doi.org/10.1682/jrrd.2011.10.0207

Hebert, J. S., Lewicke, J., Williams, T. R., & Vette, A. H. (2014). Normative data for modified box and blocks test measuring upper-limb function via motion capture. *Journal of Rehabilitation Research and Development*, *51*(6), 918–932. http://doi.org/10.1682/jrrd.2013.10.0228

Hernandez, T. D., & Schallert, T. (1988). Seizures and recovery from experimental brain damage. *Experimental Neurology*, *102*(3), 318–324. http://doi.org/10.1016/0014-4886(88)90226-9

Higgins, J., Mayo, N. E., Desrosiers, J., Salbach, N. M., & Ahmed, S. (2005). Upper-limb function and recovery in the acute phase poststroke. *The Journal of Rehabilitation Research and Development*, *42*(1), 65. http://doi.org/10.1682/jrrd.2003.10.0156

Horie, N., Maag, A.-L., Hamilton, S. A., Shichinohe, H., Bliss, T. M., & Steinberg, G. K. (2008). Mouse model of focal cerebral ischemia using endothelin-1. *Journal of Neuroscience Methods*, *173*(2), 286–290. http://doi.org/10.1016/j.jneumeth.2008.06.013

Howells, D. W., Porritt, M. J., Rewell, S. S. J., O'Collins, V., Sena, E. S., van der Worp, H. B., … Macleod, M. R. (2010). Different strokes for different folks: The rich diversity of animal models of focal cerebral ischemia. *Journal of Cerebral Blood Flow & Metabolism*, *30*(8), 1412–1431. http://doi.org/10.1038/jcbfm.2010.66

Hwang, E. J., Dahlen, J. E., Hu, Y. Y., Aguilar, K., Yu, B., Mukundan, M., … Komiyama, T. (2019). Disengagement of motor cortex from movement control during long-term learning. *Science Advances*, *5*(10). http://doi.org/10.1126/sciadv.aay0001

Ikegami, S. (2000). Muscle Weakness, hyperactivity, and impairment in fear conditioning in tau-deficient mice. *Neuroscience Letters*, *279*(3), 129–132. http://doi.org/10.1016/s0304-3940(99)00964-7

Ivanco, T. L., & Greenough, W. T. (2000). Physiological consequences of morphologically detectable synaptic plasticity: Potential uses for examining recovery following damage. *Neuropharmacology*, *39*(5), 765–776. http://doi.org/10.1016/s0028-3908(00)00004-6

Jones, T. A., Chu, C. J., Grande, L. A., & Gregory, A. D. (1999). Motor skills training enhances lesion-induced structural plasticity in the motor cortex of adult rats. *The Journal of Neuroscience*, 19(22), 10153–10163. doi:10.1523/jneurosci.19-22-10153.1999

Joseph, J. A., Roth, G. S., & Lippa, A. S. (1986). Reduction of motor behavioral deficits in senescent animals via chronic prolactin administration I. Rotational behavior. *Neurobiology of Aging*, *7*(1), 31–35. http://doi.org/10.1016/0197-4580(86)90023-0

Kakanos, S. G., Gadiagellan, D., Kim, E., Cash, D., & Moon, L. D. (2022). ReachingBot: An Automated and Scalable Benchtop Device for Highly Parallel Single Pellet Reach-and-Grasp Training and Assessment in Mice. *bioRxiv*. doi:10.1101/2022.06.17.496542

Kamper, D. G., Fischer, H. C., Cruz, E. G., & Rymer, W. Z. (2006). Weakness is the primary contributor to finger impairment in chronic stroke. *Archives of Physical Medicine and Rehabilitation*, *87*(9), 1262–1269. http://doi.org/10.1016/j.apmr.2006.05.013

Karnath, H.-O. (2004). The anatomy of spatial neglect based on Voxelwise Statistical Analysis: A study of 140 patients. *Cerebral Cortex*, *14*(10), 1164–1172. http://doi.org/10.1093/cercor/bhh076

Kawai, R., Markman, T., Poddar, R., Ko, R., Fantana, A. L., Dhawale, A. K., … Ölveczky, B. P. (2015). Motor cortex is required for learning but not for executing a motor skill. *Neuron*, *86*(3), 800–812. http://doi.org/10.1016/j.neuron.2015.03.024

Kellor, M., Frost, J., Silberberg, N., Iversen, I., & Cummings, R. (1971). Hand strength and dexterity. *The American journal of occupational therapy: official publication of the American Occupational Therapy Association*, *25*(2), 77–83.

Kleim, J. A., & Jones, T. A. (2008). Principles of experience-dependent neural plasticity: Implications for rehabilitation after Brain Damage. *Journal of Speech, Language, and Hearing Research*, 51(1). doi:10.1044/1092-4388(2008/018)

Kleim, J. A., Bruneau, R., VandenBerg, P., MacDonald, E., Mulrooney, R., & Pocock, D. (2003). Motor cortex stimulation enhances motor recovery and reduces peri-infarct dysfunction following ischemic insult. *Neurological Research*, *25*(8), 789–793. http://doi.org/10.1179/016164103771953862

Klit, H., Finnerup, N. B., Andersen, G., & Jensen, T. S. (2011). Central poststroke pain: A population-based study. *Pain*, *152*(4), 818–824. http://doi.org/10.1016/j.pain.2010.12.030

Kontson, K., Marcus, I., Myklebust, B., & Civillico, E. (2017). Targeted box and blocks test: Normative data and comparison to standard tests. *PLOS ONE*, *12*(5). http://doi.org/10.1371/journal.pone.0177965

Kuriakose, D., & Xiao, Z. (2020). Pathophysiology and treatment of stroke: Present status and future perspectives. *International Journal of Molecular Sciences*, *21*(20), 7609. http://doi.org/10.3390/ijms21207609

Lang, C. E., Bland, M. D., Bailey, R. R., Schaefer, S. Y., & Birkenmeier, R. L. (2013). Assessment of upper extremity impairment, function, and activity after stroke: Foundations for Clinical Decision making. *Journal of Hand Therapy*, *26*(2), 104–115. http://doi.org/10.1016/j.jht.2012.06.005

Langhorne, P., Bernhardt, J., & Kwakkel, G. (2011). Stroke rehabilitation. *The Lancet*, *377*(9778), 1693–1702. http://doi.org/10.1016/s0140-6736(11)60325-5

Lansberg, M. G., Christensen, S., Kemp, S., Mlynash, M., Mishra, N., Federau, C., … Albers, G. W. (2017). Computed tomographic perfusion to predict response to recanalization in ischemic stroke. *Annals of Neurology*, *81*(6), 849–856. http://doi.org/10.1002/ana.24953

Lee, J.-K., Park, M.-S., Kim, Y.-S., Moon, K.-S., Joo, S.-P., Kim, T.-S., … Kim, S.-H. (2007). Photochemically induced cerebral ischemia in a mouse model. *Surgical Neurology*, *67*(6), 620–625. http://doi.org/10.1016/j.surneu.2006.08.077

Levin, M. F., Kleim, J. A., & Wolf, S. L. (2008). What do motor "recovery" and "compensation" mean in patients following stroke? *Neurorehabilitation and Neural Repair*, *23*(4), 313–319. http://doi.org/10.1177/1545968308328727

Levin, M. F., Michaelsen, S. M., Cirstea, C. M., & Roby-Brami, A. (2002). Use of the trunk for reaching targets placed within and beyond the reach in adult hemiparesis. *Experimental Brain Research*, *143*(2), 171–180. http://doi.org/10.1007/s00221-001-0976-6

Li, S. (2017). Spasticity, motor recovery, and neural plasticity after stroke. *Frontiers in Neurology*, *8*. http://doi.org/10.3389/fneur.2017.00120

Li, X., Blizzard, K. K., Zeng, Z., DeVries, A. C., Hurn, P. D., & McCullough, L. D. (2004). Chronic behavioral testing after focal ischemia in the mouse: Functional recovery and the effects of gender. *Experimental Neurology*, *187*(1), 94–104. http://doi.org/10.1016/j.expneurol.2004.01.004

Liepert, J., Restemeyer, C., Kucinski, T., Zittel, S., & Weiller, C. (2005). Motor strokes: the lesion location determines motor excitability changes. *Stroke*, *36*(12), 2648–2648. http://doi.org/10.1161/01.str.0000189629.10603.02

Liu, Z., Li, Y., Zhang, R. L., Cui, Y., & Chopp, M. (2011). Bone marrow stromal cells promote skilled motor recovery and enhance contralesional axonal connections after ischemic stroke in adult mice. *Stroke*, *42*(3), 740–744. http://doi.org/10.1161/strokeaha.110.607226

Lyle, R. C. (1981). A performance test for assessment of upper limb function in physical rehabilitation treatment and research. *International Journal of Rehabilitation Research*, *4*(4), 483–492. http://doi.org/10.1097/00004356-198112000-00001

Macrae, I. M., Robinson, M. J., Graham, D. I., Reid, J. L., & McCulloch, J. (1993). Endothelin-1-induced reductions in cerebral blood flow: Dose dependency, time course, and neuropathological consequences. *Journal of Cerebral Blood Flow & Metabolism*, *13*(2), 276–284. http://doi.org/10.1038/jcbfm.1993.34

Maldonado, M. A., Allred, R. P., Felthauser, E. L., & Jones, T. A. (2008). Motor skill training, but not voluntary exercise, improves skilled reaching after unilateral ischemic lesions of the sensorimotor cortex in rats. *Neurorehabilitation and Neural Repair*, *22*(3), 250–261. http://doi.org/10.1177/1545968307308551

Masaki, T. (1998). The discovery of Endothelins. *Cardiovascular Research*, *39*(3), 530–533. http://doi.org/10.1016/s0008-6363(98)00153-9

Mathiowetz, V., Weber, K., Kashman, N., & Volland, G. (1985). Adult norms for the nine hole peg test of Finger Dexterity. *The Occupational Therapy Journal of Research*, *5*(1), 24–38. http://doi.org/10.1177/153944928500500102

McCrea, P. H., Eng, J. J., & Hodgson, A. J. (2005). Saturated muscle activation contributes to compensatory reaching strategies after stroke. *Journal of Neurophysiology*, *94*(5), 2999–3008. http://doi.org/10.1152/jn.00732.2004

Meschia, J. F., & Brott, T. (2017). Ischaemic stroke. *European Journal of Neurology*, *25*(1), 35–40. http://doi.org/10.1111/ene.13409

Michaelsen, S. M., & Levin, M. F. (2004). Short-term effects of practice with trunk restraint on reaching movements in patients with chronic stroke. *Stroke*, *35*(8), 1914–1919. http://doi.org/10.1161/01.str.0000132569.33572.75

Michaelsen, S. M., Dannenbaum, R., & Levin, M. F. (2006). Task-specific training with trunk restraint on arm recovery in stroke. *Stroke*, *37*(1), 186–192. http://doi.org/10.1161/01.str.0000196940.20446.c9

Michaelsen, S. M., Luta, A., Roby-Brami Agnès, & Levin, M. F. (2001). Effect of trunk restraint on the recovery of reaching movements in Hemiparetic patients. *Stroke*, *32*(8), 1875–1883. http://doi.org/10.1161/01.str.32.8.1875

Mirza Agha, B., Akbary, R., Ghasroddashti, A., Nazari-Ahangarkolaee, M., Whishaw, I. Q., & Mohajerani, M. H. (2020). Cholinergic upregulation by optogenetic stimulation of nucleus basalis after photothrombotic stroke in forelimb somatosensory cortex improves endpoint and motor but not sensory control of skilled reaching in mice. *Journal of Cerebral Blood Flow & Metabolism*, 41(7), 1608–1622. doi:10.1177/0271678x20968930

Modo, M., Stroemer, R. P., Tang, E., Veizovic, T., Sowniski, P., & Hodges, H. (2000). Neurological sequelae and long-term behavioural assessment of rats with transient middle cerebral artery occlusion. *Journal of Neuroscience Methods*, *104*(1), 99–109. http://doi.org/10.1016/s0165-0270(00)00329-0

Mudie, M. H., & Matyas, T. A. (2000). Can simultaneous bilateral movement involve the undamaged hemisphere in reconstruction of neural networks damaged by stroke? *Disability and Rehabilitation*, *22*(1-2), 23–37. http://doi.org/10.1080/096382800297097

Musuka, T. D., Wilton, S. B., Traboulsi, M., & Hill, M. D. (2015). Diagnosis and management of acute ischemic stroke: Speed is critical. *Canadian Medical Association Journal*, *187*(12), 887–893. http://doi.org/10.1503/cmaj.140355

Naess, H., Lunde, L., & Brogger, J. (2012). The effects of fatigue, pain, and depression on quality of life in ischemic stroke patients: The bergen stroke study. *Vascular Health and Risk Management*, 407. http://doi.org/10.2147/vhrm.s32780

Nagasawa, H., & Kogure, K. (1989). Correlation between cerebral blood flow and histologic changes in a new rat model of middle cerebral artery occlusion. *Stroke*, *20*(8), 1037–1043. http://doi.org/10.1161/01.str.20.8.1037

Nath, T., Mathis, A., Chen, A. C., Patel, A., Bethge, M., & Mathis, M. W. (2019). Using DeepLabCut for 3D markerless pose estimation across species and behaviors. *Nature Protocols*, *14*(7), 2152–2176. http://doi.org/10.1038/s41596-019-0176-0

National Institute of Neurological Disorders and Stroke rt-PA Stroke Study Group. (1995). Tissue plasminogen activator for acute ischemic stroke. *New England Journal of Medicine*, *333*(24), 1581–1588. http://doi.org/10.1056/nejm199512143332401

Nemchek, V., Haan, E. M., & Kerr, A. L. (2020). Intermittent skill training results in moderate improvement in functional outcome in a mouse model of ischemic stroke. *Neurorehabilitation and Neural Repair*, 35(1), 79–87. doi:10.1177/1545968320975423

Nudo, R. (2003a). Adaptive plasticity in motor cortex: Implications for rehabilitation after Brain Injury. *Journal of Rehabilitation Medicine, 35*, 7–10. http://doi.org/10.1080/16501960310010070

Nudo, R. J. (2003b). Functional and structural plasticity in motor cortex: Implications for stroke recovery. *Physical Medicine and Rehabilitation Clinics of North America*, *14*(1). http://doi.org/10.1016/s1047-9651(02)00054-2

Nudo, R. J., Barvay, S., & Kleim, J. A. (2000). Role of neuroplasticity in functional recovery after stroke. In H. S. Levin & J. Grafman (Eds.), *Cerebral reorganization of function after Brain Damage* (pp. 168–200). essay, Oxford: Oxford University Press.

O'Bryant, A. J., Allred, R. P., Maldonado, M. A., Cormack, L. K., & Jones, T. A. (2011). Breeder and batch-dependent variability in the acquisition and performance of a motor skill in adult long–evans rats. *Behavioural Brain Research*, *224*(1), 112–120. http://doi.org/10.1016/j.bbr.2011.05.028

Oliff, H. S., Weber, E., Eilon, G., & Marek, P. (1995). The role of strain/vendor differences on the outcome of focal ischemia induced by intraluminal middle cerebral artery occlusion in the rat. *Brain Research*, *675*(1-2), 20–26. http://doi.org/10.1016/0006-8993(95)00033-m

Olsen, T. S. (1986). Regional cerebral blood flow after occlusion of the middle cerebral artery. *Acta Neurologica Scandinavica*, *73*(4), 321–337. http://doi.org/10.1111/j.1600-0404.1986.tb03286.x

O'Neill, N., Mah, K. M., Badillo-Martinez, A., Jann, V., Bixby, J. L., & Lemmon, V. P. (2022). Markerless tracking enables distinction between strategic compensation and functional recovery after Spinal Cord Injury. *Experimental Neurology*, *354*, 114085. http://doi.org/10.1016/j.expneurol.2022.114085

Ono, H., Imai, H., Miyawaki, S., Nakatomi, H., & Saito, N. (2016). Rat white matter injury model induced by endothelin-1 injection: Technical modification and pathological evaluation. *Acta Neurobiologiae Experimentalis*, *76*(3), 212–224. http://doi.org/10.21307/ane-2017-021

Page, S. J., Sisto, S. A., Johnston, M. V., & Levine, P. (2002). Modified constraint-induced therapy after Subacute Stroke: A preliminary study. *Neurorehabilitation and Neural Repair*, *16*(3), 290–295. http://doi.org/10.1177/154596830201600307

Page, S. J., Sisto, S. A., Johnston, M. V., Levine, P., & Hughes, M. (2001). Modified constraint induced therapy: a randomized feasibility and efficacy study. *Journal of Rehabilitation and Development*, *38*(5), 583–590.

Pelton, T., van Vliet, P., & Hollands, K. (2012). Interventions for improving coordination of reach to grasp following stroke: A systematic review. *International Journal of Evidence-Based Healthcare*, *10*(2), 89–102. http://doi.org/10.1111/j.1744-1609.2012.00261.x

Powers, W. J., Rabinstein, A. A., Ackerson, T., Adeoye, O. M., Bambakidis, N. C., Becker, K., … Tirschwell, D. L. (2019). Guidelines for the early management of patients with acute ischemic stroke: 2019 update to the 2018 guidelines for the early management of acute ischemic stroke: A guideline for healthcare professionals from the American Heart Association/American Stroke Association. *Stroke*, *50*(12), e344–418. http://doi.org/10.1161/str.0000000000000211

Puchades, M. A., Csucs, G., Ledergerber, D., Leergaard, T. B., & Bjaalie, J. G. (2019). Spatial registration of serial microscopic brain images to three-dimensional reference atlases with the quicknii tool. *PLOS ONE*, *14*(5). http://doi.org/10.1371/journal.pone.0216796

Raghavan, P. (2015). Upper Limb Motor Impairment after stroke. *Physical Medicine and Rehabilitation Clinics of North America*, *26*(4), 599–610. http://doi.org/10.1016/j.pmr.2015.06.008

Raghavan, P., Santello, M., Gordon, A. M., & Krakauer, J. W. (2010). Compensatory motor control after stroke: An alternative joint strategy for object-dependent shaping of hand posture. *Journal of Neurophysiology*, *103*(6), 3034–3043. http://doi.org/10.1152/jn.00936.2009

Renner, C. I. E., Bungert-Kahl, P., & Hummelsheim, H. (2009). Change of strength and rate of rise of tension relate to functional arm recovery after stroke. *Archives of Physical Medicine and Rehabilitation*, *90*(9), 1548–1556. http://doi.org/10.1016/j.apmr.2009.02.024

Rensink, M., Schuurmans, M., Lindeman, E., & Hafsteinsdóttir, T. (2009). Task-oriented training in rehabilitation after stroke: Systematic review. *Journal of Advanced Nursing*, *65*(4), 737–754. http://doi.org/10.1111/j.1365-2648.2008.04925.x

Rioult-Pedotti, M.-S., Friedman, D., Hess, G., & Donoghue, J. P. (1998). Strengthening of horizontal cortical connections following skill learning. *Nature Neuroscience*, *1*(3), 230–234. http://doi.org/10.1038/678

Robinson, M. J., Macrae, I. M., Todd, M., Reid, J. L., & McCulloch, J. (1990). Reduction of local cerebral blood flow to pathological levels by endothelin-1 applied to the middle cerebral artery in the rat. *Neuroscience Letters*, *118*(2), 269–272. http://doi.org/10.1016/0304-3940(90)90644-o

Robinson, M. J., Macrae, I. M., Todd, M., Reid, J. L., & McCulloch, J. (1991). Reduction in local cerebral blood flow induced by endothelin-1 applied topically to the middle cerebral artery in the rat. *Journal of Cardiovascular Pharmacology*, *17*. http://doi.org/10.1097/00005344-199100177-00101

Roby-Brami, A., Jacobs, S., Bennis, N., & Levin, M. F. (2003). Hand orientation for grasping and arm joint rotation patterns in healthy subjects and hemiparetic stroke patients. *Brain Research*, *969*(1-2), 217–229. http://doi.org/10.1016/s0006-8993(03)02334-5

Rogers, D. C., Campbell, C. A., Stretton, J. L., & Mackay, K. B. (1997). Correlation between motor impairment and infarct volume after permanent and transient middle cerebral artery occlusion in the rat. *Stroke*, *28*(10), 2060–2066. http://doi.org/10.1161/01.str.28.10.2060

Ruan, J., & Yao, Y. (2020). Behavioral tests in rodent models of stroke. *Brain Hemorrhages*, *1*(4), 171–184. http://doi.org/10.1016/j.hest.2020.09.001

Ryait, H., Bermudez-Contreras, E., Harvey, M., Faraji, J., Mirza Agha, B., Gomez-Palacio Schjetnan, A., … Luczak, A. (2019). Data-driven analyses of motor impairments in animal models of neurological disorders. *PLOS Biology*, *17*(11). http://doi.org/10.1371/journal.pbio.3000516

Sacco, R. L., Kasner, S. E., Broderick, J. P., Caplan, L. R., Connors, J. J., Culebras, A., Elkind, M. S. V., George, M. G., Hamdan, A. D., Higashida, R. T., Hoh, B. L., Janis, L. S., Kase, C. S., Kleindorfer, D. O., Lee, J. M., Moseley, M. E., Peterson, E. D., Turan, T. N., Valderrama, A. L., and Vinters, H. v. (2013) An updated definition of stroke for the 21st century: A statement for healthcare professionals from the American heart association/American stroke association. Stroke. 44, 2064–2089

Saes, M., Mohamed Refai, M. I., van Kordelaar, J., Scheltinga, B. L., van Beijnum, B.-J. F., Bussmann, J. B., … Kwakkel, G. (2021). Smoothness metric during reach-to-grasp after stroke: Part 2. Longitudinal Association with Motor Impairment. *Journal of NeuroEngineering and Rehabilitation*, 18(1). doi:10.1186/s12984-021-00937-w

Salameh, G., Jeffers, M. S., Wu, J., Pitney, J., & Silasi, G. (2020). The home-cage automated skilled reaching apparatus (HASRA): Individualized training of group-housed mice in a single pellet reaching task. *Eneuro*, *7*(5). http://doi.org/10.1523/eneuro.0242-20.2020

Salter K, Campbell N, Richardson M, Nehta S, Jutai J, Zettler L, Moses M, McClure A, Mays R, Foley N, Teasell R. (2013). Outcome measures in stroke rehabilitation. In: Evidence-Based Review of Stroke Rehabilitation. London, ON, Canada: EBRSR.

Saver, J. L., Goyal, M., Bonafe, A., Diener, H.-C., Levy, E. I., Pereira, V. M., … Jahan, R. (2015). Stent-retriever thrombectomy after intravenous T-pa vs. T-pa alone in stroke. *New England Journal of Medicine*, *372*(24), 2285–2295. http://doi.org/10.1056/nejmoa1415061

Schallert, T., Fleming, S. M., Leasure, J. L., Tillerson, J. L., & Bland, S. T. (2000). CNS plasticity and assessment of forelimb sensorimotor outcome in unilateral rat models of stroke, cortical ablation, parkinsonism and spinal cord injury. *Neuropharmacology*, *39*(5), 777–787. http://doi.org/10.1016/s0028-3908(00)00005-8

Schneider, C. A., Rasband, W. S., & Eliceiri, K. W. (2012). NIH image to imagej: 25 years of image analysis. *Nature Methods*, *9*(7), 671–675. http://doi.org/10.1038/nmeth.2089

Shah, F. A., Li, T., Kury, L. T., Zeb, A., Khatoon, S., Liu, G., … Li, S. (2019). Pathological comparisons of the hippocampal changes in the transient and permanent middle cerebral artery occlusion rat models. *Frontiers in Neurology*, *10*. http://doi.org/10.3389/fneur.2019.01178

Sharkey, J. (1993). Perivascular microapplication of endothelin-1: A new model of focal cerebral ischaemia in the rat. *Journal of Cerebral Blood Flow and Metabolism*, *13*(5), 865–871. http://doi.org/10.1038/jcbfm.1993.108

Shelton Fátima de, & Reding, M. J. (2001). Effect of lesion location on upper limb motor recovery after stroke. *Stroke*, *32*(1), 107–112. http://doi.org/10.1161/01.str.32.1.107

Shumway-Cook, A., & Woollacott, M. H. (2001). *Motor control: Theory and practical applications*. Philadelphia: Lippincott Williams & Wilkins.

Slager, C. J., Wentzel, J. J., Gijsen, F. J. H., Thury, A., Van der Wal, A. C., Schaar, J. A., & Serruys, P. W. (2005). The role of shear stress in the destabilization of vulnerable plaques and related therapeutic implications. *Nature Clinical Practice Cardiovascular Medicine*, *2*(9), 456–464. http://doi.org/10.1038/ncpcardio0298

Sommer, C. (2016). Histology and Infarct Volume Determination in Rodent Models of Stroke. In *Rodent Models of Stroke* (2nd ed., Vol. 120, pp. 263–277). essay, Humana New York.

Stecco, A., Stecco, C., & Raghavan, P. (2014). Peripheral mechanisms contributing to spasticity and implications for treatment. *Current Physical Medicine and Rehabilitation Reports*, *2*(2), 121–127. http://doi.org/10.1007/s40141-014-0052-3

Stewart, K. C., Cauraugh, J. H., & Summers, J. J. (2006). Bilateral Movement Training and stroke rehabilitation: A systematic review and meta-analysis. *Journal of the Neurological Sciences*, *244*(1-2), 89–95. http://doi.org/10.1016/j.jns.2006.01.005

Stinear, C. M., Barber, P. A., Coxon, J. P., Fleming, M. K., & Byblow, W. D. (2008). Priming the motor system enhances the effects of upper limb therapy in chronic stroke. *Brain*, *131*(5), 1381–1390. http://doi.org/10.1093/brain/awn051

Stoll, G., Kleinschnitz, C., & Nieswandt, B. (2008). Molecular mechanisms of thrombus formation in ischemic stroke: Novel insights and targets for treatment. *Blood*, *112*(9), 3555–3562. http://doi.org/10.1182/blood-2008-04-144758

Suresh, N. L., Ping Zhou, & Rymer, W. Z. (2008). Abnormal EMG-force slope estimates in the first dorsal interosseous of hemiparetic stroke survivors. *2008 30th Annual International Conference of the IEEE Engineering in Medicine and Biology Society*. http://doi.org/10.1109/iembs.2008.4649975

Talley Watts, L., Zheng, W., Garling, R. J., Frohlich, V. C., & Lechleiter, J. D. (2015). Rose Bengal photothrombosis by confocal optical imaging in vivo: a model of single vessel stroke. *Journal of Visualized Experiments*, (100). http://doi.org/10.3791/52794

Taub, E., Miller, N. E., Novack, T. A., Cook, E. W., Fleming, W. C., Nepomuceno, C. S., … Crago, J. E. (1993). Technique to improve chronic motor deficit after stroke. *Archives of Physical Medicine and Rehabilitation* , *74*, 347–354.

Teka, W. W., Hamade, K. C., Barnett, W. H., Kim, T., Markin, S. N., Rybak, I. A., & Molkov, Y. I. (2017). From the motor cortex to the movement and back again. *PLOS ONE*, *12*(6). http://doi.org/10.1371/journal.pone.0179288

Thielman, G. T., Dean, C. M., & Gentile, A. M. (2004). Rehabilitation of reaching after stroke: Task-related training versus progressive resistive exercise. *Archives of Physical Medicine and Rehabilitation*, *85*(10), 1613–1618. http://doi.org/10.1016/j.apmr.2004.01.028

Thomalla, G., Cheng, B., Ebinger, M., Hao, Q., Tourdias, T., Wu, O., … Gerloff, C. (2011). Dwi-flair mismatch for the identification of patients with acute ischaemic stroke within 4·5 h of symptom onset (PRE-FLAIR): A multicentre observational study. *The Lancet Neurology*, *10*(11), 978–986. http://doi.org/10.1016/s1474-4422(11)70192-2

Torres-Espín, A., Forero, J., Schmidt, E. K. A., Fouad, K., & Fenrich, K. K. (2018). A motorized pellet dispenser to deliver high intensity training of the single pellet reaching and grasping task in rats. *Behavioural Brain Research*, *336*, 67–76. http://doi.org/10.1016/j.bbr.2017.08.033

Turton, A. J., Cunningham, P., van Wijck, F., Smartt, H. J. M., Rogers, C. A., Sackley, C. M., … van Vliet, P. (2016). Home-based reach-to-grasp training for people after stroke is feasible: A pilot randomised controlled trial. *Clinical Rehabilitation*, *31*(7), 891–903. http://doi.org/10.1177/0269215516661751

Uluç, K., Miranpuri, A., Kujoth, G. C., Aktüre, E., & Başkaya, M. K. (2011). Focal cerebral ischemia model by endovascular suture occlusion of the middle cerebral artery in the rat. *Journal of Visualized Experiments*, (48). http://doi.org/10.3791/1978

Ustinova, K. I., Goussev, V. M., Balasubramaniam, R., & Levin, M. F. (2004). Disruption of coordination between arm, trunk, and center of pressure displacement in patients with hemiparesis. *Motor Control*, *8*(2), 139–159. http://doi.org/10.1123/mcj.8.2.139

Uswatte, G., Taub, E., Morris, D., Barman, J., & Crago, J. (2006). Contribution of the shaping and restraint components of constraint-induced movement therapy to treatment outcome. *NeuroRehabilitation*, *21*(2), 147–156. http://doi.org/10.3233/nre-2006-21206

Urton, M. L., Kohia, M., Davis, J., & Neill, M. R. (2007). Systematic literature review of treatment interventions for upper extremity hemiparesis following stroke. *Occupational Therapy International*, *14*(1), 11–27. http://doi.org/10.1002/oti.220

van Delden, A. E. Q., Peper, C., Beek, P. J., & Kwakkel, G. (2012). Unilateral versus bilateral upper limb exercise therapy after stroke: A systematic review. *Journal of Rehabilitation Medicine*, *44*(2), 106–117. http://doi.org/10.2340/16501977-0928

Van der Lee, J. H., de Groot, V., Beckerman, H., Wagenaar, R. C., Lankhorst, G. J., & Bouter, L. M. (2001). The intra- and interrater reliability of the action research arm test: A practical test of upper extremity function in patients with stroke. *Archives of Physical Medicine and Rehabilitation*, *82*(1), 14–19. http://doi.org/10.1053/apmr.2001.18668

Waller, S. M. C., & Whitall, J. (2008). Bilateral arm training: Why and who benefits? *NeuroRehabilitation*, *23*(1), 29–41. http://doi.org/10.3233/nre-2008-23104

Wang, X., Liu, Y., Li, X., Zhang, Z., Yang, H., Zhang, Y., … He, Z. (2017). Deconstruction of corticospinal circuits for goal-directed motor skills. *Cell*, 171(2). doi:10.1016/j.cell.2017.08.014

Watson, B. D., Dietrich, W. D., Busto, R., Wachtel, M. S., & Ginsberg, M. D. (1985). Induction of reproducible brain infarction by photochemically initiated thrombosis. *Annals of Neurology*, *17*(5), 497–504. http://doi.org/10.1002/ana.410170513

Watson, C., Paxinos, G., & Puelles, L. (2012). *The mouse nervous system* (1st ed.). Waltham, Massachusetts: Elsevier Academic Press.

Whishaw, I. Q., & Pellis, S. M. (1990). The structure of skilled forelimb reaching in the rat: A proximally driven movement with a single distal rotatory component. *Behavioural Brain Research*, *41*(1), 49–59. http://doi.org/10.1016/0166-4328(90)90053-h

Wolf, S. L., Winstein, C. J., Miller, J. P., Taub, E., Uswatte, G., Morris, D., … Nichols-Larsen, D. (2006). Effect of constraint-induced movement therapy on upper extremity function 3 to 9 months after stroke. *JAMA*, *296*(17), 2095–2104. http://doi.org/10.1001/jama.296.17.2095

Wolff, S. B., Ko, R., & Ölveczky, B. P. (2022). Distinct roles for motor cortical and thalamic inputs to striatum during motor skill learning and execution. *Science Advances*, *8*(8). http://doi.org/10.1126/sciadv.abk0231

Wong, C. C., Ramanathan, D. S., Gulati, T., Won, S. J., & Ganguly, K. (2015). An automated behavioral box to assess forelimb function in rats. *Journal of Neuroscience Methods*, *246*, 30–37. http://doi.org/10.1016/j.jneumeth.2015.03.008

Woodbury, M. L., Howland, D. R., McGuirk, T. E., Davis, S. B., Senesac, C. R., Kautz, S., & Richards, L. G. (2008). Effects of trunk restraint combined with intensive task practice on poststroke upper extremity reach and function: A pilot study. *Neurorehabilitation and Neural Repair*, *23*(1), 78–91. http://doi.org/10.1177/1545968308318836

Xie, Q., Sheng, B., Huang, J., Zhang, Q., & Zhang, Y. (2022). A pilot study of compensatory strategies for reach-to-grasp-pen in patients with stroke. *Applied Bionics and Biomechanics*, *2022*, 1–13. http://doi.org/10.1155/2022/6933043

Yates, S. C., Groeneboom, N. E., Coello, C., Lichtenthaler, S. F., Kuhn, P.-H., Demuth, H.-U., … Bjaalie, J. G. (2019). Quint: Workflow for quantification and spatial analysis of features in histological images from Rodent Brain. *Frontiers in Neuroinformatics*, *13*. http://doi.org/10.3389/fninf.2019.00075

Yozbatiran, N., Der-Yeghiaian, L., & Cramer, S. C. (2007). A standardized approach to performing the Action Research Arm Test. *Neurorehabilitation and Neural Repair*, *22*(1), 78–90. http://doi.org/10.1177/1545968307305353

Zhang, L., Schallert, T., Zhang, Z. G., Jiang, Q., Arniego, P., Li, Q., … Chopp, M. (2002). A test for detecting long-term sensorimotor dysfunction in the mouse after focal cerebral ischemia. *Journal of Neuroscience Methods*, *117*(2), 207–214. http://doi.org/10.1016/s0165-0270(02)00114-0

Zhao, L., Biesbroek, J. M., Shi, L., Liu, W., Kuijf, H. J., Chu, W. W. C., … Wong, A. (2017). Strategic infarct location for post-stroke cognitive impairment: A multivariate lesion-symptom mapping study. *Journal of Cerebral Blood Flow & Metabolism*, *38*(8), 1299–1311. http://doi.org/10.1177/0271678x17728162

Ziemann, U., Iliać, T. V., Pauli, C., Meintzschel, F., & Ruge, D. (2004). Learning modifies subsequent induction of long-term potentiation-like and long-term depression-like plasticity in human motor cortex. *The Journal of Neuroscience*, *24*(7), 1666–1672. http://doi.org/10.1523/jneurosci.5016-03.2004